AD-A193 372 AUTOMATED DIAPHRAGM LOADING FOR THE LB/TS (LARGE ... 1/2
BLAST/THERMAL SIMULATOR).. (U) SCIENCE APPLICATIONS INC
SAN DIEGO CA I B OSOFSKY ET AL. 28 FEB 86 SAIC-86-1529
UNCLASSIFIED DNA-TR-86-66 DNA001-85-C-0315 F/G 14/2 NL

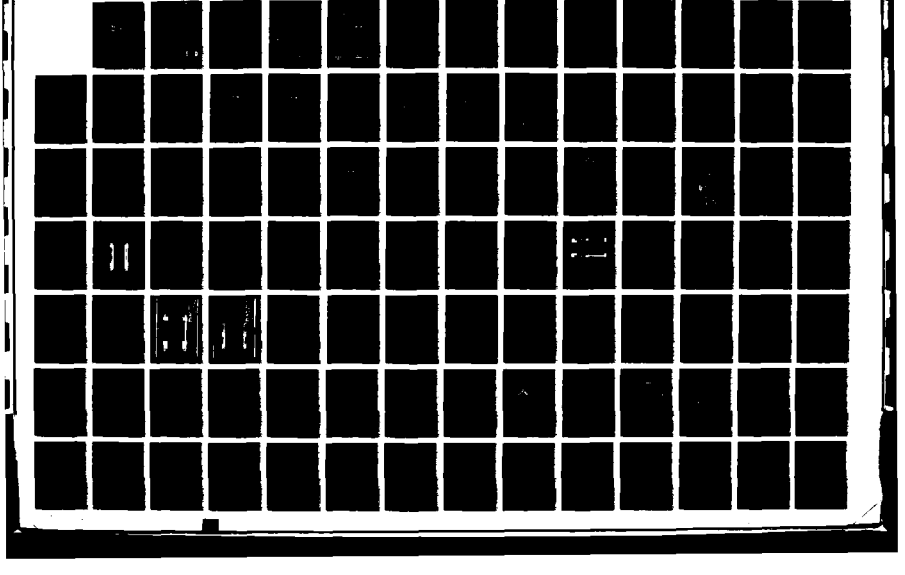

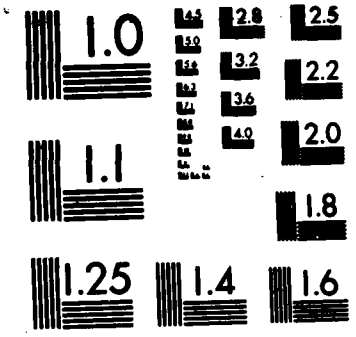

MICROCOPY RESOLUTION TEST CHART
NATIONAL BUREAU OF STANDARDS-1963-A

(4)

DNA-TR-86-66

AUTOMATED DIAPHRAGM LOADING FOR THE LB/TS

I. B. Osofsky
G. P. Mason
D. T. Hove
Science Applications International Corporation
10260 Campus Point Drive
San Diego, CA 92121

28 February 1986

Technical Report

CONTRACT No. DNA 001-85-C-0315

THIS WORK WAS SPONSORED BY THE DEFENSE NUCLEAR AGENCY
UNDER RDT&E RMSS CODE X345085469 Q67QMXGR00002 H2590D.

Prepared for
Director
DEFENSE NUCLEAR AGENCY
Washington, DC 20305-1000

DISTRIBUTION LIST UPDATE

This mailer is provided to enable DNA to maintain current distribution lists for reports. We would appreciate your providing the requested information.

- ☐ Add the individual listed to your distribution list.
- ☐ Delete the cited organization/individual.
- ☐ Change of address.

NAME: _____

ORGANIZATION: _____

OLD ADDRESS	CURRENT ADDRESS
_____	_____
_____	_____
_____	_____

TELEPHONE NUMBER: ( ) _____

SUBJECT AREA(s) OF INTEREST:

_____	_____
_____	_____
_____	_____

DNA OR OTHER GOVERNMENT CONTRACT NUMBER: _____

CERTIFICATION OF NEED-TO-KNOW BY GOVERNMENT SPONSOR (if other than DNA):

SPONSORING ORGANIZATION: _____

CONTRACTING OFFICER OR REPRESENTATIVE: _____

SIGNATURE: _____

CUT HERE AND RETURN

Director
Defense Nuclear Agency
ATTN: [redacted] TITL
Washington, DC 20305-1000

Director
Defense Nuclear Agency
ATTN: [redacted] TITL
Washington, DC 20305-1000

UNCLASSIFIED
SECURITY CLASSIFICATION OF THIS PAGE

A192372

REPORT DOCUMENTATION PAGE

1a. REPORT SECURITY CLASSIFICATION UNCLASSIFIED	1b. RESTRICTIVE MARKINGS
2a. SECURITY CLASSIFICATION AUTHORITY N/A since Unclassified	3. DISTRIBUTION/AVAILABILITY OF REPORT Approved for public release; distribution is unlimited.
2b. DECLASSIFICATION/DOWNGRADING SCHEDULE N/A since Unclassified	
4. PERFORMING ORGANIZATION REPORT NUMBER(S) SAIC-86-1529	5. MONITORING ORGANIZATION REPORT NUMBER(S) DNA-TR-86-66
6a. NAME OF PERFORMING ORGANIZATION Science Applications International Corporation 6b. OFFICE SYMBOL (If applicable) SAIC	7a. NAME OF MONITORING ORGANIZATION Director Defense Nuclear Agency
6c. ADDRESS (City, State, and ZIP Code) 10260 Campus Point Drive San Diego, CA 92121	7b. ADDRESS (City, State, and ZIP Code) Washington, DC 20305-1000
8a. NAME OF FUNDING/SPONSORING ORGANIZATION 8b. OFFICE SYMBOL (If applicable)	9. PROCUREMENT INSTRUMENT IDENTIFICATION NUMBER DNA 001-85-C-0315
8c. ADDRESS (City, State, and ZIP Code)	10. SOURCE OF FUNDING NUMBERS PROGRAM ELEMENT NO. 62715H; PROJECT NO. Q67QMXG; TASK NO. R; WORK UNIT ACCESSION NO DH251594

11. TITLE (Include Security Classification)
AUTOMATED DIAPHRAGM LOADING FOR THE LB/TS

12. PERSONAL AUTHOR(S) Osofsky, I.B.; Mason, G.P.; Hove, D.T.

13a. TYPE OF REPORT	13b. TIME COVERED	14. DATE OF REPORT (Year, Month, Day)	15. PAGE COUNT
Technical	FROM 850930 TO 860228	860228	112

16. SUPPLEMENTARY NOTATION
This work was sponsored by the Defense Nuclear Agency under RDT&E RMSS Code X345085469 Q67QMXGR00002 H2590D.

17 COSATI CODES		
FIELD	GROUP	SUB-GROUP
14	2	
20	11	

18. SUBJECT TERMS (Continue on reverse if necessary and identify by block number)
Explosive forging, Fast acting valve, FLSC, Driver, Diaphragm, Shock tube, Shock wave, Cartridge, Rupture

19. ABSTRACT (Continue on reverse if necessary and identify by block number)

This study describes a design investigation of a cartridge loading diaphragm system for the LB/TS. A diaphragm geometry was evaluated; a number of materials were investigated for use in the diaphragms and cartridge system. Cooling and heating analyses were conducted. A mechanical diaphragm opener was investigated. Manufacturing techniques and costs were investigated. Structural analyses were conducted.

(Keywords:

20. DISTRIBUTION/AVAILABILITY OF ABSTRACT ☐ UNCLASSIFIED/UNLIMITED ☒ SAME AS RPT ☐ DTIC USERS	21. ABSTRACT SECURITY CLASSIFICATION UNCLASSIFIED
22a. NAME OF RESPONSIBLE INDIVIDUAL Sandra E. Young	22b. TELEPHONE (Include Area Code) (202) 325-7042 22c. OFFICE SYMBOL DNA/CSTI

DD FORM 1473, 84 MAR 83 APR edition may be used until exhausted. All other editions are obsolete.

SECURITY CLASSIFICATION OF THIS PAGE
UNCLASSIFIED

18. SUBJECT TERMS (Continued)

Quick-opening valve
Peak overpressure
Cost
Maintenance
Heating
Cooling
Pressurization
Petal

PREFACE

This project was sponsored by the Defense Nuclear Agency (DNA) under Contract No. DNA 001-85-C-0315 entitled "Automated Diaphragm Loading for the LB/TS."

Mr. Thomas Kennedy was the DNA Technical Monitor. He was assisted by Captain James Taylor, the DNA Contract Technical Manager. The SAIC Principal Investigator was Dr. Irving B. Osofsky. Dynamics Technology, Inc. (DTI) provided design support to Science Applications International Corporation (SAIC). Duane Hove was the DTI Principal Investigator. Gregory Mason of SAIC performed the structural analyses of the diaphragm and participated in the mechanical design of the loading system.

CONVERSION TABLE

Conversion factors for U.S. Customary to metric (SI) units of measurement.

MULTIPLY → TO GET	BY	TO GET ← DIVIDE
angstrom	$1.000\ 000 \times 10^{-10}$	meters (m)
atmosphere (normal)	$1.013\ 25 \times 10^{+2}$	kilo pascal (kPa)
bar	$1.000\ 000 \times 10^{+2}$	kilo pascal (kPa)
barn	$1.000\ 000 \times 10^{-28}$	meter^2 (m^2)
British thermal unit (thermochemical)	$1.054\ 350 \times 10^{+3}$	joule (J)
calorie (thermochemical)	4.184 000	joule (J)
cal (thermochemical)/cm^2	$4.184\ 000 \times 10^{-2}$	mega joule/m^2 (MJ/m^2)
curie	$3.700\ 000 \times 10^{+1}$	*giga becquerel (GBq)
degree (angle)	$1.745\ 329 \times 10^{-2}$	radian (rad)
degree Fahrenheit	$t_K = (t^\circ f + 459.67)/1.8$	degree kelvin (K)
electron volt	11605.4	degree kelvin (K)
erg	$1.000\ 000 \times 10^{-7}$	joule (J)
erg/second	$1.000\ 000 \times 10^{-7}$	watt (W)
foot	$3.048\ 000 \times 10^{-1}$	meter (m)
foot-pound-force	1.355 818	joule (J)
gallon (U.S. liquid)	$3.785\ 412 \times 10^{-3}$	meter^3 (m^3)
inch	$2.540\ 000 \times 10^{-2}$	meter (m)
jerk	$1.000\ 000 \times 10^{+9}$	joule (J)
joule/kilogram (J/kg) (radiation dose absorbed)	1.000 000	Gray (Gy)
kilotons	4.183	terajoules (TJ)
kip (1000 lbf)	$4.448\ 222 \times 10^{+3}$	newton (N)
kip/inch^2 (ksi)	$6.894\ 757 \times 10^{+3}$	kilo pascal (kPa)
ktap	$1.000\ 000 \times 10^{+2}$	newton-second/m^2 (N-s/m^2)
micron	$1.000\ 000 \times 10^{-6}$	meter (m)
mil	$2.540\ 000 \times 10^{-5}$	meter (m)
mile (international)	$1.609\ 344 \times 10^{+3}$	meter (m)
ounce	$2.834\ 952 \times 10^{-2}$	kilogram (kg)
pound-force (lbs avoirdupois)	4.448 222	newton (N)
pound-force inch	$1.129\ 848 \times 10^{-1}$	newton-meter (N-m)
pound-force/inch	$1.751\ 268 \times 10^{+2}$	newton/meter (N/m)
pound-force/foot^2	$4.788\ 026 \times 10^{-2}$	kilo pascal (kPa)
pound-force/inch^2 (psi)	6.894 757	kilo pascal (kPa)
pound-mass (lbm avoirdupois)	$4.535\ 924 \times 10^{-1}$	kilogram (kg)
pound-mass-foot^2 (moment of inertia)	$4.214\ 011 \times 10^{-2}$	kilogram-meter^2 (kg m^2)
pound-mass/foot^3	$1.601\ 846 \times 10^{+1}$	kilogram/meter^3 (kg/m^3)
rad (radiation dose absorbed)	$1.000\ 000 \times 10^{-2}$	**Gray (Gy)
roentgen	$2.579\ 760 \times 10^{-4}$	coulomb/kilogram (C/kg)
shake	$1.000\ 000 \times 10^{-8}$	second (s)
slug	$1.459\ 390 \times 10^{+1}$	kilogram (kg)
torr (mm Hg, 0° C)	$1.333\ 22 \times 10^{-1}$	kilo pascal (kPa)

*The becquerel (Bq) is the SI unit of radioactivity; 1 Bq = 1 event/s.
**The Gray (Gy) is the SI unit of absorbed radiation.

TABLE OF CONTENTS

Section		Page
1	INTRODUCTION	1
2	BACKGROUND	2
	2.1 CONVENTIONAL DIAPHRAGM SYSTEMS	2
	2.1.1 Conventional Diaphragm Opening	5
	2.2 LB/TS DIAPHRAGM OPERATING PARAMETERS	5
	2.2.1 Unheated Driver Gas	5
	2.2.2 Heated Driver Gas	10
3	DIAPHRAGM AUTOMATED LOADING SYSTEM DESIGNS	13
	3.1 DESIGN CRITERIA	13
	3.2 DIAPHRAGM DESIGN CONCEPTS	13
	3.2.1 Diaphragm Arrangement	13
	3.2.1.1 Single Stage Diaphragms	13
	3.2.1.2 Dual Stage Diaphragms	16
	3.2.2 Mechanical Fastening Techniques	18
	3.2.3 Hydraulic Fastening Techniques	24
	3.3 MATERIALS SELECTION	27
	3.4 STRESS ANALYSIS	27
	3.4.1 Cartridge Assembly	30
	3.4.1.1 Minimum Wall Thickness	30
	3.4.1.2 Hydrostatic Pressure and Compression Loads	31
	3.4.1.3 Bolted Flange Design	34
	3.4.1.4 Integral Cooling System	35
	3.4.1.5 Pressure Seals	35
	3.4.2 Cartridge Housing Assembly	36
	3.4.2.1 Hydraulic Clamp Assembly	36
	3.4.2.2 Cartridge Housing Structure	40
	3.5 DESIGN AND DIAGRAMS	43

TABLE OF CONTENTS (continued)

Section			Page
4	HEAT TRANSFER ANALYSES		50
	4.1	HEAT TRANSFER METHODOLOGY	51
	4.2	HEAT TRANSFER CALCULATIONS	52
		4.2.1 Wall Temperature	52
		4.2.2 Diaphragm Temperature	54
	4.3	INTERPRETATION OF THE CALCULATIONS	54
	4.4	SYSTEM COOLING CONCEPT	59
5	DIAPHRAGM DESIGN CONCEPTS		61
	5.1	DIAPHRAGM OPENING MECHANISMS	61
		5.1.1 Explosive Methods	61
		5.1.2 Pressure Rupture Methods	71
		5.1.3 Mechanical Methods	73
		5.1.4 Petal Formation	75
	5.2	DIAPHRAGM STRUCTURAL ANALYSIS	76
		5.2.1 Design Criteria	77
		5.2.2 Diaphragm Materials Selection	78
		5.2.3 Diaphragm Stress Analysis	81
	5.3	DIAPHRAGM FABRICATION TECHNOLOGY	85
		5.3.1 Fabrication Methods	85
		5.3.1.1 Explosive Forming	86
		5.3.2 Hydroform	88
		5.3.3 Forging	88
		5.3.4 Spinning	88
		5.3.5 Hydraulic Forming	91
6	OPENING TECHNIQUES DEMONSTRATION TEST PLAN		93
	6.1	FLSC CHARACTERIZATION TESTS	93
	6.2	DIAPHRAGM OVERPRESSURE TESTS	94
	6.3	DIAPHRAGM EXPLOSIVE OPENING TESTS	94
	6.4	DUAL DIAPHRAGM EXPLOSIVE OPENING TESTS	95

TABLE OF CONTENTS (concluded)

Section		Page
7	CONCLUSIONS	97
	7.1 HEATING	97
	7.2 DIAPHRAGMS	97
	7.3 DIAPHRAGM CARTRIDGES	97
	7.4 STRUCTURES	98
8	RECOMMENDATIONS	99
9	LIST OF REFERENCES	100

LIST OF ILLUSTRATIONS

Figure		Page
1	Conventional bolted diaphragm installation	3
2	Conventional flanged diaphragm installation	4
3	Schematic 15 driver arrangement LB/TS	6
4	Explosive cutting charge layout	7
5	Test station waveforms for unheated driver gas, Δp = 35 psi	9
6	Test station waveform for heated driver gas, Δp = 35 psi	11
7	Single diaphragm installation	14
8	Dual series diaphragm installation	17
9	Diaphragm pressure force diagram	19
10	Schematic bolted flange	22
11	Schematic insertion and removal of quick-loading diaphragm - cartridge type	23
12	Schematic hydraulically-clamped diaphragm installation	25
13	Diaphragm loading system design	29
14	Cartridge housing assembly	37
15	Hydraulic clamp parts and pressure load diagram	38
16	Cartridge housing structure	41
17	Cartridge housing structure design	42
18	Diaphragm loading system cartridge assembly	44
19	Diaphragm loading system cartridge assembly	45
20	Typical diaphragm control system	47
21	Wall temperature profiles	53
22	Wall temperature profiles with cooling	55
23	Wall temperature profiles with insulation	56
24	Diaphragm region temperature history - insulated walls	57
25	Diaphragm region temperature history - no wall insulation	58
26	Heated dual diaphragm schematic	60
27	Diaphragm opening pattern	62
28	FLSC characteristics	64
29	Performance of RDX/Aluminum configuration IV LSC	66
30	Cutting profiles into stainless	67
31	Explosive charge overpressure diaphragms opener	70

LIST OF ILLUSTRATIONS (Concluded)

Figure		Page
32	Dual diaphragm opening concepts	72
33	Mechanical diaphragm opener	74
34	LB/TS diaphragm schematic	83
35	Explosive forming of diaphragms precision die method	87
36	Power spinning at Spincraft	90
37	Hydraulic forming of diaphragm	92

LIST OF TABLES

Table		Page
1	Driver system characteristics	8
2	Diaphragm automated loading system (DALS) design criteria . .	15
3	Bolt characteristics	20
4	Hydraulic cylinder characteristics	26
5	Selected ASME materials Specifications for diaphragm loading system parts	28
6	Minimum shell thickness for diaphragm loading system based on circumferential stress (equation 1)	31
7	Rupture diaphragm design criteria	79
8	Strength and elongation properties of selected high strength steel alloys	82
9	Diaphragm structural design results for 1150 and 2300 psi . .	85

SECTION 1
INTRODUCTION

During a previous study of the Large Blast/Thermal Simulator (LB/TS) driver system for DNA [Ref. 1], it became apparent that additional research was required on the diaphragms that are to be used to initiate the gas flow from the high pressure storage vessels (drivers) to the test chamber. In the proposed design for the LB/TS, there are on the order of 15 drivers internally pressurized as high as 2200 psia. Each driver may contain room temperature gas at 2200 psia or may contain gas at 1250 psia that is heated to 600° F. The pressurized gas is contained in each driver vessel by a metal diaphragm that is one meter in diameter.

It is important to the operation of the LB/TS that all of the diaphragms be ruptured simultaneously. Also, because the diaphragms are used to contain heated gas at high pressure, they must be designed from material that can withstand the elevated temperatures and the diaphragm opening system must be designed to operate at these temperatures.

During the previous LB/TS driver system study, it was pointed out that an automated "cartridge" loading diaphragm should be used to facilitate installation and removal of the 15 driver diaphragms for each shot. Conventional diaphragm installations rely upon the use of bolted flanged joints to contain the diaphragms and seal the pressure vessel. Because of the size and quantity of the bolts required for these one-meter diameter diaphragms, the installation and subsequent removal of 15 or more diaphragms per shot would result in a time consuming, manpower intensive operation. The automated cartridge diaphragm installation is also necessary so that turnaround time between shots will not be unduly compromised.

This study describes a design investigation of a cartridge loading diaphragm system for the LB/TS.

SECTION 2
BACKGROUND

2.1 CONVENTIONAL DIAPHRAGM SYSTEMS.

SAIC investigated methods of automating the installation and removal of diaphragms on the LB/TS. Diaphragms area used to operate the driver system and are used in the driver system of the large shock tube facility at Gramat in France. The LB/TS is designed to have 15 to 16 drivers, each with its own diaphragm or pair of diaphragms. A conventional diaphragm usually consists of a preformed dished steel sheet that is clamped between two flanges secured by a large number of bolts closely spaced around the periphery of the flanges as schematically illustrated in Figure 1. The diaphragm is also held radially by the bolts. Sealing is usually accomplished with an "O" ring.

Figure 2 illustrates a conventional flanged diaphragm that is radially restrained by a circumferential ring.

The forces on the bolts of such installations are very high. For example, if the inside diameter of the bore was one meter and the seal diameter was 48 inches, the load on the flange due to pressure (2185 psig) acting out to the seal face would be 3,954,000 lbs. If we used one-inch diameter bolts, each capable of being stressed to 50,000 psi, then each bolt would carry 39,000 lbs. of force (neglecting the threads) and we would require 102 bolts just to contain the pressure load. At least 50 more bolts would be required to preload the seal and prevent the joint from opening up. Thus, 152 one-inch diameter bolts would be required.

For the LB/TS with 15 drivers and 15 diaphragms, it would be a costly, time consuming task to take apart and reinstall 2,280 1.0-inch bolts or 1,020 1.5-inch bolts every time that diaphragms have to be replaced. If dual conventional diaphragms are used, 4,560 1.0-inch bolts or 2,040 1.5-inch bolts would be used.

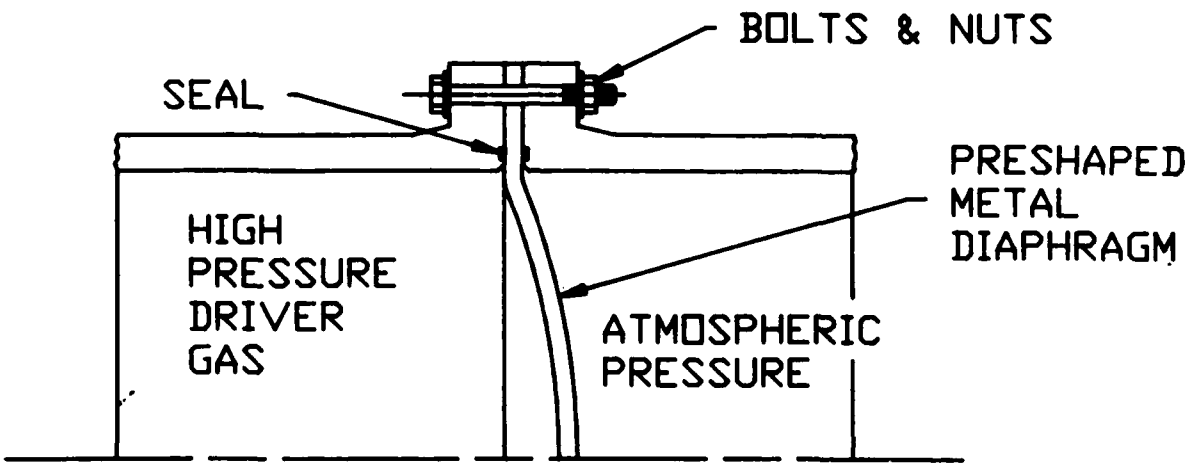

Figure 1. Conventional bolted diaphragm installation.

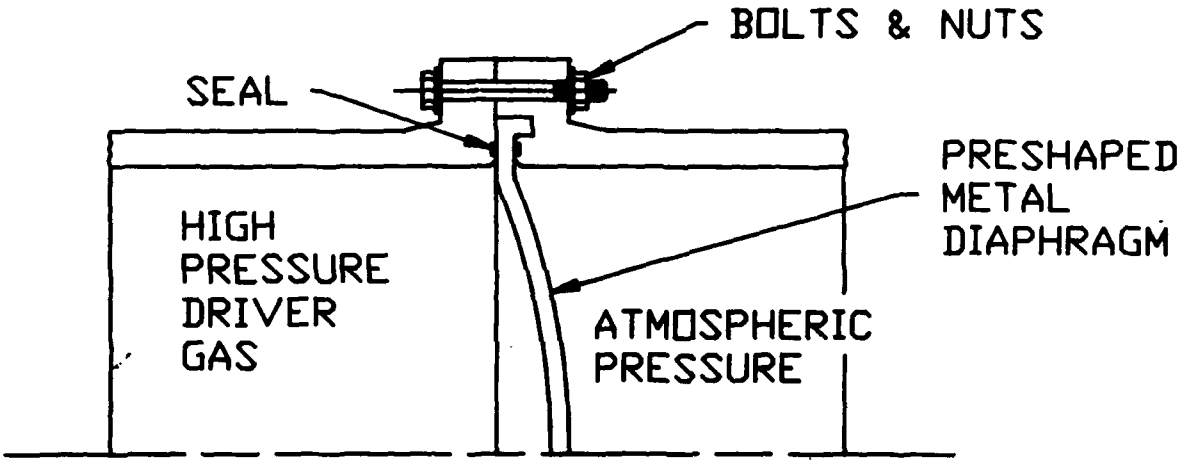

Figure 2. Conventional flanged diaphragm installation.

2.1.1 Conventional Diaphragm Opening.

Because there are 15 widely separated diaphragm installations arranged as illustrated in schematic fashion in Figure 3, it is apparent that only an electrically initiated explosive cutting system can simultaneously rupture the diaphragms into gores and allow the compressed gas to flow from the drivers to the test section simultaneously as required to form the planar shock wave in the test section of the LB/TS. The detonation speed of explosive is in the order of 7,000 meters/second so that a linear shaped charge initiated at the center of a one-meter diameter diaphragm takes only 0.07 milliseconds to finish cutting the gore pattern. No mechanical cutting system can operate so swiftly.

Explosive cutting of diaphragms as described here is state of the art in many shock tubes. Depending on the thickness of the diaphragm, linear shaped charges or lengths of "rope" explosive like "primacord" are attached to the downstream diaphragm surface, usually in the form of a six- or eight-pointed asterisk depending on the number of gores that are desired as illustrated in Figure 4. Unfortunately, the explosives that can be used to cut the diaphragms are not safe and usable at the elevated temperatures that will be experienced in the heated drivers of the LB/TS.

Therefore, special attention was paid to designs for maintaining the explosive cutting charge at safe temperatures.

2.2 LB/TS DIAPHRAGM OPERATING PARAMETERS.

2.2.1 Unheated Driver Gas.

The previous LB/TS study [Ref. 1] resulted in design data for the driver systems. These data are tabulated in Table 1 and were used in the design of the diaphragm system. The calculations for unheated Driver System V2 showed serious discrepancies in the generated static and dynamic pressure wave forms at static overpressure levels of 35 psi. Figure 5 shows test station wave forms for unheated driver gas and the dynamic pressure is on the order of three times too great. Only a single diaphragm would be required for

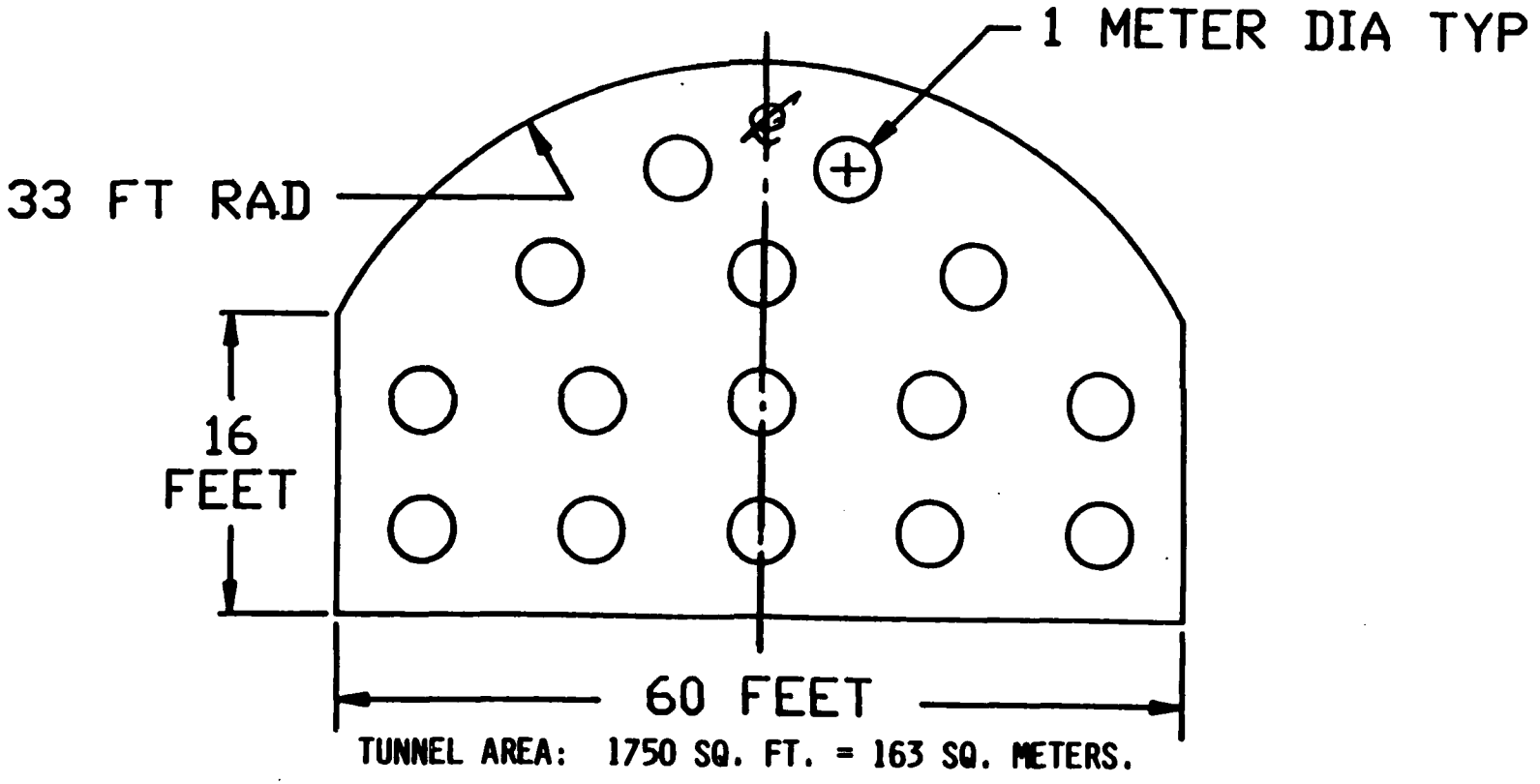

Figure 3. Schematic 15 driver arrangement LB/TS.

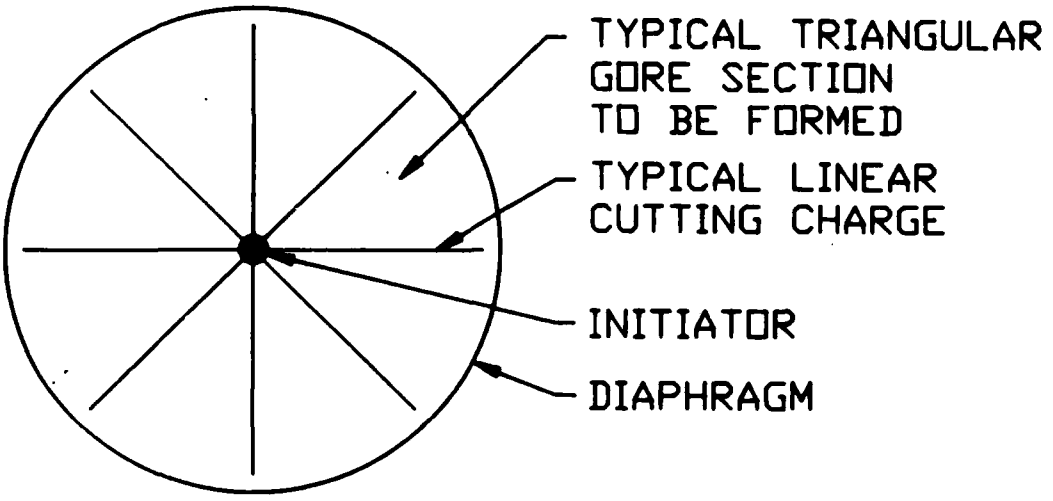

Figure 4. Explosive cutting charge layout.

Table 1. Driver system characteristics.

DRIVER SYSTEM	VOLUME $FT^3/(M^3)$	NUMBER OF DRIVERS	DRIVER		TEMPERATURE ^oR	DESIGN PRESSURE PSIA	AIR WEIGHT 10^3 LBS	AIR VOLUME 10^6 FT^3 @ 14.7 PSIA @ 530^oR
			AVERAGE LENGTH FT/(M)	DIAMETER FT/(M)				
V1	24700 (700)	7	102 (31)	6.6 (2)	530	4070	512.5	6.84
					1060	2250	141.6	1.89
V2	37760 (1071)	15	200 (61)	4.0 (1.2)	530	2200	423.5	5.65
					1060	1250	120.3	1.61
V3	77630 (2200)	16	295 (90)	4.6 (1.4)	530	1700	673.7	8.98
					1060	970	191.9	2.56

DIAPHRAGMS ARE ASSUMED TO BE ONE METER IN DIAMETER

System V2 was used for this study.

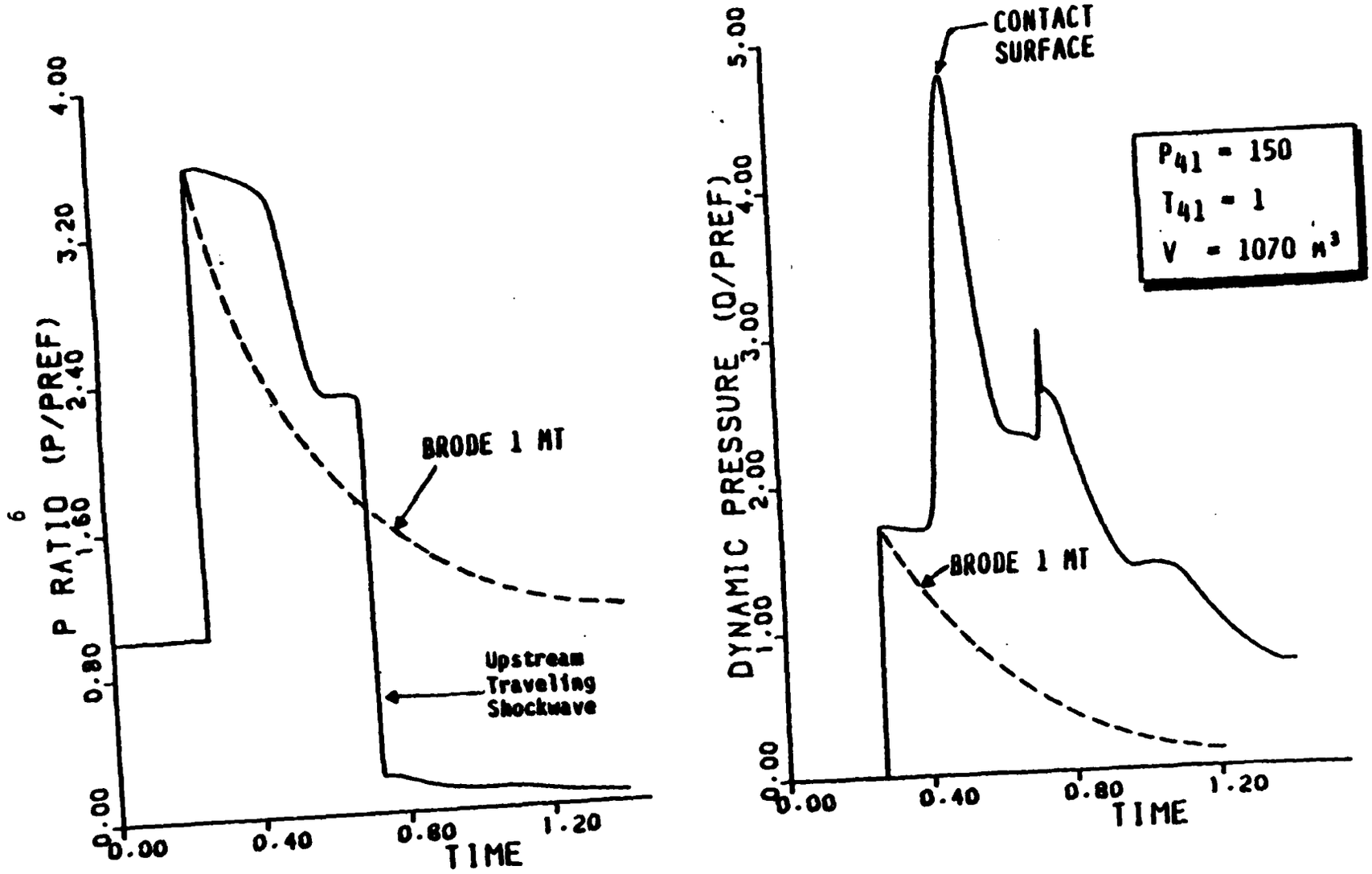

Driver System V2

Figure 5. Test station waveforms for unheated driver gas, Δp = 35 psi.

the unheated case but it would be designed for a working pressure of 2200 psia and would be approximately 0.44 inches thick if a steel with 150,000 psi minimum yield strength was used and a safety factor of 1.5 was included. If two diaphragms in series were used, each operating at half the pressure, the metal thickness would decrease to 0.22 inches per diaphragm. These thicknesses do not account for engineering or fabrication tolerances, notch sensitivity, metal variations or grooving.

The study concluded that for the configurations that were studied, unheated driver gas could not be used in the LB/TS at high overpressures unless a wave-shaping valve was used to control the dynamic pressure.

Examination of the driver data in Table 1 shows that there is a strong sensitivity of the required internal pressure to driver volume and to operating temperature. For example, for Driver System V1 with a driver volume of 700 M^3, design pressure is 4070 psia. As driver volume increases to 1071 M^3, the design pressure drops to 2200 psia. For System V3 with a volume of 2200 M^3, the design pressure drops to 1700 psia. If variable geometry of the system diaphragms were studied, calculations would have shown that the ratios of effective "nozzle" throat diameter to driver and driven section diameters would have been important variables in system performance. However the geometries for that part of the study were deemed to be fixed by the technical monitor and variations were not included in the calculations.

In each case, the design pressure drops by approximately 45% if the gas is heated.

The design pressure directly affects the thickness of the diaphragms and the thickness of the structure of the diaphragm system.

2.2.2 Heated Driver Gas.

The analysis performed in the previous LB/TS study showed that ideal wave forms could be substantially simulated if the driver gas was heated to 600°F (1060°R). Figure 6 shows that both the ideal static pressure and

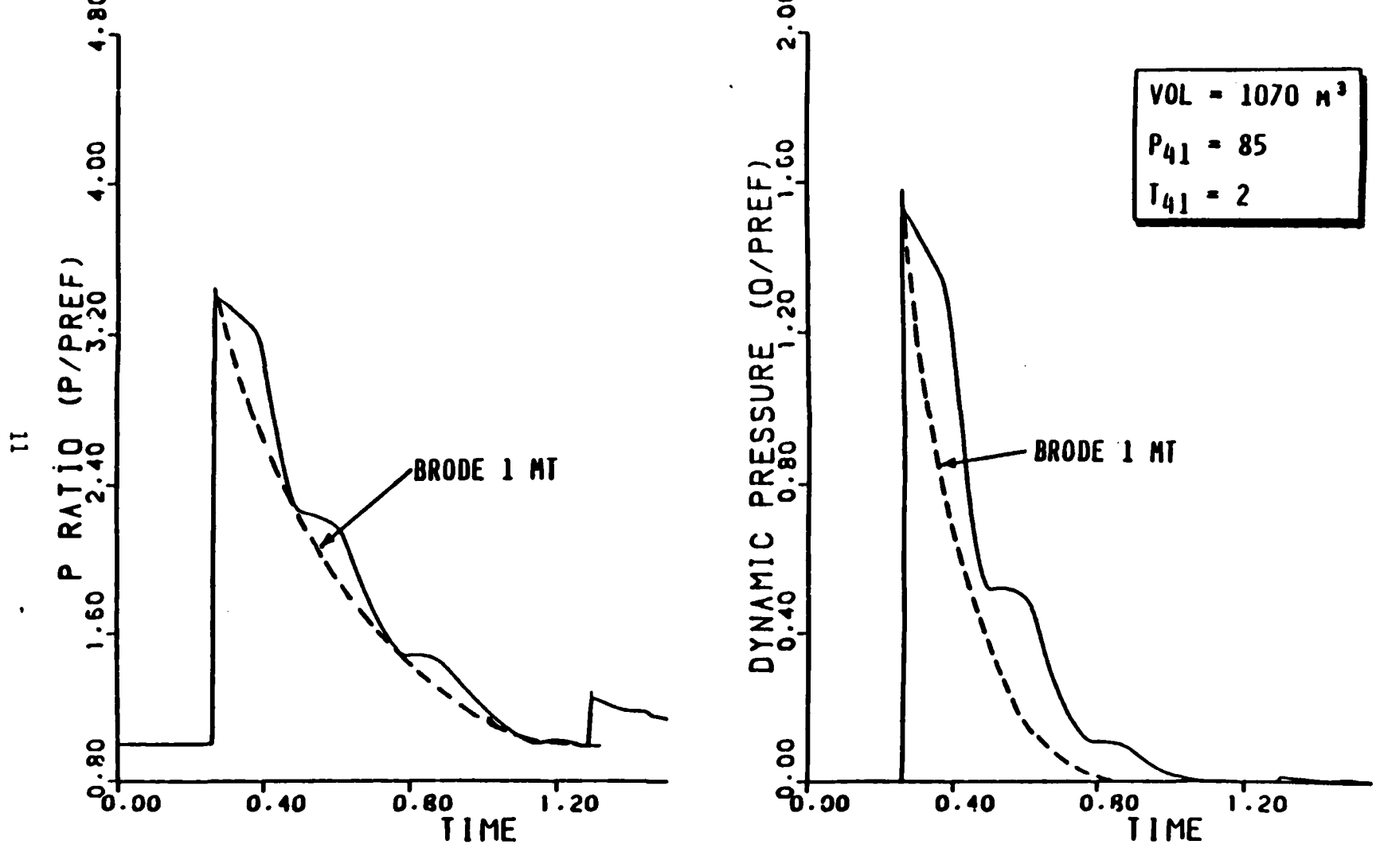

Figure 6. Test station waveform for heated driver gas, Δp = 35 psi.

dynamic pressure waves are closely simulated by the heated gas in Driver System V2. Driver pressure is 1250 psia and temperature is 600°F. A single diaphragm fabricated from 150,000 psi minimum tensile strength (at 600°F) steel would be 0.25 inches thick not accounting for manufacturing tolerances. Unfortunately, if the diaphragm is exposed to 600°F drive gas at 1250 psia, it will rapidly reach a temperature of 600°F and no explosive cutting system can survive at such elevated temperatures.

Therefore, if heated driver gas is to be used in the LB/TS, some means of isolating the explosive cutting charge from the hot diaphragm must be developed.

SECTION 3
DIAPHRAGM AUTOMATED LOADING SYSTEM DESIGNS

The conventional diaphragm is a high pressure component which is installed on the shock tube driver by means of mechanical fastening techniques as described in Section 3.2.2. It is the intent of this section to describe a means by which a diaphragm or a series of diaphragms could be installed on the shock tube driver automatically, efficiently and reliably. The basis of the design is to supply the diaphragm in a preloaded cartridge which could be easily inserted into a cartridge housing built into the shock tube driver. The cartridge sealing and retention would be accomplished by the use of mechanical and/or hydraulic clamping techniques.

3.1 DESIGN CRITERIA.

The design criteria for the diaphragm cartridge system and its driver housing is based primarily on the ASME Boiler and Pressure Vessel Code Ref. 8. The ASME Code provides the necessary safe design rules and practices for pressure containing structures when they are pressurized and operated in close proximity of any personnel or hazardous area. Additionally, the ASME Code specifies the types and grades of materials to be used under Code rated designs and tabulates allowable stress values at temperature for all the recommended materials. Table 2 summarizes the pertinent design criteria used to design the diagram loading system structure.

3.2 DIAPHRAGM DESIGN CONCEPTS.

3.2.1 Diaphragm Arrangement.

3.2.1.1 Single Stage Diaphragms. If unheated driver gas is used, a single diaphragm can be used to control the flow from each driver as schematically illustrated in Figure 7. The diaphragm is thick enough to contain all of the driver pressure with safety. For the V2 system, pressurized to 2200 psia, the minimum thickness of a high strength single diaphragm would be 0.44 inches.

The explosive cutting charge is fastened to the leeward side of the diaphragm.

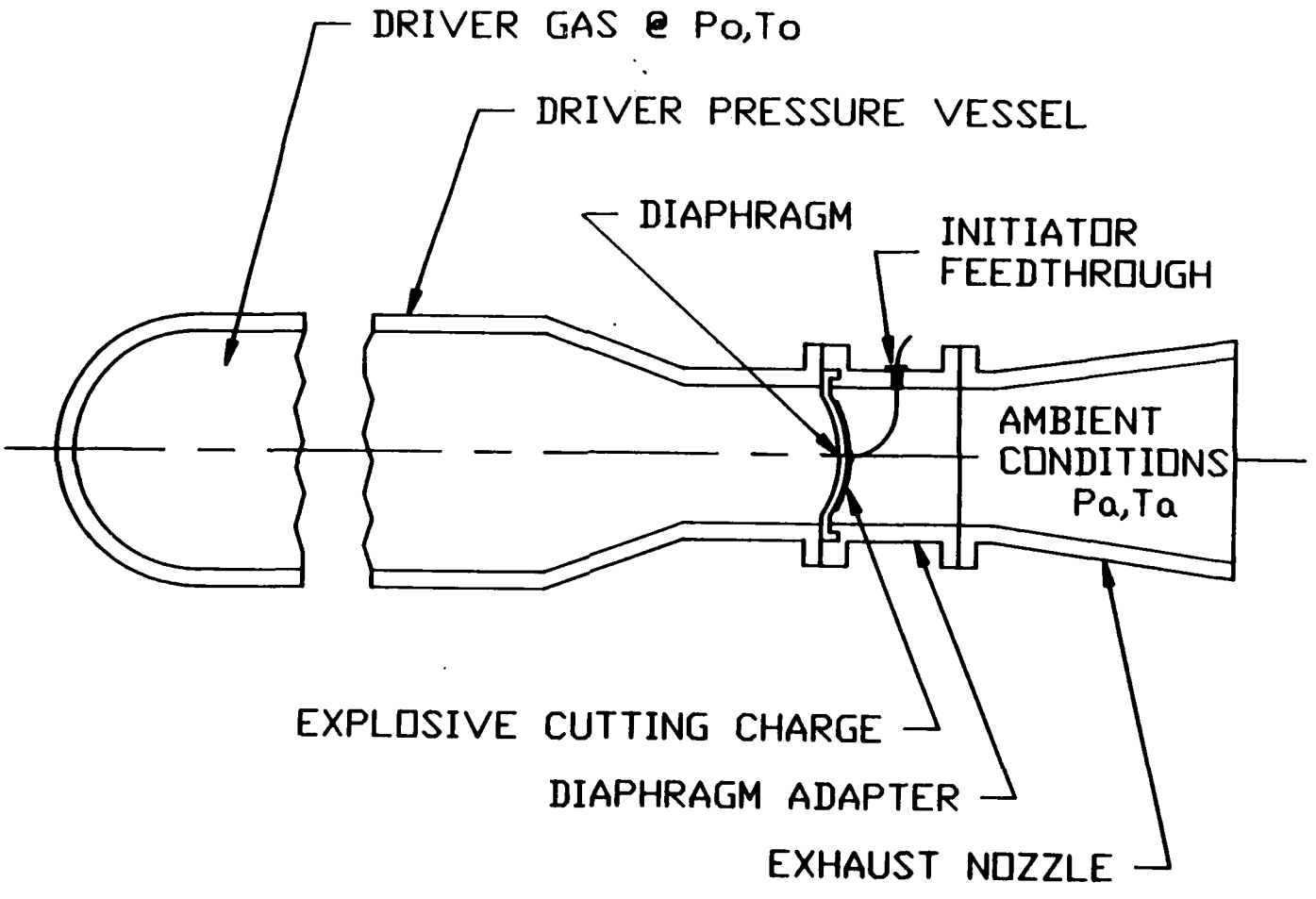

Figure 7. Single diaphragm installation.

Table 2. Diaphragm automated loading system (DALS) design criteria.

Design Criteria	DALS application or part: Hot Gas Pressure Containing Shells	Cold Gas Pressure Containing Shells	All Other Misc. Structural Parts
Service Environment	Air or Nitrogen	Air or Nitrogen	Atmospheric Conditions
Corrosion	Yes	Yes	Yes
Working Pressure (PSIG)	2300	2300	Not Applicable
Design Pressure (PSIG)	2500	2500	Not Applicable
Working Temperature (F)	700	<350	<100
Safety Factor on Tensile Strength	4.0	4.0	4.0
Min Thickness Strength Basis	ASME Code	ASME Code	ASME Code
Man Rating	Yes	Yes	Yes

If heated gas is used in the driver system, the explosive cutting charge would soon reach the temperature of the driver gas (600°F) and would either deteriorate, melt, burn or detonate.

If sufficient insulation was applied to the upstream side of the single diaphragm, it would be possible to keep the diaphragm cool enough so that an explosive cutting charge could safely be attached to the diaphragm. If insulation was applied to the downstream side of the diaphragm, the explosive cutting charge would have to penetrate the insulation as well as the diaphragm and it may interfere with the required explosive "standoff" distance.

The problem with insulation attached to the diaphragm is that some or all of it would be blown downstream towards the test chamber when the explosive charge fractures the diaphragm. Pieces of insulation would tend to

disturb the local air flow in the shock tube and would strike the test object and instrumentation at high velocity thereby creating impact damage. Therefore, it was concluded that insulated diaphragms were undesirable at this time, but in the future, if a tenacious insulation similar to silicone rubber could be developed, that would survive the heat, the explosive decompression, the explosive generated shock and the flexure of the diaphragm gores as they petal open, such a system would be a worthy candidate to consider.

3.2.1.2 Dual Stage Diaphragms. If a dual stage diaphragm as schematically illustrated in Figure 8 is used, a number of conditions make the system advantageous. As in the single diaphragm system, the driver vessel contains gas pressurized at Po and at temperature T_0. For the unheated case (System V2) P_0 = 2200 psia, T_0 = 60°F. The forward diaphragm adapter would be pressurized to 1100 psia at 60°F. Therefore, the pressure differential across either diaphragm is half the amount that a single diaphragm experiences and diaphragm thickness would decrease from 0.44 inches to 0.22 inches. This would decrease the amount of explosive charge required to cut the downstream diaphragm. When the downstream diaphragm is opened by the explosive charge, the upstream diaphragm which was also designed to contain $P_0/2$ psi (1100 psia) suddenly sees the full pressure differential, 2185 psig, and ruptures. The time required for such a rupture would be the time required for the expansion wave to travel from the open downstream diaphragm to the upstream diaphragm. This would be in the order of four milliseconds.

If the driver contained heated pressurized gas, driver gas between the two diaphragms at 1100 psia could be cooled to room temperature and the explosive cutting charge could safely be attached to the room temperature downstream diaphragm.

In this type of design, insulation and/or cooling of the forward diaphragm adapter may be required.

Also, because the downstream diaphragm is unheated, less expensive materials may be used.

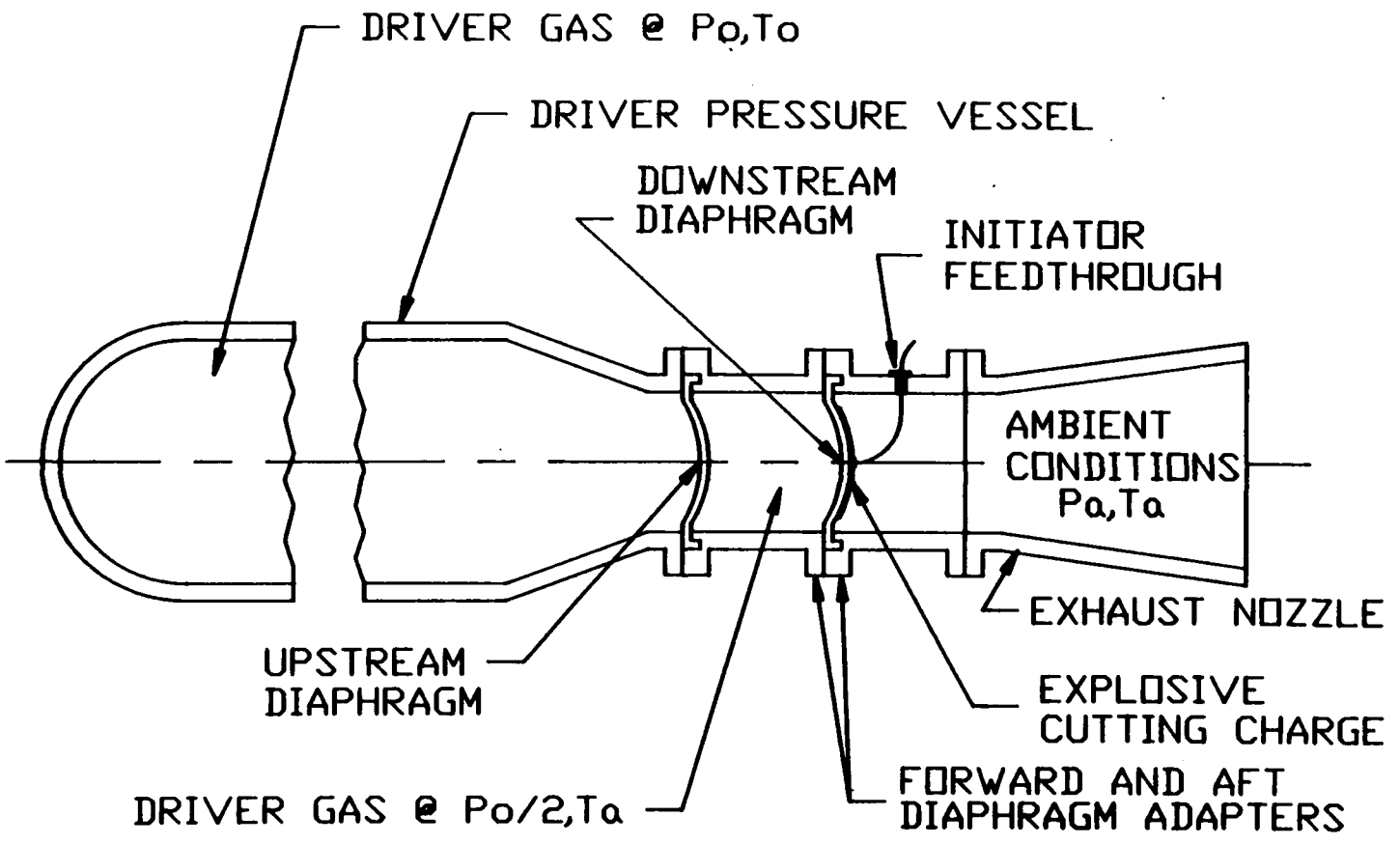

Figure 8. Dual series diaphragm installation.

3.2.2 Mechanical Fastening Techniques.

In the previous LB/TS study, [Ref. 1] a number of techniques were briefly examined for use in fastening the diaphragm section to the driver vessel and nozzle. Some of these are discussed below.

An explanation of the forces on the fasteners is given below. Figure 9 schematically illustrates a diaphragm assembly.

F = force acting on the diaphragm, lbs.

$$F = P_o A - P_d A = (P_o - P_d) A$$

$$A = \frac{\pi d_s^2}{4}$$

$$F = (P_o - P_d) \frac{\pi d_s^2}{4}$$

where:

P_o = 2,200 psia

P_d = 14.7 psia (single diaphragm)

P_d = 1,100 psia (dual diaphragm)

d_s = diameter of the seal

$d_s \simeq 48$ inches

$A = 1{,}810$ inches^2

$F = 3{,}955{,}000$ lbs. on a single diaphragm with $P_d = 2{,}200$ psia

$F = 1{,}964{,}000$ lbs. on each dual diaphragm with $P_d = 1{,}100$ psia

If bolts are used to fasten the flanges together, not only must they withstand the diaphragm force, but they must have a preload sufficient to prevent leakage. Also, the bolts stretch when under tensile force.

$$\text{Bolt elongation} = \Delta L = \frac{F_b \ell}{AE} = \delta, \text{ inches}$$

F_b = force in the bolt, lbs.

ℓ = length of the bolt, inches

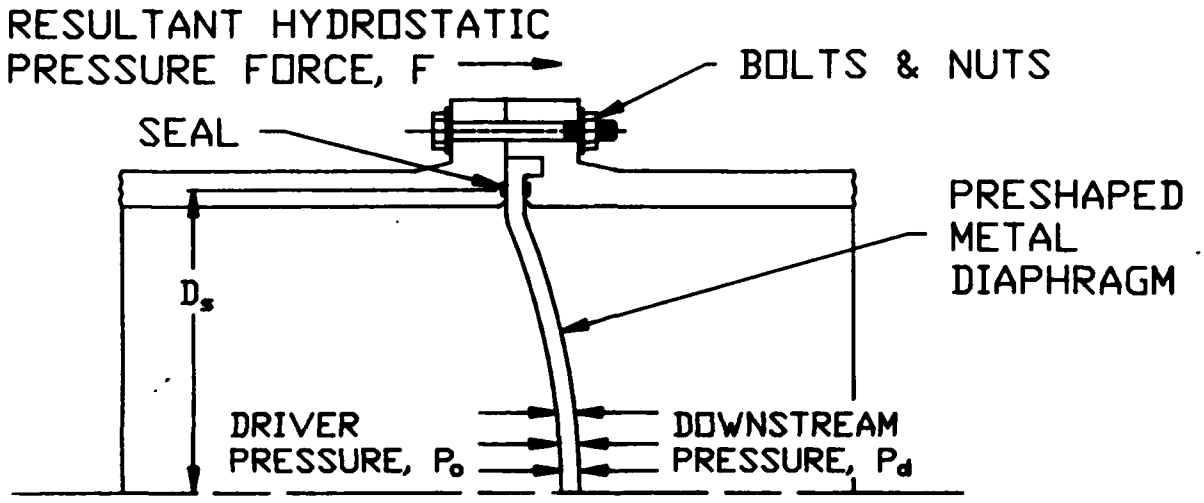

Figure 9. Diaphragm pressure force diagram.

A = Cross sectional area of the bolt, inches^2

E = Modulus of elasticity of the bolt, psi

Table 3 shows the number of bolts required to sustain the diaphragm force and gives their elongation if the bolts are eight inches long between the head and nut. Bolts are stressed to 50,000 psi at the thread root.

Table 3. Bolt characteristics.

				Number of Bolts Required			
Bolt Dia In.	Bolt Root Dia., In.	Bolt Force Lbs.	Bolt Elong-ation, In.*	Single Diaphragm Stress	Single Diaphragm Actual	Dual Diaphragm Stress	Dual Diaphragm Actual
1	.8446	28,010	.0097	141	282	70	140
1.25	1.0725	45,170	.0110	88	175	43	86
1.5	1.2955	65,910	.0102	60	120	30	60
1.75	1.5022	88,620	.0100	45	89	22	44
2	1.7245	116,790	.0101	34	68	17	34

* For purposes of discussion, all bolts were assumed to have indentical stresses but actual stresses will differ slightly, depending on ratio of root diameter area to outer diameter area.

This indicates that all of the bolts will stretch almost identical amounts when stressed to 50,000 psi at the minor thread diameter and will allow the seals to leak. The solution is to preload the flanges so that deflection is reduced to zero. This is normally accomplished by stressing the bolts to 100% greater than the expected load, thereby keeping joint and gasket deflection to zero. Usually this is accomplished by doubling the numbers of bolts.

A problem arises with a large number of bolts. The flange generally must have a space between the bolts that is at least equal to 1.5 bolt diameters. Therefore, it is difficult to make a single row of bolts hold all of the bolts that are required.

For example, the minimum bolt circle diameter can be calculated as follows:

$$\text{B.C Dia} = \frac{nd_b'}{\pi} = \frac{n(1 + 1.5)db'}{\pi}$$

$$\text{B.C Dia} = \frac{n(2.5d_b')}{\pi}$$

where:

B.C. Dia = diameter of the bolt circle, inches

n = number of bolts

d_b' = bolt diameter plus clearance

For cases previously calculated, the minimum diameters of the bolt circles are shown below for a nominal clearance = 0.063 inches.

Bolt Dia. Inches	No. of Bolts	B.C. Dia. Inches
1	282	239
1	140	101
1.25	175	183
1.25	87	79
1.5	120	149
1.5	60	64
1.75	89	129
1.75	44	55
2.00	68	111
2.00	34	48

Note that these diameters are much larger than the space available so that a bolted flange would probably require two concentric rows of preloaded bolts as illustrated in Figure 10.

Therefore, it is more practical to design the diaphragm containment system so that the full force of the diaphragm pressure load is not reacted by the bolts. This is accomplished in the SAIC cartridge design which is schematically illustrated in Figure 11. In this design, the diaphragm pressure load is not reacted by bolts but is reacted directly by a containment frame. Sealing pressure is generated by an annular hydraulic piston. Such a diaphragm system is much simpler than a bolted system and is easier to install and remove.

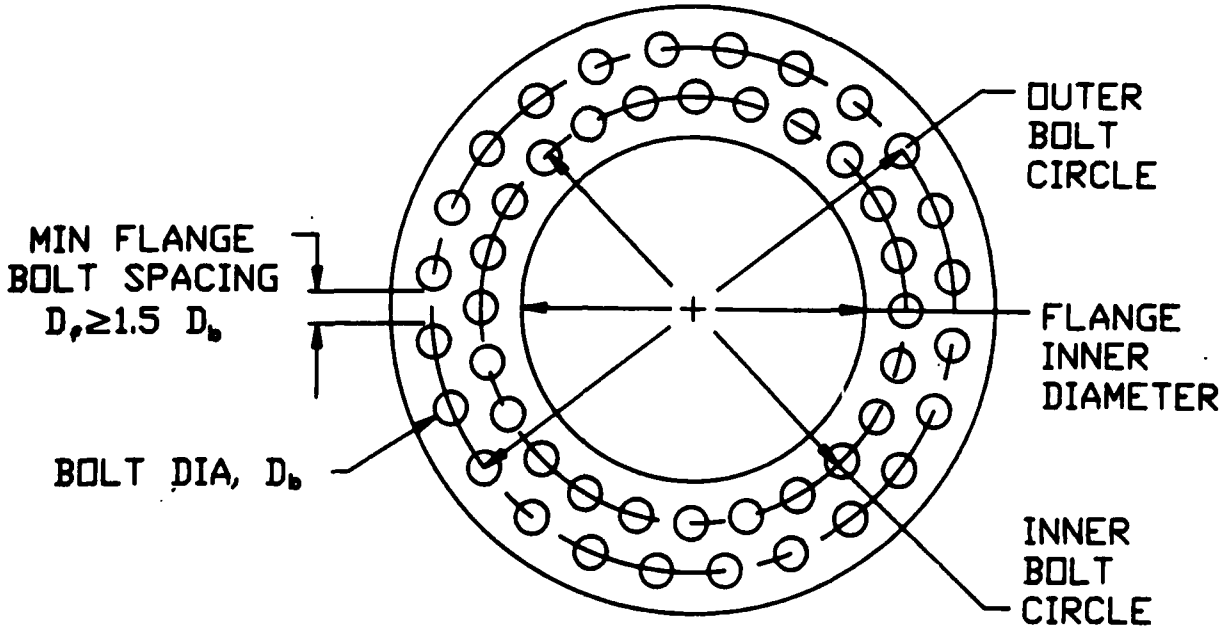

Figure 10. Schematic bolted flange.

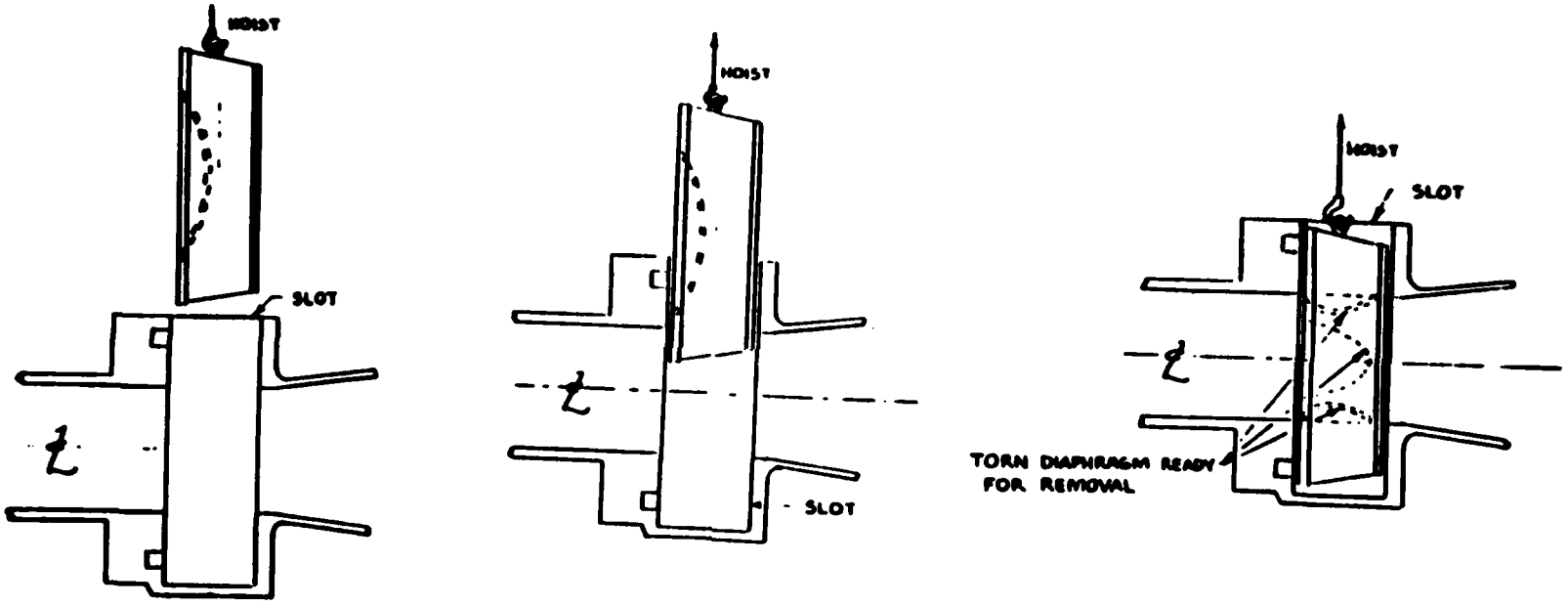

Figure 11. Schematic insertion and removal of quick-loading diaphragm - cartridge type.

Other mechanical fastening techniques were discussed in Reference 1, but were not considered for this study because they are expensive and require very accurate positioning of heavy parts during installation and disassembly. Such systems included breech lock interrupted threaded joints, hydraulic cylinder clamps, and vee clamps. Although these systems were all feasible, they were much more expensive to implement than the cartridge system described and required the maintenance of precision joints and precise orientation of massive parts for assembly.

3.2.3 Hydraulic Fastening Techniques.

If hydraulic cylinders were to be used to provide clamping force as schematically illustrated in Figure 12, the sizing would proceed as follows.

Assume that the sealing force on a single diaphragm is 3,955,000 lbs. (as calculated in Section 3.2.2) and 1,964,000 lbs. for a dual diaphragm. Let the hydraulic pressure in the actuating cylinders be 10,000 psi, which is the maximum pressure commercial system available (Enerpac). If the clamping force is $F_c = 2F_p$, then the net hydraulic clamping area, A_c, can be calculated as follows:

F_{ps} = 3,955,000 lbs. (single diaphragm)
F_{pd} = 1,964,000 lbs. (dual diaphragm)
F_{cs} = 7,910,000 lbs.
F_{cd} = 3,928,000 lbs.
Hydraulic area $A_{cs} = F_{cs}/10{,}000 = 791$ inches^2
$A_{cd} = F_{cd}/10{,}000 = 393$ inches^2
Net area/cylinder = cylinder area - piston rod area

Maximum tensile stress allowable on the piston is 50,000 psi (same as the bolts.)

$$A_{cyl} = \frac{\pi}{4}(d_c^2 - d_p^2)$$

$$F_{cyl} = P_c A_c$$

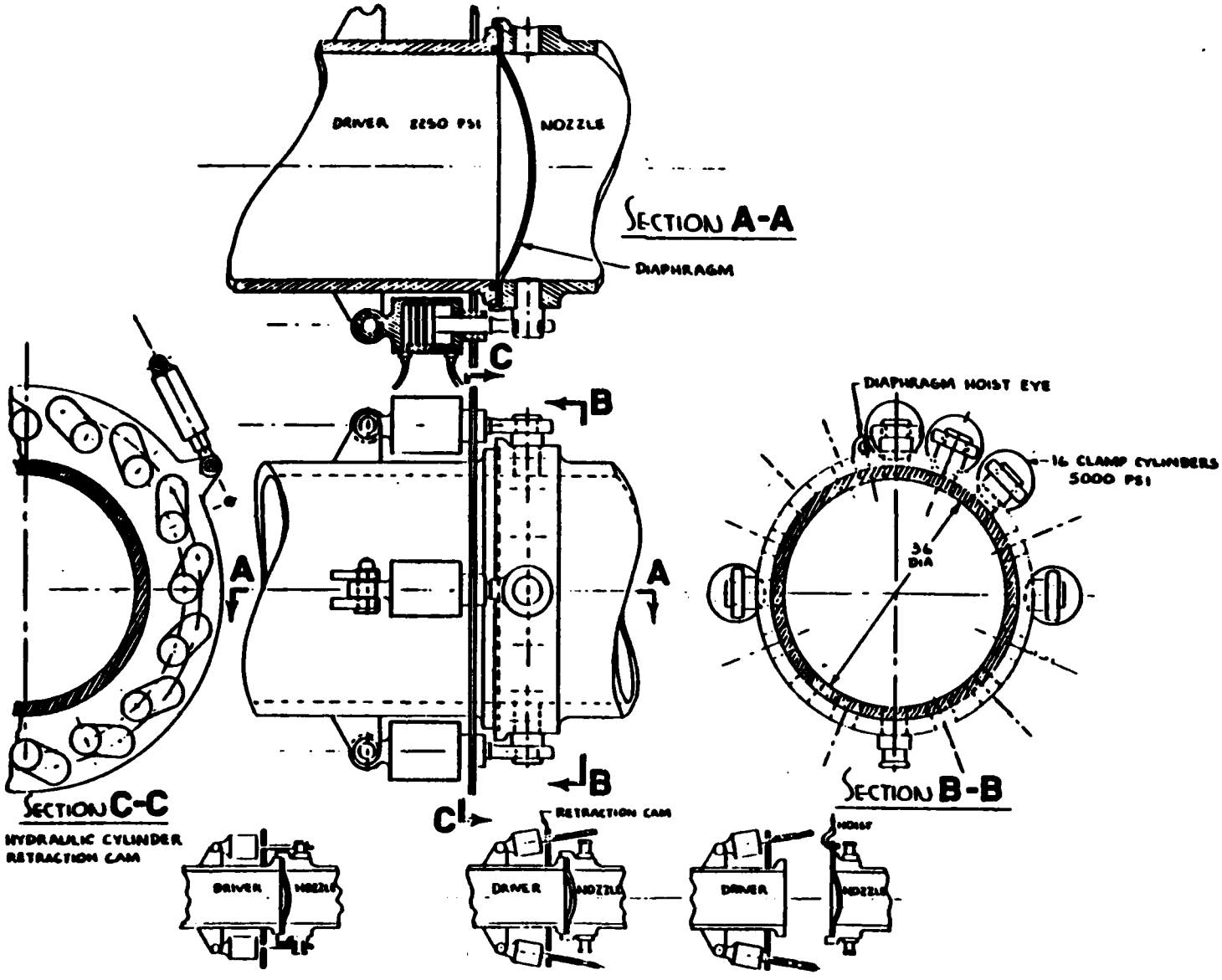

Figure 12. Schematic hydraulically-clamped diaphragm installation.

A_p = area of the piston rods = $F_c/50,000$

A_{cn} = Net area of the cylinders = $F_c/10,000$

A_{cg} = gross area of the cylinders = $A_{cn} + A_p$

$A_{cg} = F_c/50,000 + F_c/10,000$

$A_{cg} = 6\ F_c/50,000$

Solving for a single diaphragm.

$A_{cgs} = 949$ inches^2

$A_{cgd} = 471$ inches^2

Now, if we look at the physical space allowed for placing these cylinders parallel to the flow duct as shown in Figure 12, we shall calculate the number of cylinders required to clamp the diaphragms in place.

$$N = \frac{\text{Area Required}}{\text{Area/Cylinder}} = \frac{A_{cgs}}{A_c} \text{ or } \frac{A_{cgd}}{A_c}$$

$$A_c = \frac{\pi d_c^2}{4}$$

Table 4. Hydraulic cylinder characteristics.

Cyl. Dia. Inches	A_c Inches^2	N_s Single	N_d Dual	PD_s Inches	PD_d Inches
3	7.07	135	68	170	86
4	12.57	76	38	103	52
6	28.27	34	17	52	26

If a one inch radial thickness for the cylinder wall assembly is allowed, the pitch circle diameter of the cylinder can be calculated as follows:

$$PD = \frac{n(d_c + 2)}{\pi}$$

These diameters indicate that cylinders which are at least four inches in

diameter must be used and the number of required cylinders is considerable. The mechanism required to engage and disengage the cylinders is complicated and expensive.

A 10,000 psi working hydraulic pressure is now commercial state of the art in pumps, lines, fittings, valves and cylinders are available from stock.

3.3 MATERIALS SELECTION.

The diaphragm loading system materials selection is based primarily upon the application, service environment and the fabrication methods used. Additionally, cost considerations must be taken into account when manufacturing heavy components which require thousands of pounds of material. As a rule of thumb the least expensive materials are carbon steel followed by low alloy steel, high alloy steel and stainless steel, respectively. Aluminum, titanium, and other nonferrous materials are not recommended because of their relative high cost compared to similar strength ferrous materials. The ASME code specifies the materials under several classes of applications. These are: bolting (all fasteners used in ASME pressure vessels); fittings (all parts specified as pressure containing piping fittings); plate and sheets (all pressure vessels manufactured from plate and sheet by rolling and welding); seamless pipe and tube (pipe and tube manufactured by extrusion methods); electric resistance welded pipe and tube (all pipe and tube manufactured by plate/sheet forming and welding); and forgings, castings, and structural shapes (all other materials used other construction of pressure containing or structural parts). Under each application, a specification for material is given which supplies information as to the applicability of the material to the service environment (i.e., high temperature, cryogenic, etc.), the material constraints (if any), the fabrication and heat treatment methods, the composition, and the testing requirements (i.e., tensile test, composition test, etc.). Table 5 shows materials that were selected from the ASME Code for use in the various diaphragm loading system parts.

3.4 STRESS ANALYSIS.

Table 5. Selected ASME materials specifications for diaphragm loading system parts.

Steel Type	Spec No.	Grade	Application	Specified Min. Yield ksi	Specified Min. Tensile ksi	Maximum -20 to 650°F ksi	Allowable Stress 700°F ksi	750°F ksi
Carbon	SA-36	--	Structural Steel Plates and Shapes	36	58	12.7	--	--
Carbon	SA-105	--	Forgings for Flanges, FTGS, and General Piping	36	70	17.5	16.6	16.6
Carbon	SA-283	A	Low and Intermediate	24	45	10.4	--	--
		B	Tensile Strength Plates,	27	50	11.5	--	--
		C	Shapes and Bars	30	55	12.7	--	--
		D		33	60	12.7	--	--
Carbon	SA-285	A	Pressure Vessel Plates	24	45	11.3	11.0	10.3
		B	Low- and Intermediate-	27	50	12.5	12.1	11.2
		C	Tensile Strength	30	55	13.8	13.3	12.1
Carbon	SA-516	55	Pressure Vessel Plates	30	55	13.8	13.3	12.1
		60	For Intermediate and	32	60	15.0	14.4	13.0
		65	Higher Temperature	35	65	16.3	15.5	13.9
		70	Service	38	70	17.5	16.6	14.8
Low-Alloy	SA-182	F1	Forged or Rolled Pipe	40	70	17.5	17.5	17.5
		F5	Flanges, Forged FTGS,	40	70	16.3	16.0	15.4
		F5a	and Valves and Parts	65	90	20.9	20.5	19.8
		F9	High Temperature	55	85	19.7	19.4	18.7
		F21	Service	45	75	17.7	17.5	17.2
		F22		45	75	17.7	17.2	17.2
Low-Alloy	SA-302	A	Pressure Vessel Plates	45	75	18.8	18.8	18.3
		B	Managanese-Molybdenum	50	80	20.0	20.0	19.6
		C	Mang-Moly-Nickel	50	80	20.0	20.0	19.6
		D		50	80	20.0	20.0	19.6

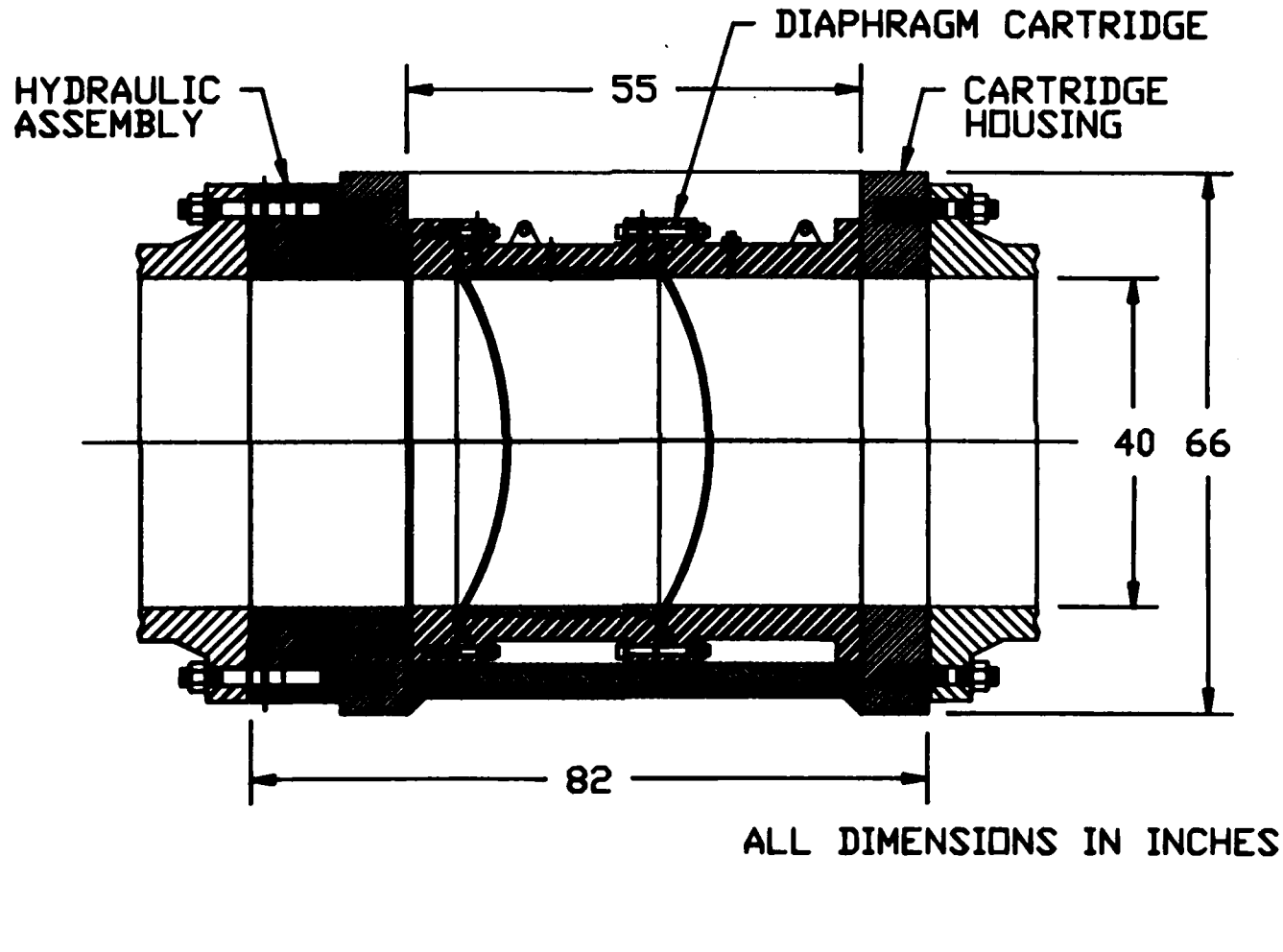

Figure 13. Diaphragm loading system design.

The diaphragm loading system design is shown in Figure 13. Shown are the various dimensions of the cartridge and cartridge housing assembly which were calculated based on the diaphragm port size of 40 inches (approx. 1 meter). The calculations are based on the ASME Code rules and practices.

3.4.1 Cartridge Assembly.

3.4.1.1 Minimum Wall Thickness. For internal pressure containing cylindrical vessels of the cartridge assembly the minimum allowable wall thickness is given by the greater thickness calculated by equations 1 and 2 (ASME Code UG-27):

$$\text{CIRCUMFERENTIAL STRESS:} \quad t = \frac{PR}{SE-0.6p} \qquad (1)$$
$$t < R/2 \text{ and } P < 0.385SE$$

$$\text{LONGITUDINAL STRESS:} \quad t = \frac{PR}{2SE+0.4P} \qquad (2)$$
$$t < R/2 \text{ and } P < 1.25SE$$

where:

t = minimum required thickness of shell, excluding corrosive allowance in.

P = design pressure, psi

R = inside radius of the shell, before corrosion allowance is added, in.

S = maximum allowable stress values, psi (given by Tables in Subsection C, ASME Code)

E = joint efficiency, given by Table UW-12, ASME Code

This minimum thickness accounts only for the design pressure (shock and/or hydrostatic) which the vessel is subjected to. All other external structural and weight loads must be accounted for separately. In the first order analysis performed here, these external loads are neglected because the weight of the pressurized gas is negligible compared to the weight of the steel structure and the system is assumed to be adequately balanced to avoid any adverse moments or forces on the pressure vessel wall. Using the design criteria established in Section 3.1, calculations were made for shell thickness using several materials. The greater thickness was calculated from the

circumferential equation (Eq. 1) in all cases. These results (circumferential stress only) are tabulated in Table 6. The table gives design data required to size the pressure shells at the design pressure and several temperatures. For the hot shells (no cooling assumed) a minimum shell thickness of 6.9 inches is required compared to 6.2 inches for a cold shell utilizing standard pressure vessel grade plate SA-285-Grade A carbon steel. For the higher performance SA-516 carbon steel, a minimum thickness of approximately 5.7 inches is required for the hot shells and 3.75 inches for a cold one. For the low alloy SA-302 steel, the minimum thickness drops to about 3.5 inches for all temperature levels. The low alloy steel is less susceptible to elevated temperature strength degradation than carbon steel. The low alloy steel appears to be the most ideal material to use in the pressure shells when considering shell thickness at elevated temperature constraints. However, a more detailed analysis of the costs for fabricating the diaphragm pressure components from carbon steel versus low alloy steel should be performed. Additionally, the corrosion properties of each material should be examined if they are exposed to a hot gas/oxygen containing environment.

Table 6. Minimum shell thickness for diaphragm loading system based on circumferential stress (equation 1).

Material Spec No. (tbl 3.3.1)	Design Press psi	Inner Radius in	Joint Efficiency	Minimum Thickness <650°F in	700°F in	750°F in
SA-285-A	2500	20	0.85	6.17	6.37	6.89
SA-285-B	2500	20	0.85	5.48	5.69	6.23
SA-285-C	2500	20	0.85	4.89	5.10	5.69
SA-516-55	2500	20	0.85	4.89	5.10	5.69
SA-516-60	2500	20	0.85	4.44	4.66	5.24
SA-516-65	2500	20	0.85	4.05	4.28	4.85
SA-516-70	2500	20	0.85	3.74	3.97	4.51
SA-302-A	2500	20	0.85	3.45	3.45	3.56
SA-302-B	2500	20	0.85	3.23	3.23	3.30
SA-302-C	2500	20	0.85	3.23	3.23	3.30
SA-302-D	2500	20	0.85	3.23	3.23	3.30

3.4.1.2 Hydrostatic Pressure and Compression Loads. The operation of the hydraulic diaphragm loading system, introduces an additional strength factor

for the pressure containing shells of the cartridge assembly. When hydrostatic and hydraulic clamping loads are applied to the first (upstream) diaphragm, a compressive load is exerted on the downstream shells. This compressive load could cause the shell to fail by elastic instability. This load is calculated by the required sealing compression load on the gasket plus the hydrostatic load exerted by the internal pressure acting on the cross-sectional area. The formulae for computing this load are given by the ASME Code (Sec VIII Div 1, pg. 413) under the rules for bolted flange connections with ring type gaskets. The formulas are:

$$Wm1 = H+Hp = 0.785(G^2)P+(2b)(3.14mP) \quad (3)$$

where:

Wm1 = required bolt load for the operating conditions, lb
H = total hydrostatic end force, lb
Hp = total joint-contact surface compression (sealing) load, lb
G = diameter at gasket load reaction, in
P = design pressure, psi
b = effective gasket seating width, in
m = gasket required compression load factor

The diameter at the gasket load reaction is the effective diameter of the pressure vessel that the pressure acts upon. In the case of a ring gasket, the effective diameter is at approximately the average diameter of the gasket (i.e., the center of the gasket width). Assuming a 1 inch width gasket and a 40 inch inner shell diameter, the effective diameter, G, is approximately 42 inches (1/2-inch gasket offset from inner diameter assumed). The effective gasket seating width is calculated from the following formula (ASME Code Sec VIII-Div 1, pg. 418):

$$b = 0.5(bo)^{1/2} \quad (4)$$

where:

bo = basic gasket seating width, N/2, in
N = actual gasket width, in

For the 1 inch gasket width, b=.35 in. The gasket compression load factor, m,

is determined from the type of gasket used. In the design, a spiral-wound metal, asbestos filled carbon steel gasket material is chosen and the ASME Code (Sec VIII-Div 1-Table 2-5.1 pg. 416) specifies m=2.50 for this material. Using a design pressure of 2500 psi and the above factors, H=3,461,850 lb, Hp=576,975 and Wm1=4,038,825 lb.

The elastic instability phenomena must be taken into account in the design of the pressure shells because the ASME Code rules assume the shell is to be under positive longitudinal stress (i.e., tension). The elastic instability of a tubular shape is given by the ultimate load which is required to fail the compression member. Reference 7, pg. 422 gives the following parabolic formula for short columns:

$$P/A = Sy - k(L/r)^2 \qquad (5)$$

where:

P = ultimate load, lbs
A = section area, in^2
Sy = tensile yield strength, psi
k = correlation factor
L = l/C,column length adjustment for end conditions, in
C = 2, end condition factor for welded ends
l = column length, in
r = least radius of gyration of section, in

For the shell furthest downstream (See Figure 13), the compression load is greatest and the differential pressure load across the shell is zero. The following factors are used to compute the ultimate load on a tubular cylindrical column [Ref. 7, Roarke pg. 418]:

Sy = 36,000 psi
k = 1.172

The calculated ultimate buckling load for a 40 inch inner diameter by 4 inch wall thickness shell 50 inches long is:

$P = 20{,}000{,}000$ lbs

where:

$r = 15.6$ in

$A = 553$ in^2

The ultimate load is approximately 5 times that exerted by that gyrostatic and gasket clamping loads combined and indicates that the pressure shell will not buckle from those compression loads.

3.4.1.3 Bolted Flange Design. Pressure vessel components are commonly assembled by means of matching flanges which are bolted together with a ring type seal (i.e., gasket, O-ring, etc.). The flange design is critical to ensure that a pressure tight seal is kept under all design operating conditions. The loads under which a flange operates were previously described and consist primarily of the hydrostatic pressure load and gasket compression sealing load. This load was calculated previously to estimate the elastic stability of the diaphragm cartridge structure to compressive loading. Because the cartridge is loaded in compression, the flange design for this assembly need not take into consideration the total hydrostatic and clamping forces. Rather, these flanges are designed to efficiently assemble the cartridge and prevent damage to the assembly (especially the seals) while handling and installing. The flange design must adequately clamp and align the various pieces (i.e., diaphragms and their adapters) until the hydraulic clamping engages with the full sealing force. Bolt tension for the diaphragm cartridge assembly could realistically be allowed to decrease to zero upon hydraulic sealing and thus is not a critical factor. Therefore, the flange design becomes a function of the handling and clearance constraints which are imposed on the cartridge system. In the design, one inch bolts were considered adequate for assembly and handling stability. The flanges were then designed to allow sufficient clearance for the use of these bolts. The fact that the flanges for the cartridge assembly are not sized for the full pressure/sealing load is a benefit to the design because it allows the maximum outer diameter of the cartridge to be smaller and thus the cartridge receptacle and hydraulic clamp mechanism could be sized smaller. This greatly

decreases the size and weight of all components involved.

3.4.1.4 Integral Cooling System. The cooling parts shown in Figure 13 represent preliminary cooling system size estimates to limit metal temperatures to 350 degrees F. The cooling system is an integral part of the pressure vessel wall and is assumed not to be included in minimum wall thickness calculations (i.e., Eqs. 1 and 2). Only the upstream section is shown with a cooling capability, however, the other section could be cooled similarly. The structural design performed for the cooling system shown is for the thickness of the material from the diaphragm port inner diameter to the cooling port. The material thickness must be capable of two functions: first, to provide sufficient strength to withstand the local pressure forces (i.e., collapse of the cooling part) and second, the capability to withstand crushing by the diaphragm petals as they open and strike the wall. A one-inch thickness is considered adequate to provide strength for these loading conditions. Replaceable heavier metal sections could be added in the vicinity of the striking diaphragm petals to decrease the likelihood of cooling system failure.

3.4.1.5 Pressure Seals. Pressure sealing is usually accomplished in pressure vessel construction by ring type seals. Ring type seals generally consist of two types: first is the self-sealing type which requires no compressive load to operate; the second type of seal requires compression loading which ensures a tight seal and is usually referred to as a gasket. Both of these seal types were considered for the cartridge and the gasket type was chosen because of its simplicity in design. A self-sealing type seal, like an O-ring, requires a special groove to be machined for its installation and the mating sealing surface must be flat and without flaws or scratches. Any small scratch in the mating surface could develop a leak and result in hot, high pressure gas blowing by the seal. A compression gasket type seal, however, requires less control over the mating surface. The compression gasket is seated by clamping the surfaces together and the gasket material flows into all imperfections and flaws. There is a wide variety of gasket type seals and the application usually dictates the type of gasket material and design. For high pressure elevated temperature gas, a metal

reinforced asbestos filled gasket is commonly employed. This type of gasket has layers of spiral wound metal chevrons with asbestos material between the layers. These types of seals are widely used and have proved their reliability in all types of services.

3.4.2 Cartridge Housing Assembly.

The cartridge housing assembly is composed of two main parts as shown in Figure 14. The first part, the hydraulic clamping mechanism, engages the end of the cartridge assembly and compresses the assembly and a gasket for pressure sealing. The second part is the housing which holds the cartridge in place and transfers hydraulic clamping forces to the downstream section of the driver. The main body of the housing assembly is designed to transfer hydrostatic pressure loads from the cartridge to the upstream driver structure. Additionally, the hydraulic mechanism is exposed to hot, high pressure gas and must be designed to withstand the gas heat and pressure loads as well as the hydraulic pressure loads.

3.4.2.1 Hydraulic Clamp Assembly. Figure 15 shows the hydraulic clamp assembly parts and the operating loads that are imposed on them. The hydraulic clamp design incorporates force balancing through the use of the hydraulic pressure and driver pressure differential. The shell thickness for the various parts are designed by the differential pressure acting across their radial surfaces. Assuming that the driver and hydraulic pressure is a constant, the flange part (see Figure 15) shell thickness, t_1, is sized according to the pressure differential, P_d-P_h. The piston shell thickness, t_3, is sized according to the hydraulic pressure which acts on only the inner radial surface. The piston is also sized by the hydraulic work area, A_h (specified by t_2), which is acted on by the hydraulic pressure, P_h, to provide sufficient seal compression. The seal compression force, calculated earlier in Section 3.4.1, is constant for a given driver pressure. Assuming a driver pressure of 2500 psig, the sealing force is given as 576,975 lbs. Assuming a hydraulic supply pressure of 3000 psi, the required work area is approximately 193 square inches.

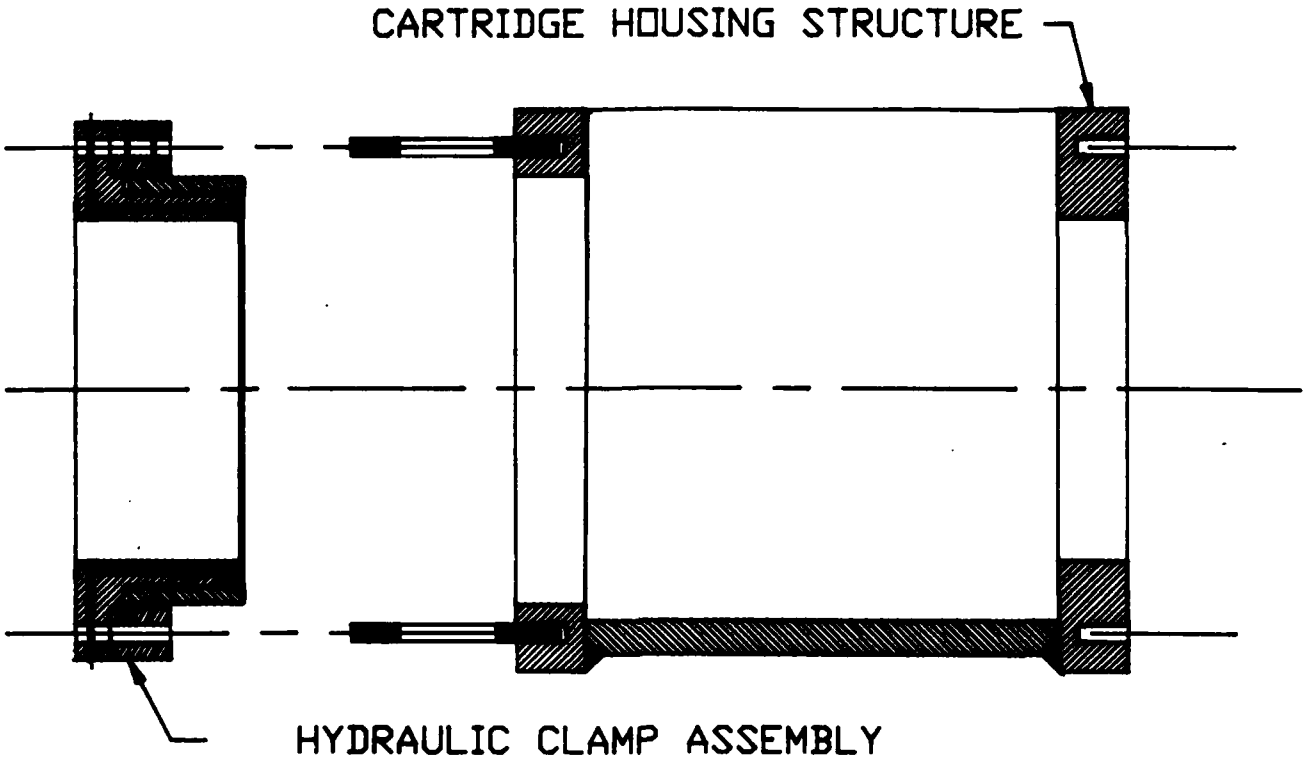

Figure 14. Cartridge housing assembly.

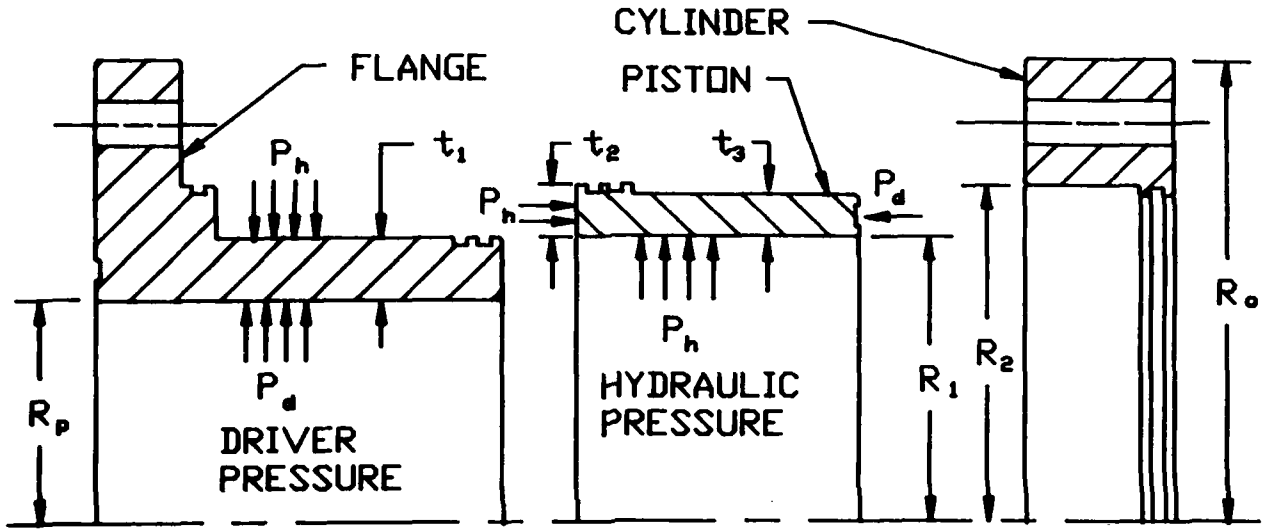

R_p, INNER RADIUS OF DIAPHRAGM PORT DIAMETER
R_o, OUTER RADIUS OF HYDRAULIC CLAMP ASSEMBLY
R_1, INNER/OUTER RADIUS OF PISTON/FLANGE PARTS
R_2, INNER RADIUS OF CYLINDER PART
t_1, THICKNESS OF FLANGE PRESSURE SHELL
t_2, THICKNESS OF PISTON AT HYDRAULIC WORK SURFACE
t_3, THICKNESS OF PISTON PRESSURE SHELL

Figure 15. Hydraulic clamp parts and pressure load diagram.

The flange shell can now be sized using a differential pressure of 500 psi, assuming that the hydraulic pressure is decreased proportionally with the driver pressure when the shock tube is operated (otherwise the differential pressure could increase to 3000 psi when the driver is vented to 0 psig and the hydraulic pressure is not decreased). The resultant flange pressure is exerted on the outer radial surface and is treated as a shell subjected to external pressure. The ASME Code provides rules for the computation of the shell thickness of a cylinder exposed to external pressure. The computation of the thickness is performed through a series of calculations using a trial and error algorithm and tables provided in the code. The following factors are used in the analysis:

D_o = outer diameter of cylindrical shell, inches
t_1 = shell thickness, inches
L = shell length, inches
A = factor from ASME Code
B = factor from ASME Code

The ASME Code factors, A and B, are each a function of the geometry and material used for the shell, respectively. Assuming a shell thickness of 3 inches and length 18 inches, the ASME factors are:

A = 0.08
B = 14,000 for SA-516-GR.C carbon steel @ <300 F

The allowable external pressure for the shell is calculated from the following formula:

$$Pa = \frac{48}{3(D_o/t_1)}$$

The pressure is calculated at approximately 1220 psi, which is roughly 2.5 times the actual working pressure. A similar calculation performed for a 2 inch shell results in an allowable pressure of 750 psi. The 3 inch value is used in the design to allow a greater safety margin to account for hydraulic and driver pressure fluctuations during shock tube blowdown.

This hydraulic piston is designed as an internal pressure shell and thus the previous ASME Code rules used for cylindrical shells will apply. Using a working pressure of 3000 psig, an allowable working stress of 25 ksi and equations 1 and 2, the shell thickness for the piston, t3, is approximately 3 inches. The last part of the hydraulic assembly, the cylinder, is sized by geometric constraints rather than by hydraulic pressure. The cylinder must be large enough to accommodate bolts to fasten the flange/piston/cylinder assembly to the cartridge housing. A outer radius, R_o, of 32 inches provides ample space for 2 inch bolts and makes the cylinder thickness equal to 6 inches.

3.4.2.2 Cartridge Housing Structure. Figures 16 and 17 show the cartridge housing structure and the operating loads that are applied on it, respectively. The total cross-sectional area of the housing, A-A, is subjected to the resultant hydrostatic pressure and sealing compression force imbalances due to the housing slot configuration. The neutral axis must pass through the same axis as that of the force, F. The neutral axis must therefore be located on the centerline of the driver/diaphragm cartridge assemblies.

The resultant force, F, was calculated previously taking into account hydrostatic pressure and sealing compression forces. This force value was given as:

$$F = 4{,}038{,}825 \text{ lb}$$

The minimum cross sectional area for the housing is given by the following equation:

$$A = F/S$$

where:

A = minimum cross sectional area, in^2

S = maximum allowable working stress, ksi

The maximum allowable working stress is given by Table 5 for SA-36 carbon

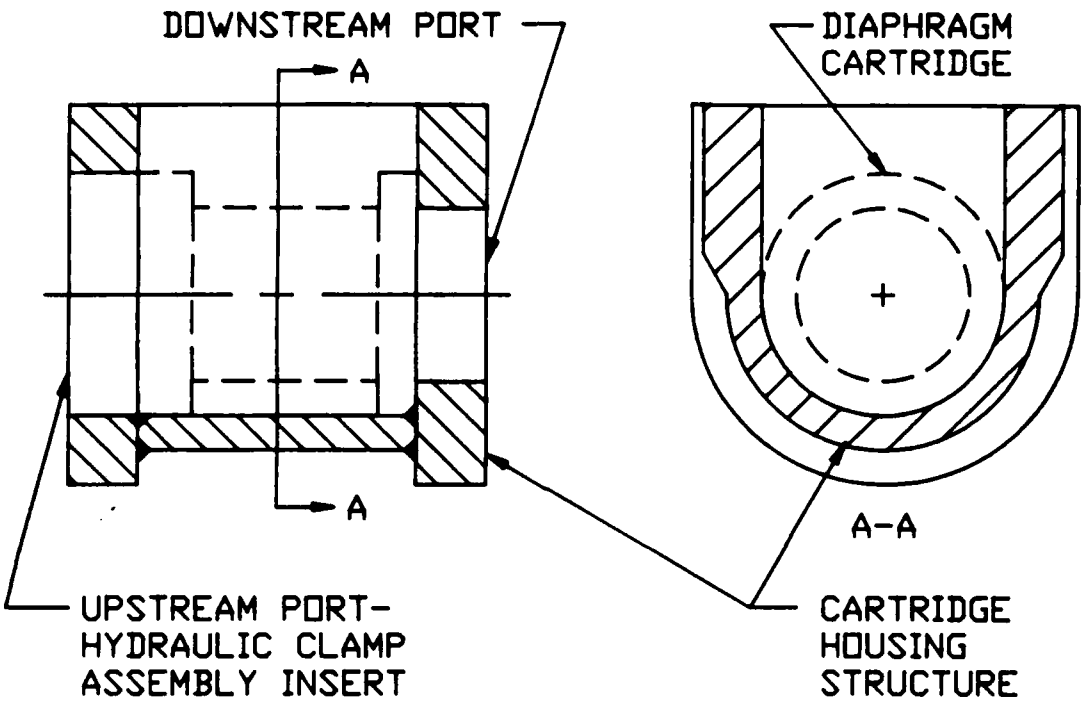

Figure 16. Cartridge housing structure.

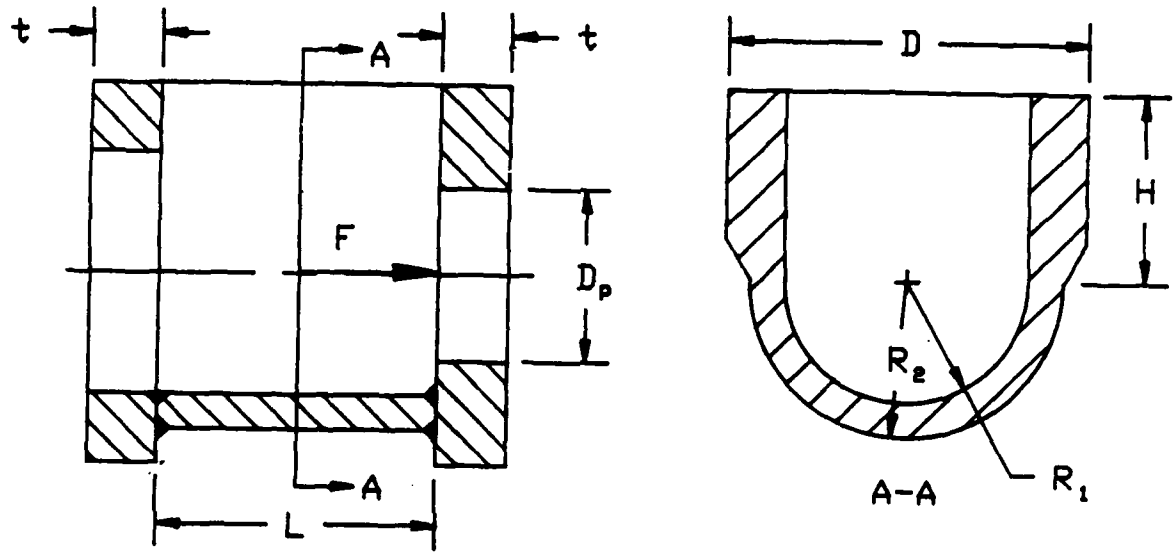

F, resultant force applied to the housing structure

Figure 17. Cartridge housing structure design.

steel as 12.7 ksi. The resulting minimum area is 318 in^2. For an internal radius, R_1, of 27 inches, the required thickness for a complete cylinder is approximately 3 inches. For the cross-section shown in Figure 17, the lower part cylindrical section is assumed to have a thickness of 3 inches and the upper rectangular section is designed so that the resultant moment is balanced. The moment is balanced if the centroid of the section falls exactly on the center of the force, F. The resulting dimensions for the section are calculated by equating the moments of inertia of the upper section about the force line with the moment of inertia of the lower cylindrical section about the force centerline. The following dimensions represent the balanced system:

R1 = 27 in
R2 = 30 in
H = 36 in
D = 64 in

These values indicate an upper rectangular section that is much heavier than the lower cylindrical one. Consequently, the actual tensile stress and deflection are greatly decreased due to the increased material thickness from the force balancing.

3.5 DESIGN AND DRAWINGS.

The preliminary design of the Diaphragm Automatic Loading System (DALS) is shown in Figure 18 and 19. The figures represent preliminary Level I drawings which were created to illustrate the mechanical design of the system. The DALS design is a first order solution to the labor and time intensive diaphragm removal and installation problem perceived in the LB/TS driver operation. The operation of the system is simple and efficient yet offers flexibility in the type of automation. After the cartridge is loaded into its housing, the various gas supply/cooling hoses and electrical sensor-/initiator lines are connected to the cartridge. The cartridge is then pressure sealed by means of a hydraulic pressure supply system. The driver system is now ready for operation. For the dual diaphragms, the gas between the two diaphragms is regulated at the proper operating pressure and tempera-

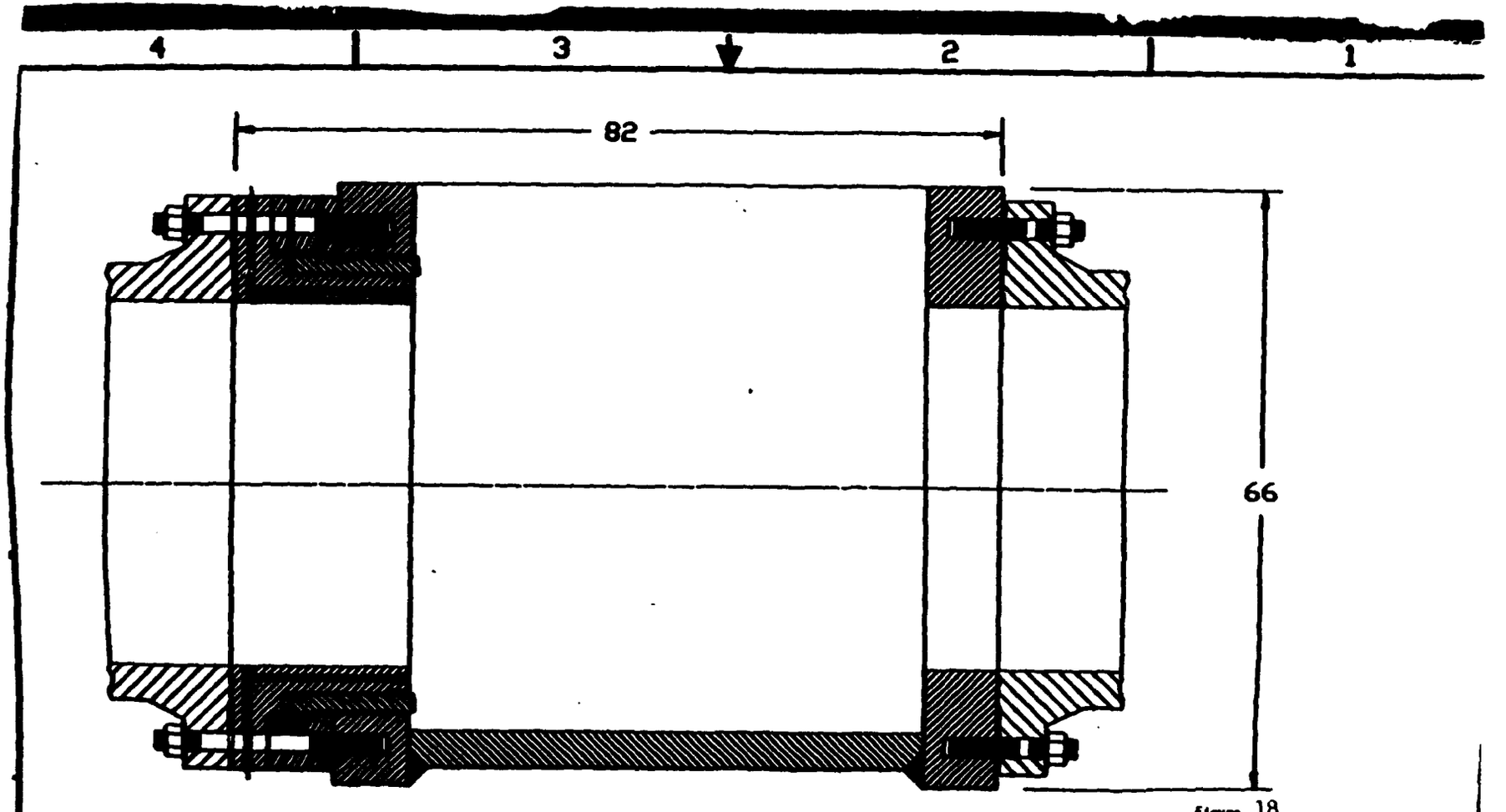

Figure 18

UNLESS OTHERWISE SPECIFIED:
ALL DIMENSIONS ARE IN INCHES

CONTRACT NO.	DNA001-85-C-0315
DRAWN	G.MASON
CHECKED	
ENGR APPROV	
MFG APPROV	
APPROVED	DNA
	SCIENCE APPLICATIONS INT'L CORPORATION
TITLE	DIAPHRAGM LOADING SYSTEM CARTRIDGE HOUSING ASSEMBLY
SIZE	B
DWG NO.	DLS882-002
SCALE	1/10
WEIGHT	
SHEET	1 OF 1

4 3 2 1

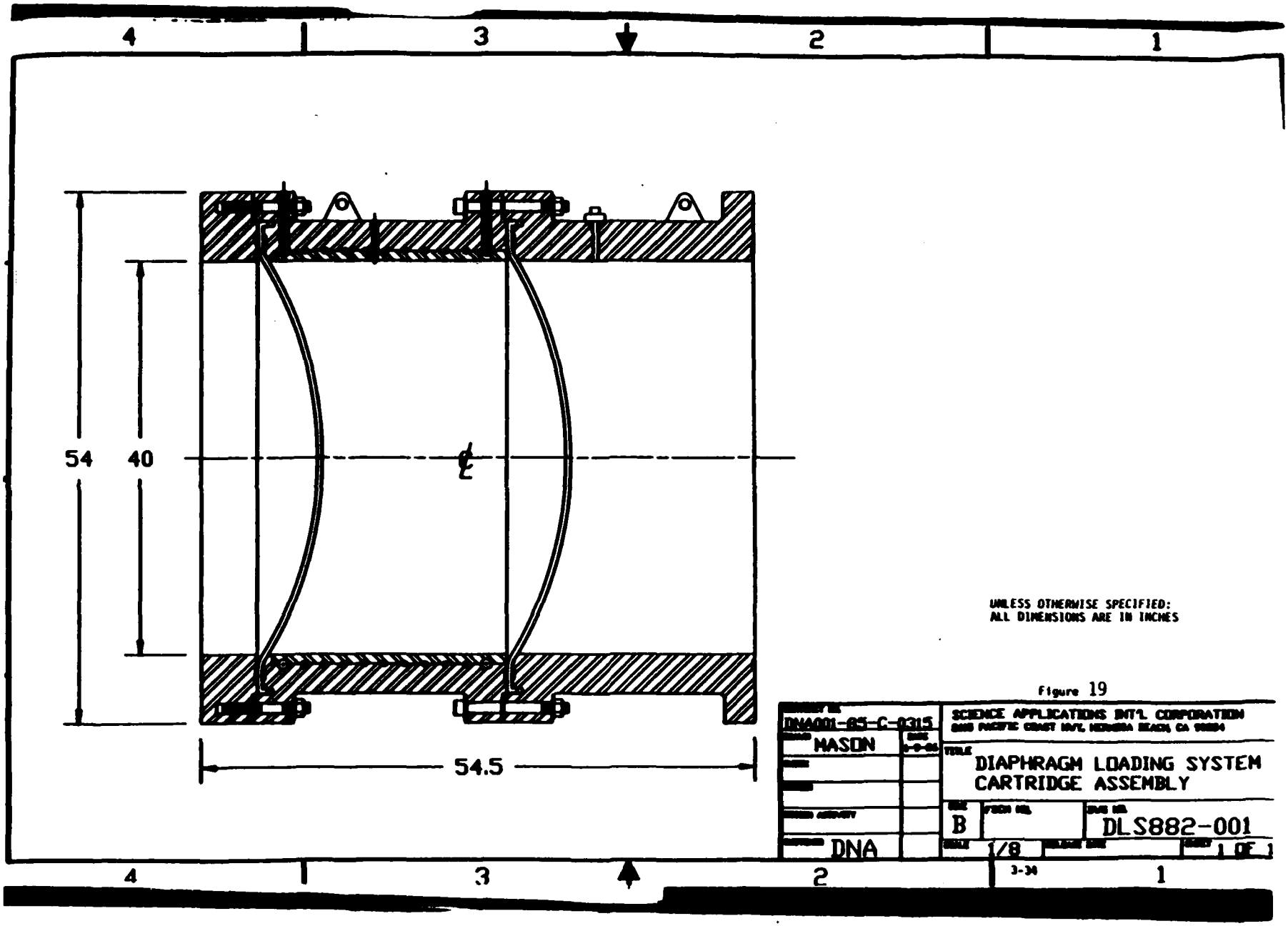
4
3
2
1
54
40
54.5
45
UNLESS OTHERWISE SPECIFIED:
ALL DIMENSIONS ARE IN INCHES
DNA001-85-C-0315
SCIENCE APPLICATIONS INT'L CORPORATION
MASON
DIAPHRAGM LOADING SYSTEM
CARTRIDGE ASSEMBLY
B
DLS882-001
DNA
1/8
3-34
1 OF 1

Figure 19

ture by means of a control system. After the diaphragms are ruptured and the subsequent shock blowdown occurs, the cartridge can be easily removed by hydraulically moving the clamp back. The cartridge assembly can then be easily lifted out and replaced with another cartridge that was previously assembled at an on site shop. The used cartridge can then be taken to the shop where it is disassembled, inspected and reassembled with new diaphragms and made ready for use again. A schematic of a typical hydraulic clamping, pressurizing, cooling, sensing (temperature and pressure) and diaphragm initiating control system is shown in Figure 20. This type of control system offers the great reliability for diaphragm system operation.

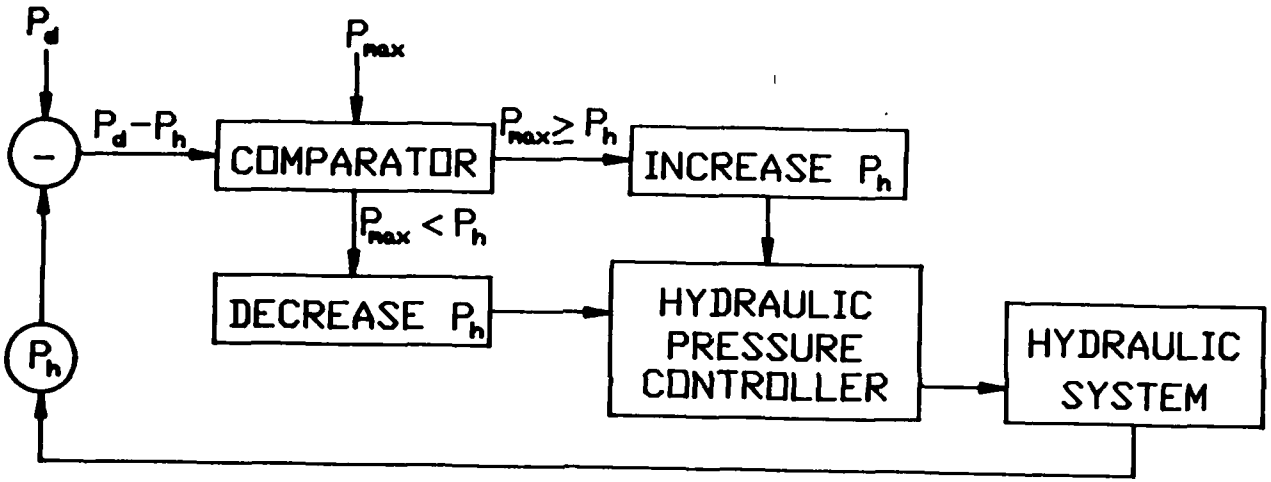

HYDRAULIC SEAL CLAMP CONTROL SYSTEM SCHEMATIC

P_d = DRIVER PRESSURE

P_h = HYDRAULIC PRESSURE

P_{SET} = SET MAXIMUM PRESSURE DIFFERENTIAL

Figure 20. Typical diaphragm control sytem.

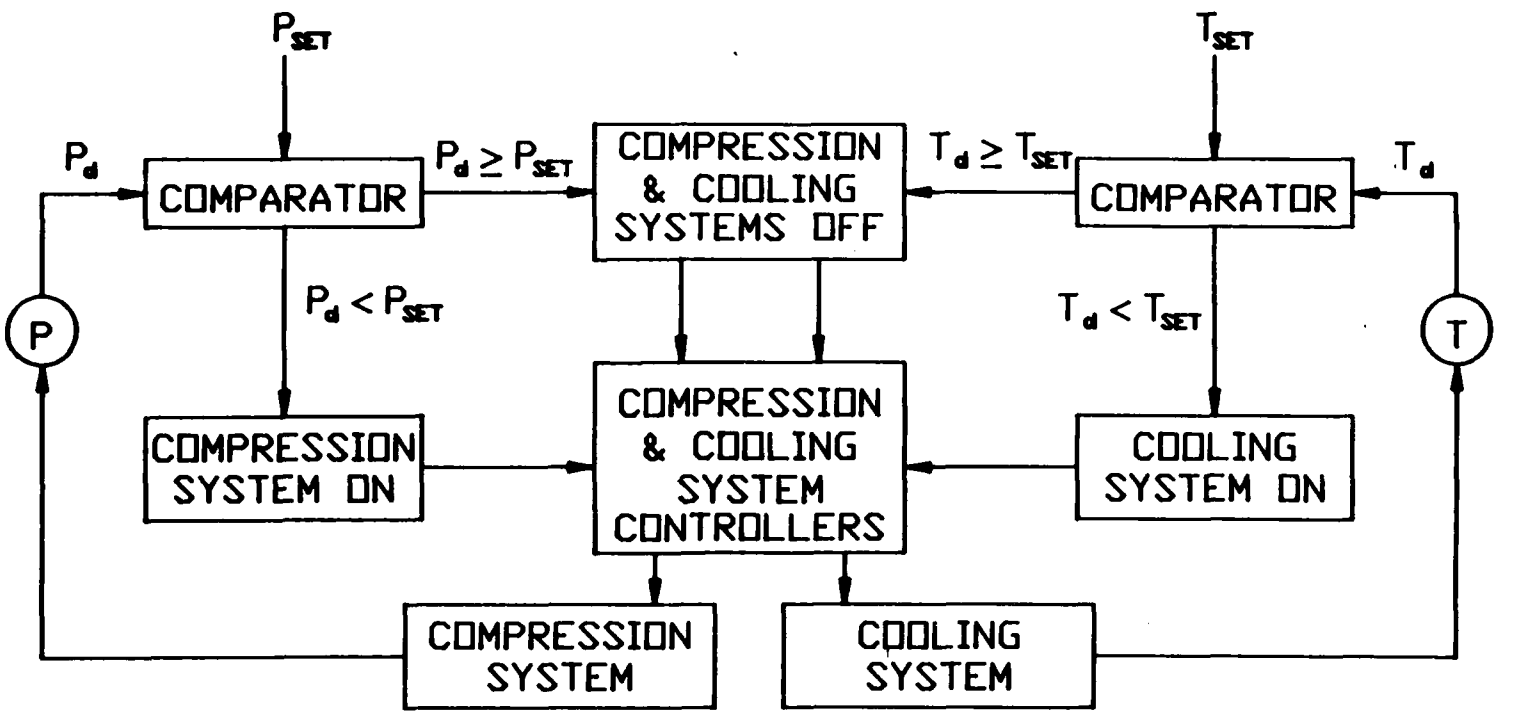

P_d, T_d = DIPAHRAGM SECTION GAS PRESSURE AND TEMPERATURE

P_{SET}, T_{SET} = DIAPHRAGM SECTION SET PRESSURE AND TEMPERATURE

DIAPHRAGM GAS PRESSURE & TEMPERATURE CONTROL SYSTEM SCHEMATIC

Figure 20. Typical diaphragm control system. (Continued)

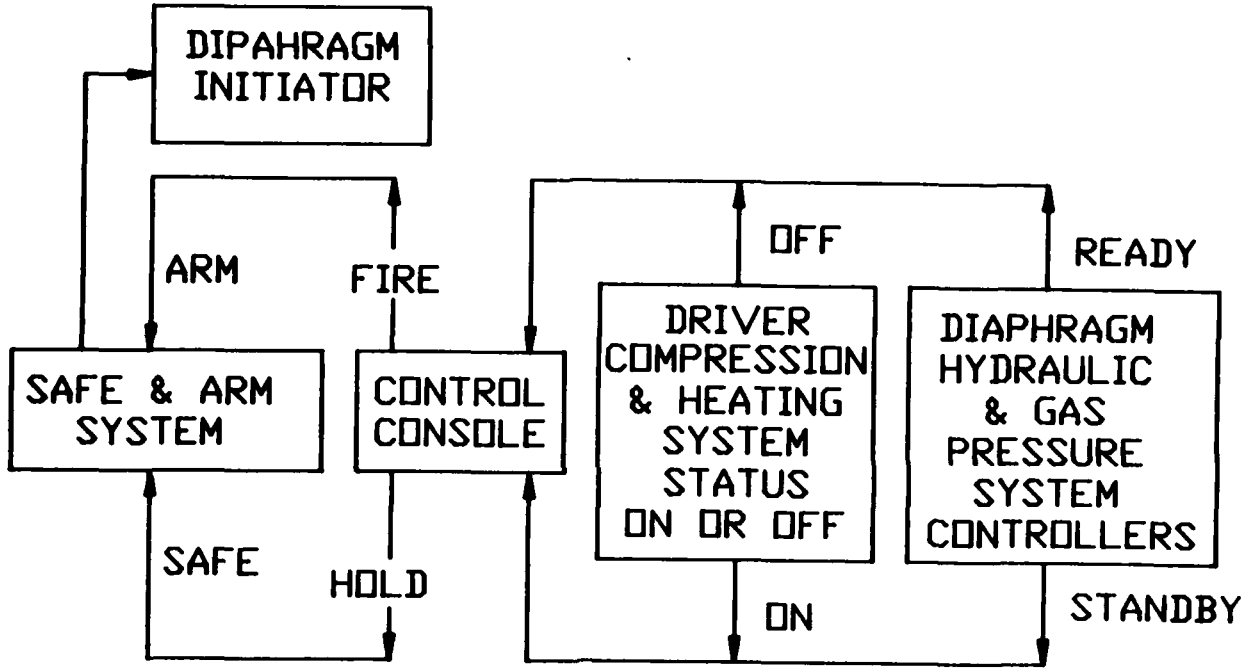

Figure 20. Typical diaphragm control system. (Concluded)

SECTION 4
HEAT TRANSFER ANALYSES

The design of the cartridge loading diaphragm system is shown on Figures 13, 14 and 15. Figure 15 is an enlarged view of the upstream annular hydraulic piston that is used to seal the cartridge assembly. A heat transfer analysis was conducted to obtain preliminary design data for the system. Cooling passages were shown in the design of the sealing piston and diaphragm cartridge. At this time, it is not certain that cooling will be required on the full-sized LB/TS system but provisions have been included for cooling. Water would be the coolant fluid.

Qualified insulation for the upstream passage between the diaphragm and driver does not exist at this time; therefore, firebrick type insulation values were used in the calculations. Similarly, no suitable insulation appears to be available for the diaphragms. Therefore, uninsulated diaphragms were calculated for this study.

To obtain estimates of the length and time scales involved in heat conduction into the steel parts of the cartridge diaphragm assembly, we consider first the simple problem of heat conduction into a semi-infinite solid slab of metal. Specifically, assume that the surface of the metal slab is quickly raised to and kept at temperature T_w and the initial solid metal slab temperature is T_o. The temperature profile in the solid is

$$T(x) - T_o = (T_w - T_o) \text{ erfc } \frac{x}{2\sqrt{\alpha t}}$$

where erfc is the complimentary error function, x is length, t is time, and α is the thermal diffusivity of the metal ($\alpha = 1.3 \times 10^{-5}$ m^2/sec for mild steel). Setting

$$\frac{T(x)-T_o}{T_w - T_o} = 0.1$$

one may conservatively estimate the "depth of heat penetration" into the metal (the temperature profile drops off rapidly with depth) as

$$\frac{x}{2\sqrt{\alpha t}} = 1.16$$

or

$$x = 2.3\ \alpha t$$

For present design considerations, t - 7200 sec (2 hours), yielding a heat penetration depth x of 0.7 meters (27.6 inches).

From this simplified exercise, it can be seen that the heat will easily conduct through an uninsulated 0.05-m (2 inches) steel wall but will not conduct significantly along the wall. This means that heat will reach areas of concern (such as the hydraulic seals) and will be lost to the atmosphere by conduction through the shock tube walls but will not reach the downstream diaphragm (one meter from the upstream diaphragm) in the times of interest (care needs to be taken for critical parts near the upstream diaphragm).

4.1 HEAT TRANSFER METHODOLOGY.

Two problems need to be addressed in more detail:

- o Heat conduction into the wall in the vicinity of the hydraulic sealing unit
- o Heat transfer across the double diaphragm cartridge to the downstream face where the explosives are located

These heat transfer problems are ideally handles by lumped parameter models governed by diffusion equations. For this work, the Systems Improved Numerical Differencing Analyzer (SINDA) code is used [Ref. 5]. SINDA is a typical thermal analyzer approach that accepts resistor-capacitor (R-C) network representations. The SINDA code uses an explicit forward differencing method to solve the transient thermal analysis equations.

In the following calculations, the properties of the steel are taken to be [Ref. 6]:

ρ = 7800 Kgm/m^3

C_p = 450 Joules/Kgm-°K

K = 50 Joules/m-°K-sec

α = 1.5 x 10^{-5} m^2/sec

Where an insulation is used (somewhat arbitrary) properties representative of fire brick were selected:

ρ = 5000 Kgm/m^3
C_p = 540 Joules/Kgm-°K
K = 1.5 Joules/m-°K-sec
α = 5 x 10^{-7} m^2/sec

Film coefficients were calculated from empirical convection heat transfer equations found in Edwards, Denny and Mills [Ref. 6].

h_{driver} = 70 Joules/m^2-°K-sec
$h_{cartridge}$ = 40 Joules/m^2-°K-sec
$h_{exterior}$ = 30 Joules/m^2-°K-sec

In the present calculations, the driver pressure was assumed to be at 85 atmospheres and the diaphragm cartridge was assumed to be at 43 atmospheres for the selection of film coefficients. A more complete analysis would specify the film coefficients as a function of the changing pressure and temperature, but the present calculations should be conservative. Radiation was examined briefly and was found to slightly lower the downstream diaphragm temperature, primarily due to heat loss to the walls.

4.2 HEAT TRANSFER CALCULATIONS.

The shock tube/diaphragm cartridge geometry assumed for the present calculations is a one-meter interior diameter (except when an insulation layer 0.03-m thick is added to the interior) tube with 0.05-m thick walls in the cartridge and 0.12-m thick walls in the hydraulic seal region. The diaphragms are one meter apart.

4.2.1 Wall Temperature.

With no active cooling or insulation, SINDA code calculations (Figure 21) indicate that the temperature at the seal will exceed the design criteria

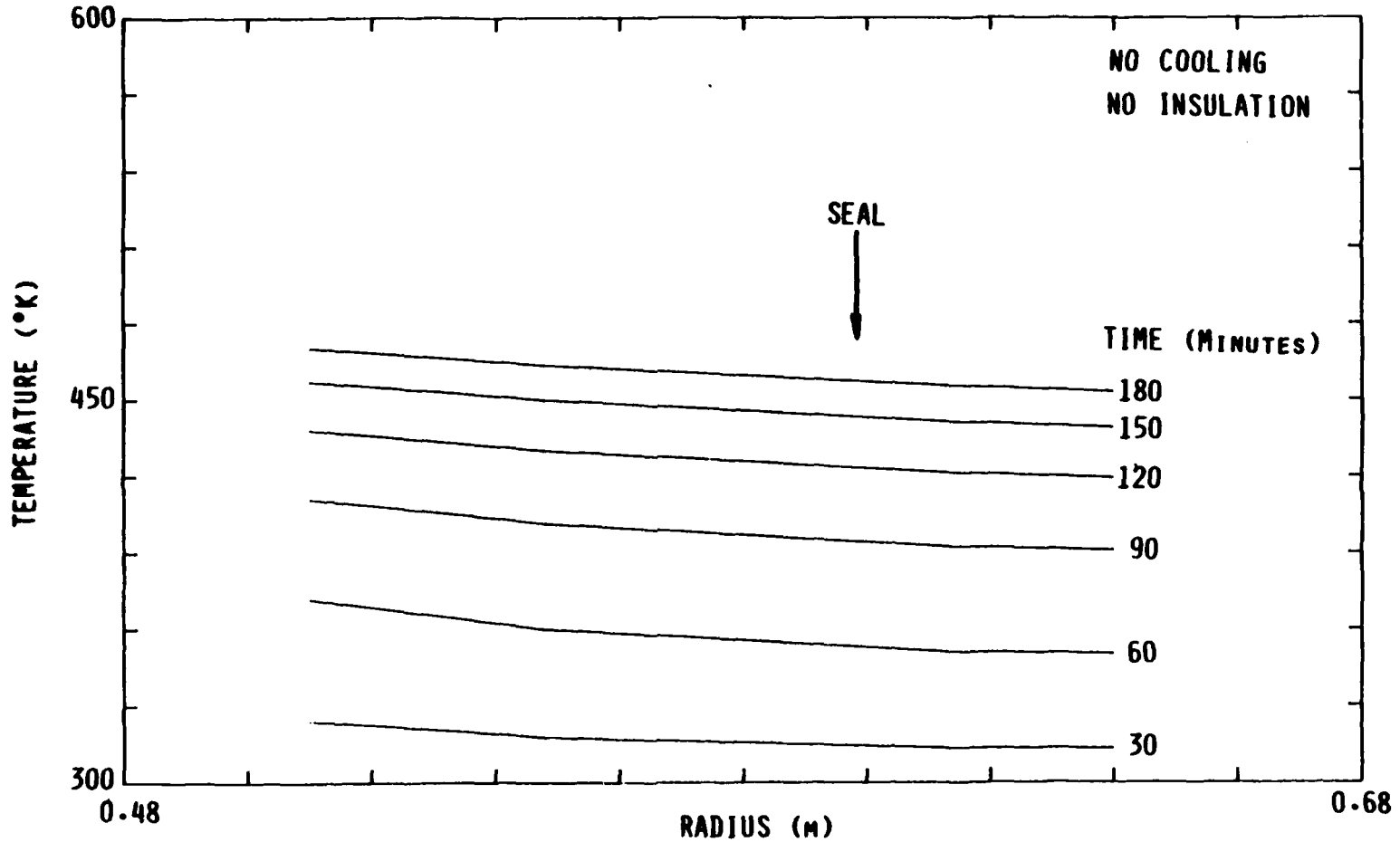

Figure 21. Wall temperature profiles.

of 400°K at about two hours after start of heating. This can be fixed by either cooling the wall (an example calculation for 5 x 10^5 J/m^2-sec is given in Figure 22) or by insulating the interior of the driver (Figure 23).

4.2.2 Diaphragm Temperature.

If the walls in the diaphragm cartridge are insulated, the temperature of the downstream diaphragm exceeds the design criteria about two hours from start of heating (Figure 24). With no insulation, there is sufficient loss of heat to the walls/atmosphere to keep the temperature of the downstream diaphragm below the design criteria (Figure 25). An active wall cooling calculation demonstrated that the downstream diaphragm could be kept at near ambient temperature, if desired.

4.3 INTERPRETATION OF THE CALCULATIONS.

From a modeling point of view, there does not appear to be any difficulty in achieving the design temperature goals either by active cooling or insulation. It must be noted that the accuracy of the present calculation is unknown because of the uncertainty in the validity of the film coefficients. As designs progress, a more detailed selection of heat transfer parameters should be done, and the predictions should be validated by a full-scale test of the diaphragm cartridge region (i.e., with a shortened driver). This could be accomplished as part of the prototype development tests at the U.S. Army Ballistic Research Laboratory, Aberdeen Proving Ground, Maryland.

The results show that the aft diaphragm can be kept cool enough to safely attach explosive cutting charges to its face. It also appears that cooling the center section walls will lower the diaphragm section air temperature so that an explosive charge can be mounted between the diaphragm, if desired.

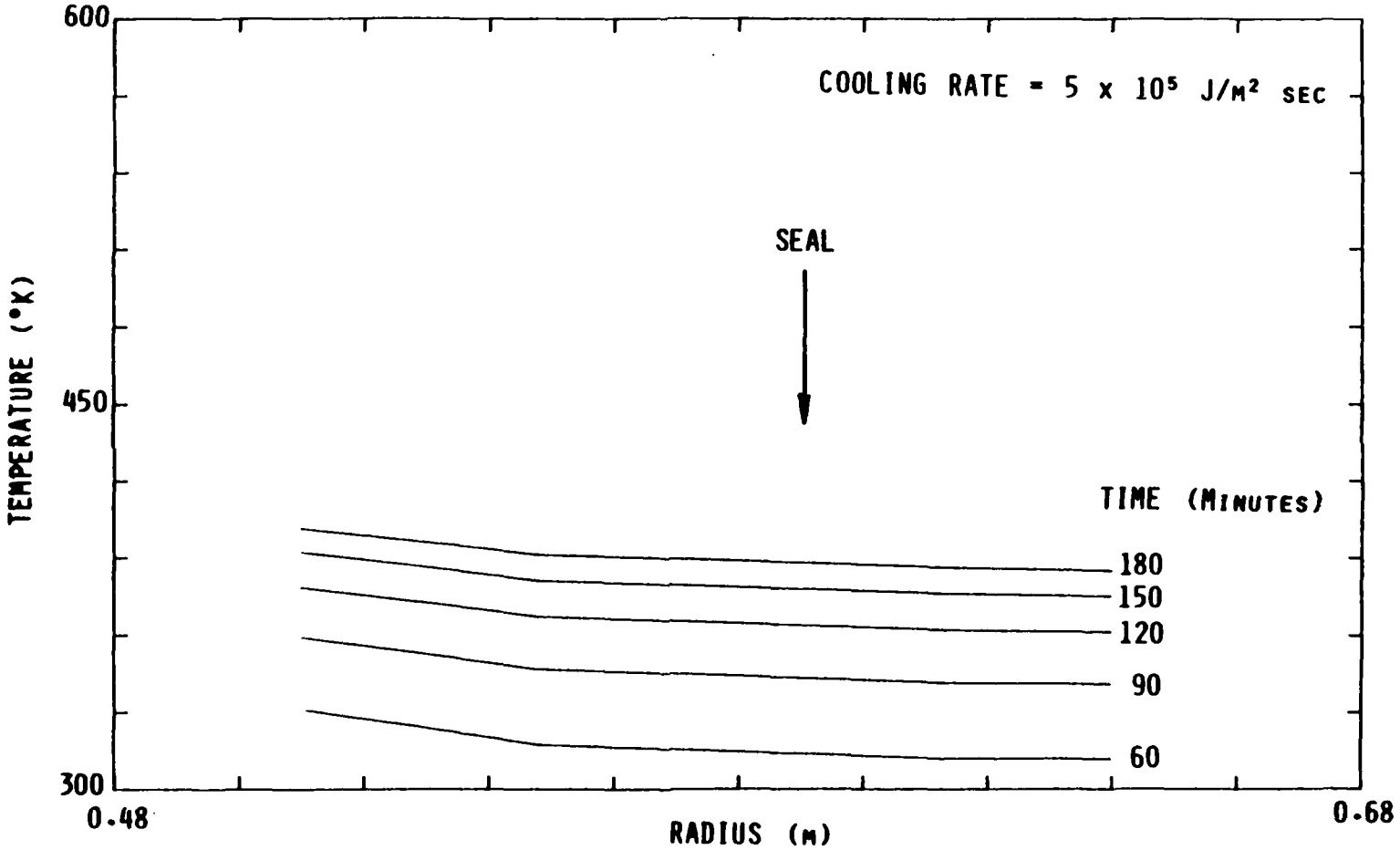

Figure 22. Wall temperature profiles with cooling.

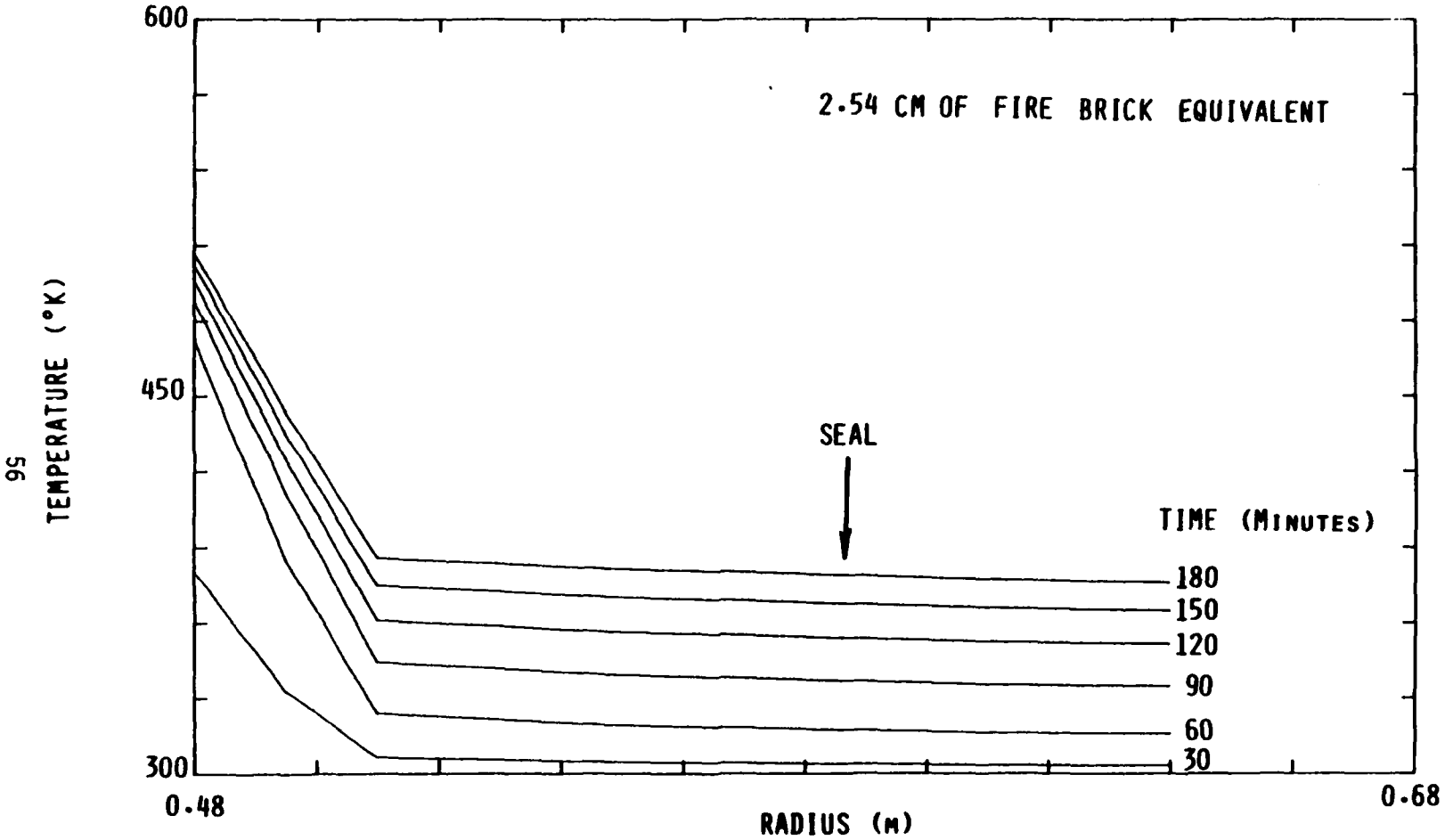

Figure 23. Wall temperature profiles with insulation.

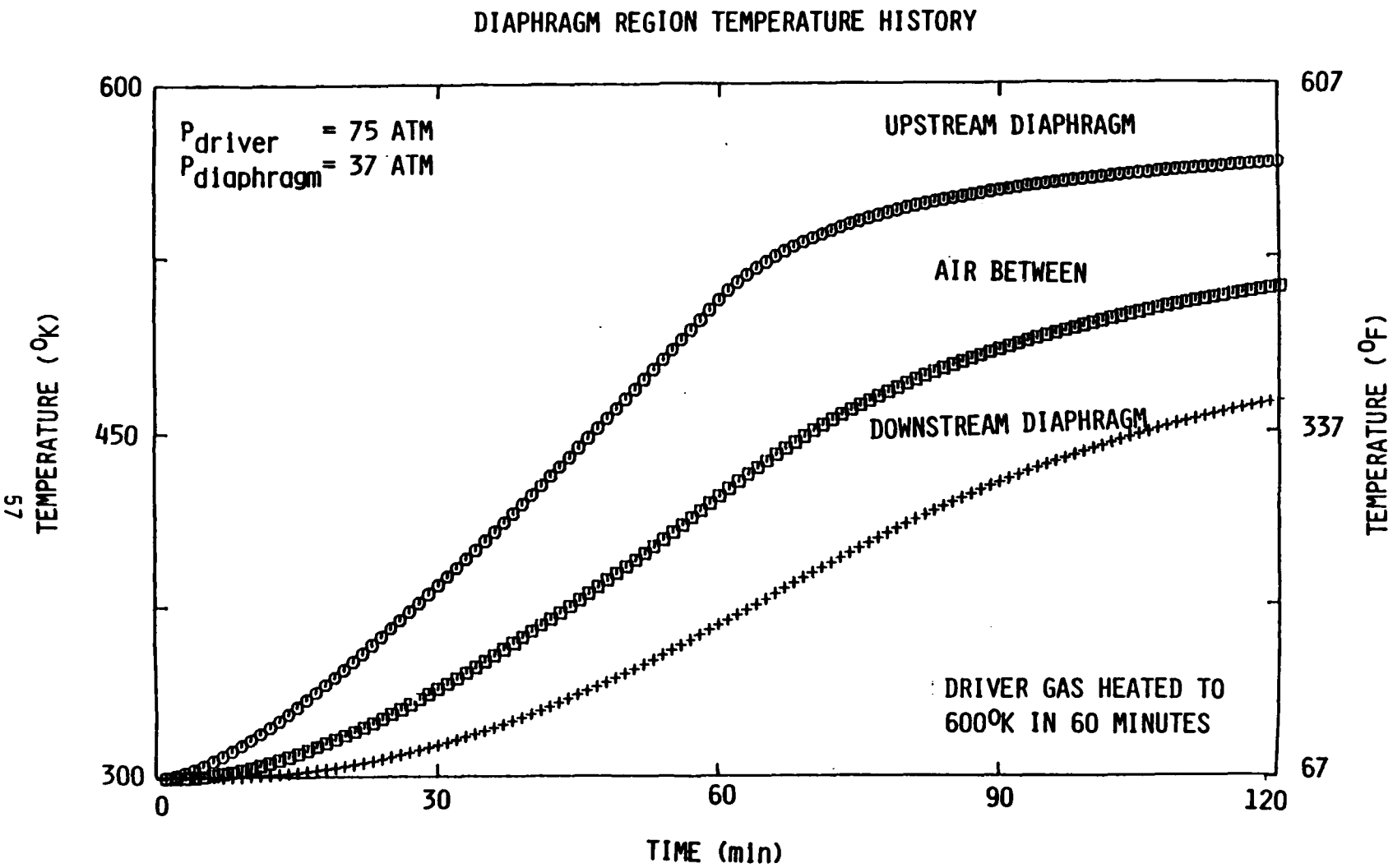

Figure 24. Diaphragm region temperature history - insulated walls.

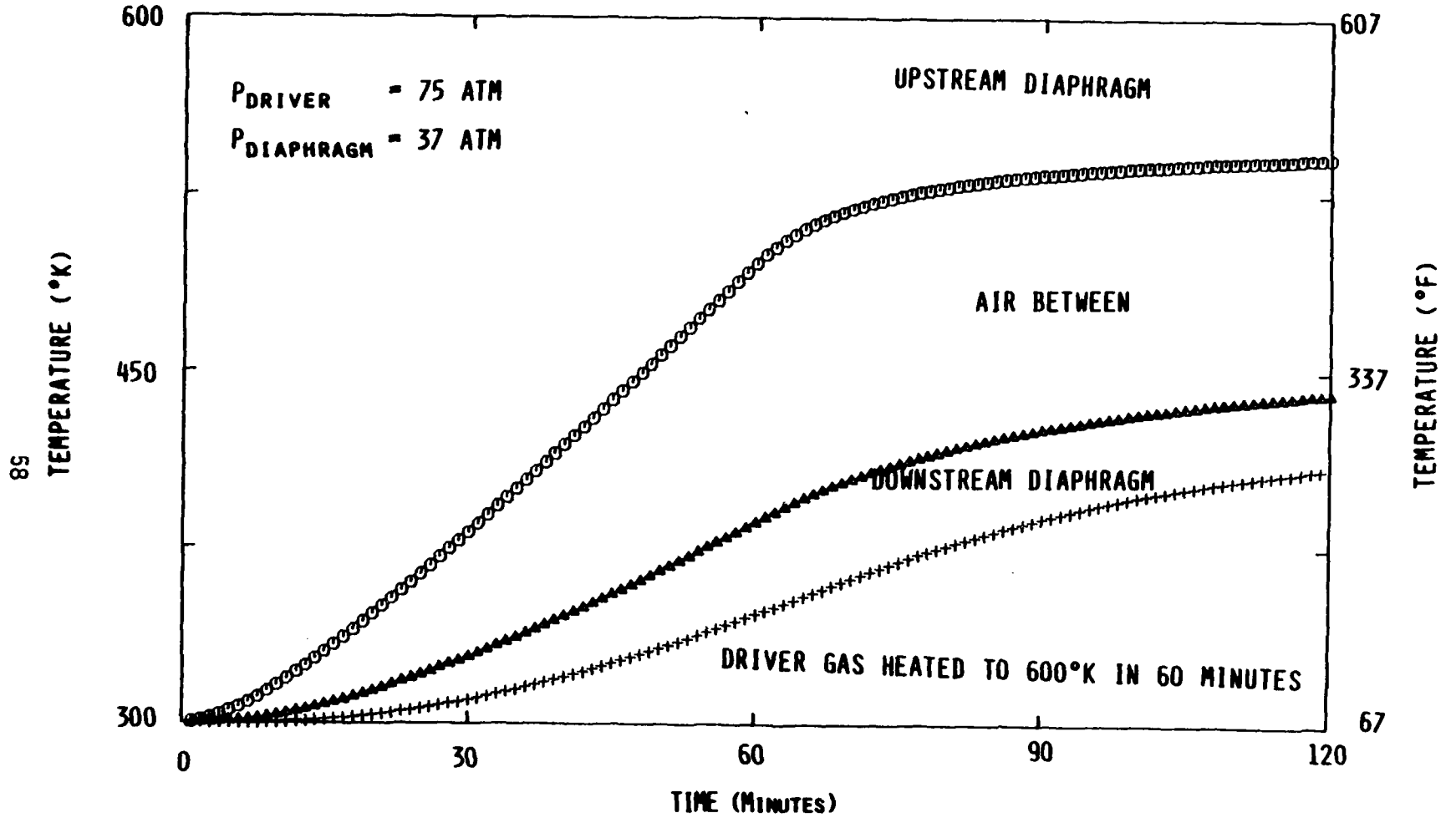

Figure 25. Diaphagm region temperature history - no wall insulation.

4.4 SYSTEM COOLING CONCEPT.

Figure 26 schematically illustrates three of the cooling concepts that were considered in the design of the heat gas diaphragm system. Figure 26a shows a driver gas compression system pumping gas through a heater that raises the system temperature to T_1. The sealing piston and cylinder temperatures must be maintained at relatively low values (on the order of 250°F) so that seals do not fail and radial clearances do not approach upper and lower limits because of thermal expansion. This is accomplished by circulating water through passages in the wall and rejecting the heat with radiators or other means. Insulation on the inner wall would reduce or eliminate the need for cooling.

The central compartment is similarly cooled by circulating water in passages in the wall.

Heated gas from the driver at temperature T_1 and pressure P_1 is cooled in a heat exchanger and passed through a pressure regulator to the central compartment at pressure P_2, which is always maintained at $P_2 = P_1/2$. Some heat is rejected across the downstream diaphragm to ambient air at P_3, T_3.

Figure 26b shows an alternate cooling system that is similar to that illustrated in Figure 26a except that unheated gas from the compression system is directly brought to a pressure regulator into the central compartment before the gas is heated. This eliminates the separate cooler.

Figure 26c shows a system that cools the central compartment by continually bleeding fresh compressed unheated high pressure gas into the compartment to replace gas heated by convection from the upstream diaphragm. Therefore, if the exchange rate, $\dot{m}_2$, is properly set, the central compartment temperature, T_2, can be maintained at the desired level. Thus, in this scheme, no gas or wall cooling of the central compartment is required.

CUTTING CHARGES ON DOWNSTREAM DIAPHRAGM

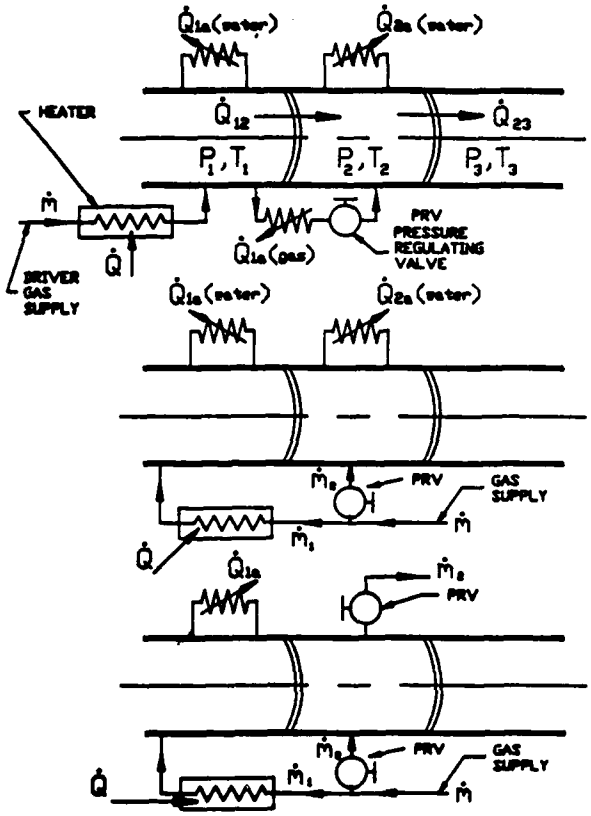

WATER COOLED WALLS
IN SECTIONS 1 AND 2
COOLED AIR @ P_2
SUPPLIED FROM SECTION 1 (a)

WATER COOLED WALLS
IN SECTIONS 1 AND 2
COOL AIR @ P_2
SUPPLIED BY COMPRESSORS (b)

WATER COOLED WALL
IN SECTION 1 ONLY
COOL AIR @ P_2
SUPPLIED BY COMPRESSORS
AND CONTINUOUSLY BLED
OUT OF SECTION 2 (c)

Figure 26. Heated dual diaphragm schematic.

SECTION 5
DIAPHRAGM DESIGN CONCEPTS

5.1 DIAPHRAGM OPENING MECHANISMS.

5.1.1 Explosive Methods.

If the diaphragm that is schematically illustrated in Figure 1 is subjected to pressure on its concave side, the shape of the diaphragm can be configured so as to put the diaphragm in tension out to the very edge. This will be discussed in detail in Section 5.2

The spherical segment of the diaphragm is in tension and is normally designed to break into triangular gores upon initiation of an opening sequence. In many designs, the downstream surface of the diaphragm is scored with sharp vee grooves as illustrated in Figure 27 where an eight-petal design in shown. In some designs, the vee grooves have a length of explosive cord such as "primacord" cemented or attached over each groove. In other cases, where pressure is relatively low, the explosive cord is fastened to an ungrooved diaphragm. Initiators, usually in the form of an exploding bridge-wire detonator, are usually installed at the apex of the explosive cord pattern so that all cuts (OA, OB, OC, OD, OE, OH) are made simultaneously. The explosive detonation wave travels at approximately 7,000 meters/second; therefore, all cuts in a 40-inch diameter (1 meter) diaphragm are made within 0.09 milliseconds. All diaphragms on a 15-driver LB/TS can be opened explosively in simultaneous fashion.

As pressures increase, thicker diaphragms are required. The equation for thickness is given below in simple fashion.

$$t = \frac{(P_u - P_d)r(f)}{2S_{ty}}$$

where

t = thickness of diaphragm, inches
P_u = upstream pressure, psig
P_d = downstream pressure, psig

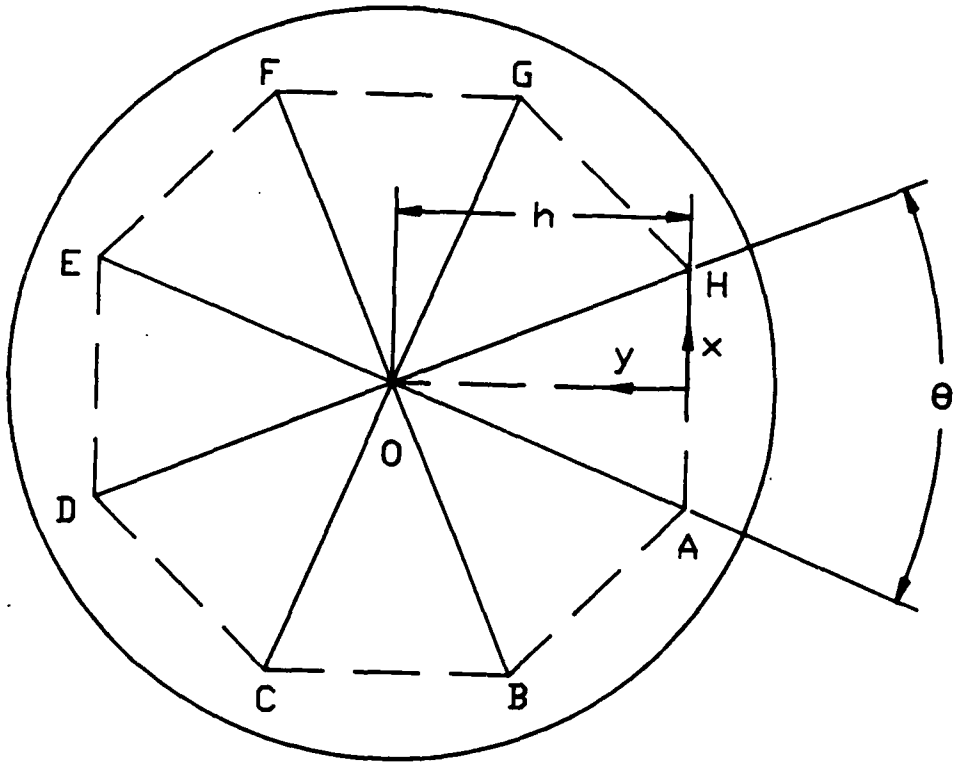

Figure 27. Diaphragm opening pattern.

r = spherical radius, inches

S_{ty} = minimum tensile yield stress, psi

f = factor of safety

For the case of interest:

P_u	= 2,200 psi	
P_d	= 0	single diaphragm
r	= 40 inches	
S_{ty}	= 35,000 psi	low carbon steel
S_{ty}	= 150,000 psi	alloy steel
f	= 1.5	

This shows that for a single diaphragm, the low carbon steel diaphragm would be 1.9 inches thick, whereas the heat treated alloy steel diaphragm (AISI 4130) would be 0.44 inches thick. A normalized alloy steel diaphragm would be 0.9 inches thick. The dual diaphragm would be approximately half as thick. Therefore, because we are interested in cutting the diaphragms with explosive, SAIC received estimates of explosive performance from two leaders in the field. These were:

1. The Ensign-Bickford Company
   Aerospace Division
   660 Hopmeadow Street
   Simsbury, Connecticut

and

2. Explosive Technology
   Fairfield, California

Both of these companies suggested that the diaphragms be cut with linear-shaped charges at the proper standoff distance. Both also suggested that sharp vee grooves be machined into the downstream side of the diaphragm to facilitate fracture at the desired locations. Both concerns make linear-shaped charges that can withstand temperatures on the order of 300°F. Figure 28 (from Ensign-Bickford) shows a cross-section and data for typical flexible linear-shaped charges (FLSC) of the type that would be used to open the diaphragm. Preliminary estimates from the explosive supplier indicate that loadings of the order of 500 grains/foot would be required.

FLSC CONFIGURATION IV
PART NUMBERS, WEIGHTS, DIMENSIONS

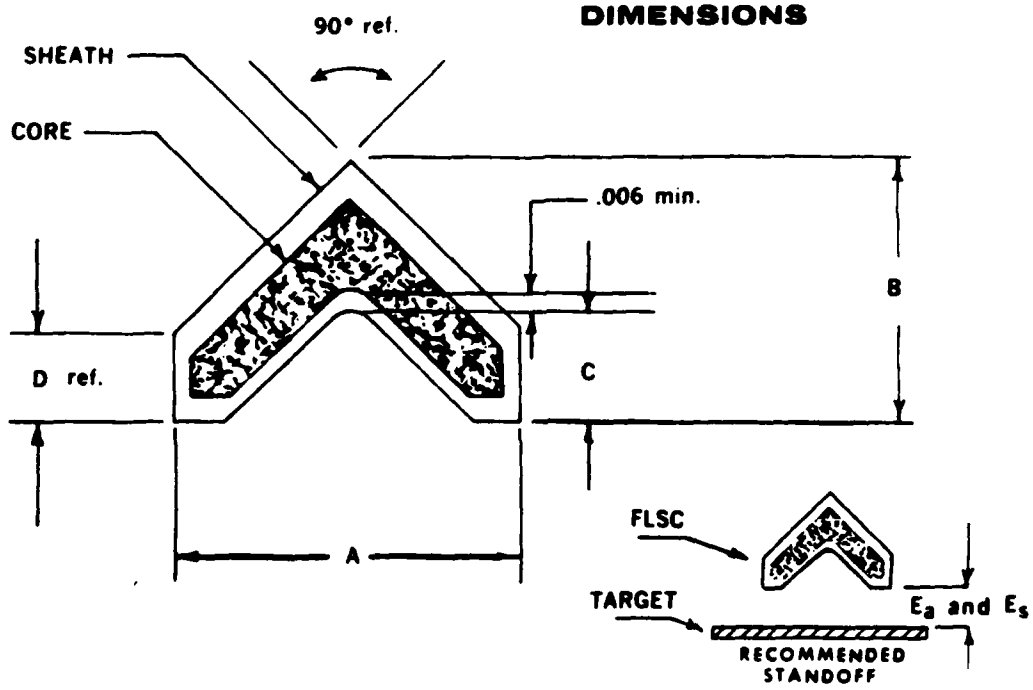

Nominal Core Load (gr/ft)	ENSIGN-BICKFORD Part Number (RDX/LEAD)	Dimensions (in inches) A	B	C	D	E_a(1)	E_s(2)	Gross Weight (lb/ft)
50	206007	.268	.205	.098	.071	.100	.100	0.0436
100	206006	.395	.296	.140	.099	.180	.100	0.1548
200	206009	.556	.422	.203	.144	.230	.230	0.2988

(1) Against 6061-T6-Al
(2) Against 304 Stainless

Figure 28. FLSC characteristics.

Note that standoff is important and the cutting charges must be supported above the surface by foam or light frangible material to obtain the proper standoff distance.

Figure 29 (from Ensign-Bickford) shows a log-log plot for the cutting of 304 stainless steel. The explosive suppliers believe that cutting the heat treated alloy steels or precipitation hardening stainless steel (17-4PH) will be much more difficult and they recommend that tests be performed to obtain data. In the interim, they suggest that a FLSC loading of 500 grains/foot be used in our estimates.

Figure 30 (from Ensign-Bickford) shows the ranges of effective standoff distances for stainless steel. It can be seen that standoff distance increases with charge weight and for 500 grains/foot, the standoff distance would be approximately 0.2 inches.

Cutting performance of the linear-shaped charge is a function of detonation rate and characteristics of the sheath material and is also affected by the hardness, strength, and density of the material being cut.

Penetration and cut of a given material are essentially proportional to the square root of the coreload. Actual data with improved shapes such as the Ensign-Bickford Configuration IV show an exponent value of 0.6; i.e.,

$$\frac{T_1}{T_2} = \left[\frac{W_1}{W_2}\right]^{0.6}$$

where

T_1 and T_2 are total cut of a given material and W_1 and W_2 are coreloads.

Using this equation, we can examine the effects of coreloads when the cutting performance of a given coreload is known. Generally, penetration is equal to about 50% of the total cut with fracture accounting for the balance. This relationship depends on the strength and hardness of the material being cut, which, in turn, relate to environmental conditions, most notably to

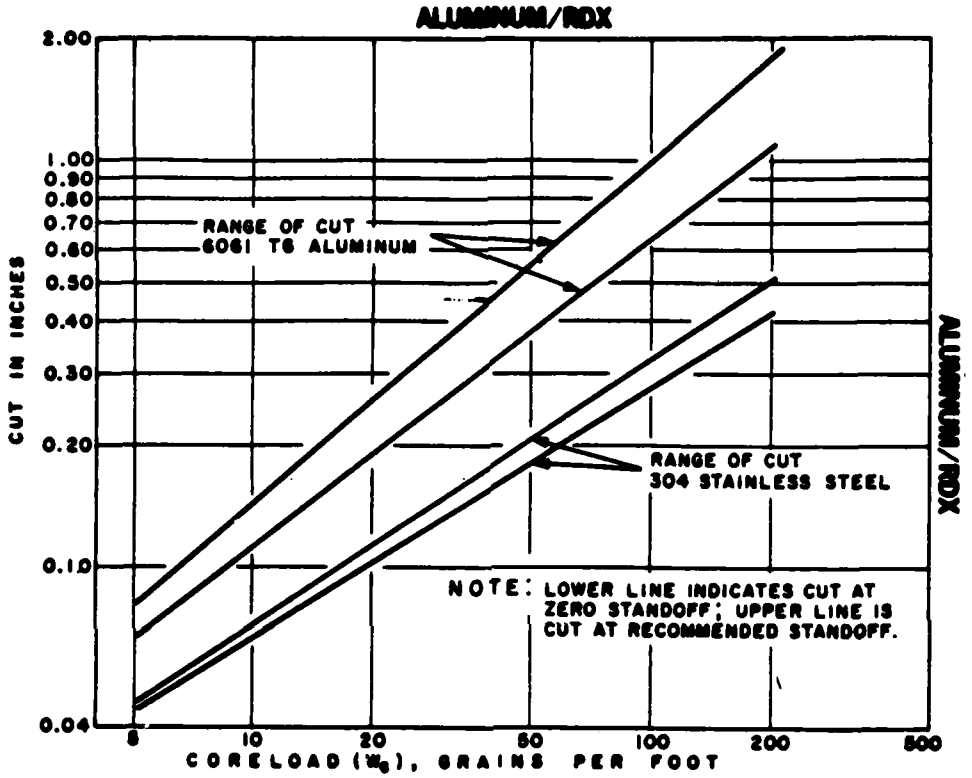

Figure 29. Performance of RDX/Aluminum Configuration IV LSC.

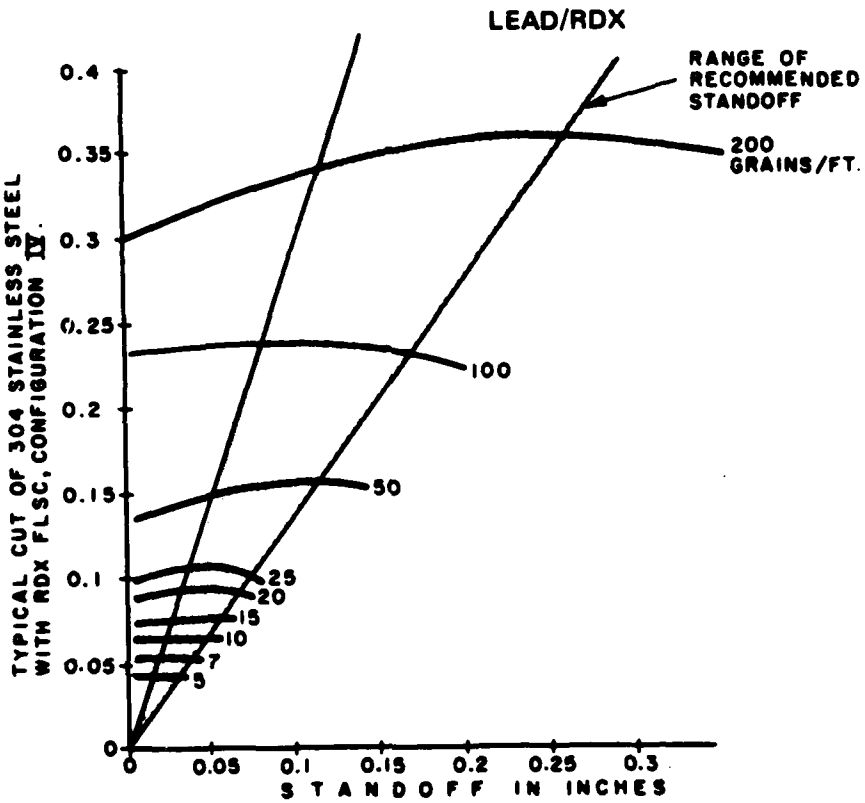

Figure 30. Cutting profiles into stainless.

temperature.

The following explosives are used in Ensign-Bickford linear-shaped charges. Data are from Ensign-Bickford.

RDX, cyclotrimethylenetrinitramine.

Specification	MIL-R-398
Melting point	190°C
Autoignition	405°C
Degradation	350°F after 1/2 hour
	325°F after 1 hour
	300°F after 4 hours
Maximum recommended prolonged storage temperature	+ 250°F
Detonation rate	8200 meters/sec @ 1.65 g/cc

RDX, cyclotetramethylenetetrainitramine, is a homolog of RDX.

Specification	MIL-H-45444
Melting point	273°C
Autoignition	380°C
Degradation	425°F after 1/2 hour
	400°F after 1 hour
	375°F after 4 hours
Maximum recommended prolonged storage temperature	+ 300°F
Detonation rate	9100 meters/sec @ 1.84 g/cc

PETN, pentaerythrtoltetranitrate, is somewhat more sensitive and slightly less powerful than RDX and is used primarily in Primacord and detonators.

Specification	MIL-P-387
Melting point	141°C
Autoignition	272°C
Degradation	250°F after 1/2 hour
	225°F after 1 hour
	200°F after 4 hours
Maximum recommended prolonged	

storage temperature	+ 150°F
Detonation rate	8300 meters/sec @ 1.7 g/cc

The explosive cutting charge should be sized so that it cuts enough metal to allow the system pressure to rupture the diaphragm along the cuts. For example, if the FLSC cuts half way through the diaphragm, and the factor of safety is less than 2, the pressure behind the diaphragm will rupture the diaphragm. It is necessary that after the cut, the following equation be fulfilled.

$$S = \frac{P_r}{2t} \geq S_{tu}$$

where

- S = actual tensile stress, psi
- P = diaphragm differential pressure, psi
- r = diaphragm spherical radius, inches
- t = thickness of diaphragm remaining uncut, inches
- S_{tu} = ultimate strength of diaphragm material

If the FLSC cuts clear through the diaphragm, it is too large a charge for the job.

An alternate method of explosively opening the diaphragm is illustrated in Figure 31. The dual diaphragms are prescored with sharp vee grooves. The upstream diaphragm is pressurized at driver pressure, P_0, and is exposed to heated gas at pressure T_0. The compartment between the two diaphragms is pressurized to half the driver pressure. $P_2 = P_0/2$ and the compartment is cooled to keep the temperature low enough so that a small explosive charge can be suspended between the two diaphragms. Upon command, this charge detonates and the overpressure fractures the downstream diaphragm and vents the central compartment whereupon the system pressure, P_0, fractures the upstream diaphragm.

Unfortunately, there may be problems with this simple system. Because the pressure wave from the explosion reflects from the upstream diaphragm with amplification that could reach considerable levels, it is possible that the

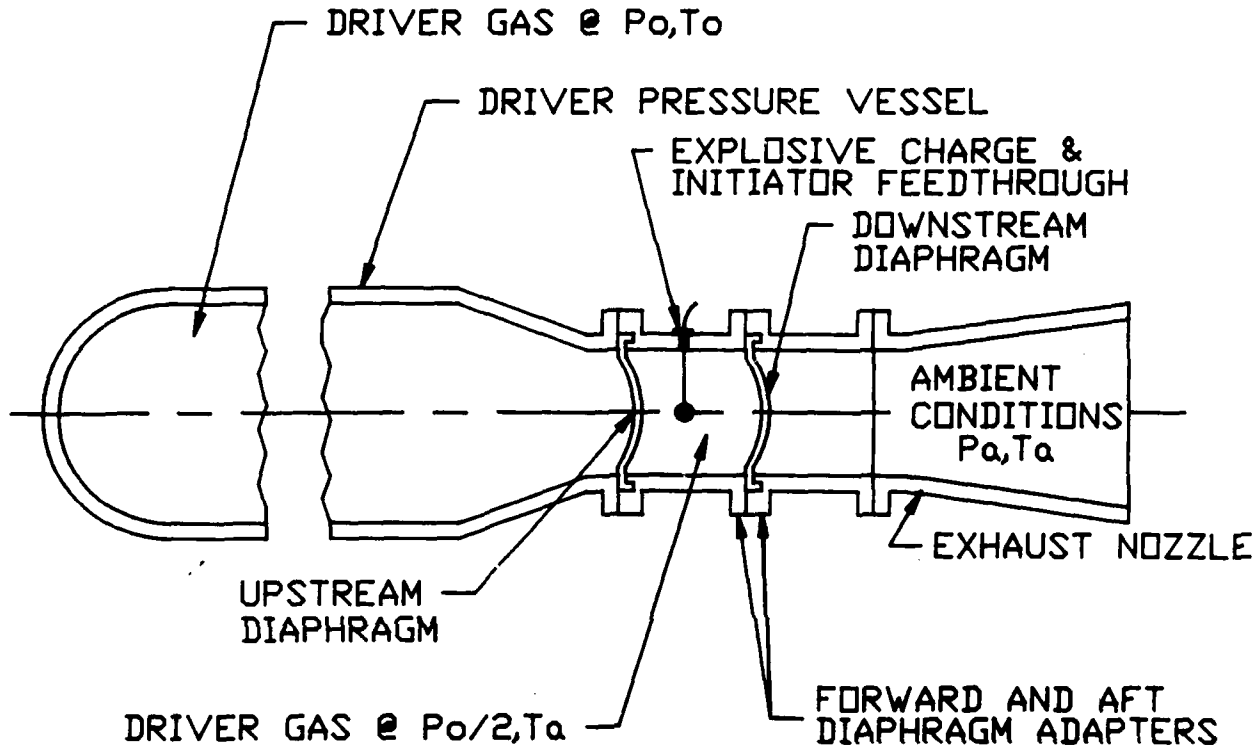

Figure 31. Explosive charge overpressure diaphragm opener.

upstream diaphragm could bend backwards (upstream) before opening and reverse its bending downstream as the pressure is vented by the downstream diaphragm, thereby causing the gores to separate at the roots due to the physical elongation in the reverse bending cycle. Perhaps this could be alleviated by facing the spherical radius upstream but then the thickness required would increase. Also, the explosive pressure loading does increase the thickness of the diaphragm compartment walls. This effect is also present on the walls around the diaphragm with the linear-shaped cutting charges but not to this degree because the FLSC are in ambient pressure rather than at half the system pressure.

5.1.2 Pressure Rupture Methods.

If there are two diaphragms in series as illustrated in Figures 8 and 32, the system pressure, P_1, is applied to the upstream diaphragm and half the system pressure, P_2, is applied to the space between the two diaphragms. Figure 32a shows that an explosive cutting charge on the downstream diaphragm 2 ruptures it, whereupon the pressure in compartment B between the diaphragm is vented to the exhaust nozzle, C. Now diaphragm 1 has the system pressure, P_1, acting on the upstream side and ambient pressure, P_a, acting on the other side. Because diaphragms 1 and 2 are designed only to withstand half the system pressure, diaphragm 1 breaks and releases the system pressure to the nozzle.

If diaphragm 1 was unscored, it would break in a random fashion and parts of it may obstruct the flow. In order for it to break cleanly, in a predetermined pattern of triangular gores, the diaphragm has a pattern of sharp vee grooves machined into the rear face to act as stress risers.

If no explosive is used, breakage of the diaphragms can be initiated as illustrated in Figures 32b and 32c. In Figure 32b, when the command to open the diaphragms is actuated, a valve, V, is opened between the diaphragms to vent compartment B to the atmosphere. When the pressure in B drops low enough, the upstream diaphragm, 1, fractures and opens. This suddenly increases the pressure in B to full system pressure, P_1, which ruptures the

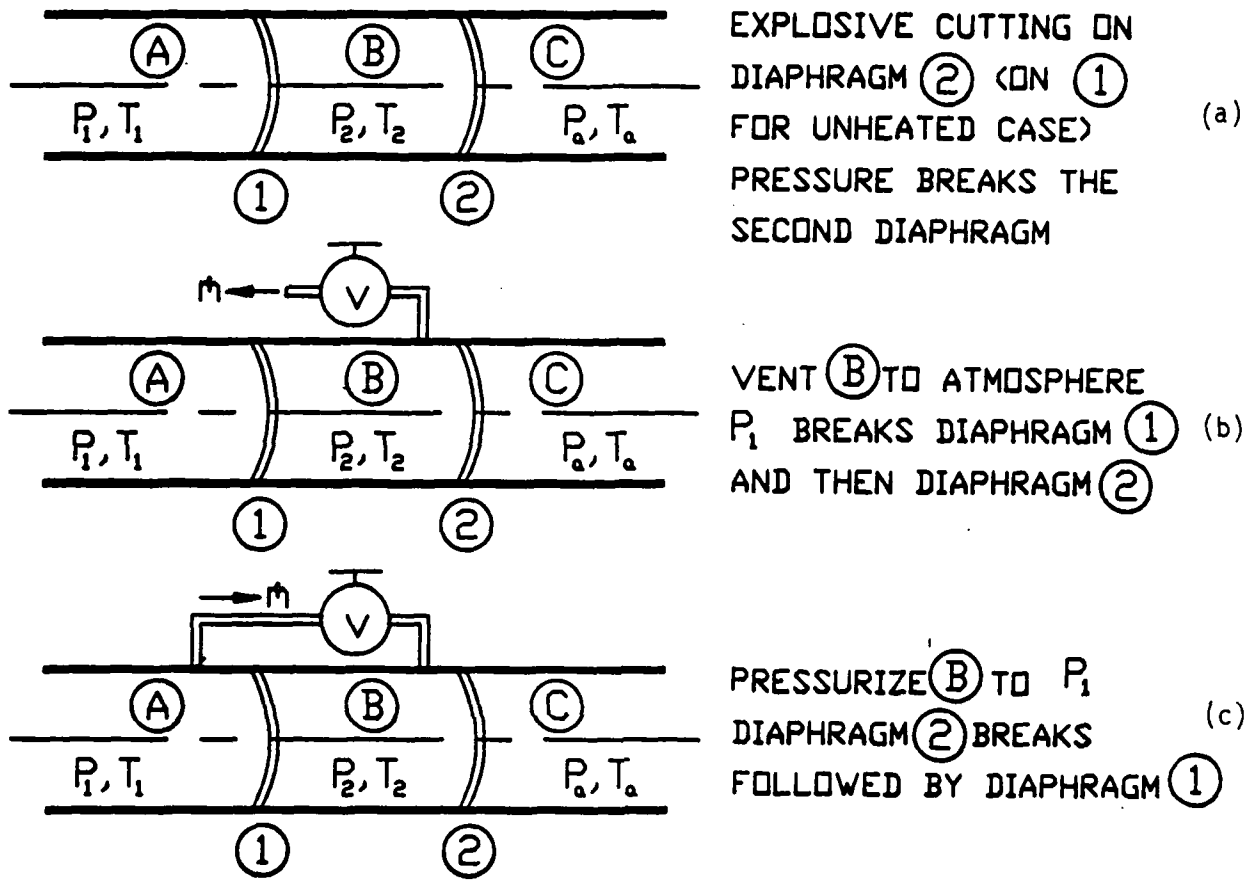

Figure 32. Dual diaphragm opening concepts.

downstream diaphragm, P_2, thereby opening the driver to the exhaust. The time period for this operation to take place depends on the time required to vent compartment B to the atmosphere. It is a function of P_2, volume B, and valve V port size and opening time.

Figure 32c shows the same physical arrangement but valve V vents high pressure air from the driver A to chamber B. As pressure P_2 in B rises to the level required, diaphragm 2 ruptures releasing chamber pressure, P_2, and the full system pressure, P_1, acting on diaphragm 1, causes it to burst. In all of these cases, the diaphragms are designed to burst at pressures below system pressure, P_1, and greater than half system pressure, P_2.

Response time depends on the venting and pressurization time and the bursting strength of the diaphragm.

5.1.3 Mechanical Methods.

Diaphragms can be opened by using a mechanical device, usually in the form of a pointed rod, to initiate the fracture at the junction of a series of radial grooves. Using this technique as illustrated in Figure 33, a piston driven by a pyrotechnic gas charge pierces the diaphragm to initiate the rupture. Action time can be on the order of 10 milliseconds depending on gas generator output and piston parameters. A gas generator similar to a shotgun cartridge is required. Electric squib initiation would start the decomposition of a gunpowder charge. Pressures on the order of 25,000 psi are attainable with simple cartridge type gas generators. The mechanical system would not require explosives and would not be affected by heated driver gas.

If compressed air or hydraulic pressure is used to drive the piston, response time will be increased and piston diameter will be increased because compressed air is not normally available at pressures greater than 2500 psia and hydraulic pressures are limited to 10,000 psi maximum. An accumulator would be required to provide hydraulic flow so the working hydraulic pressure would drop to approximately 3,000 psi over the stroke of the piston. Also, because hydraulic flow rates are limited by the pressure, response times would

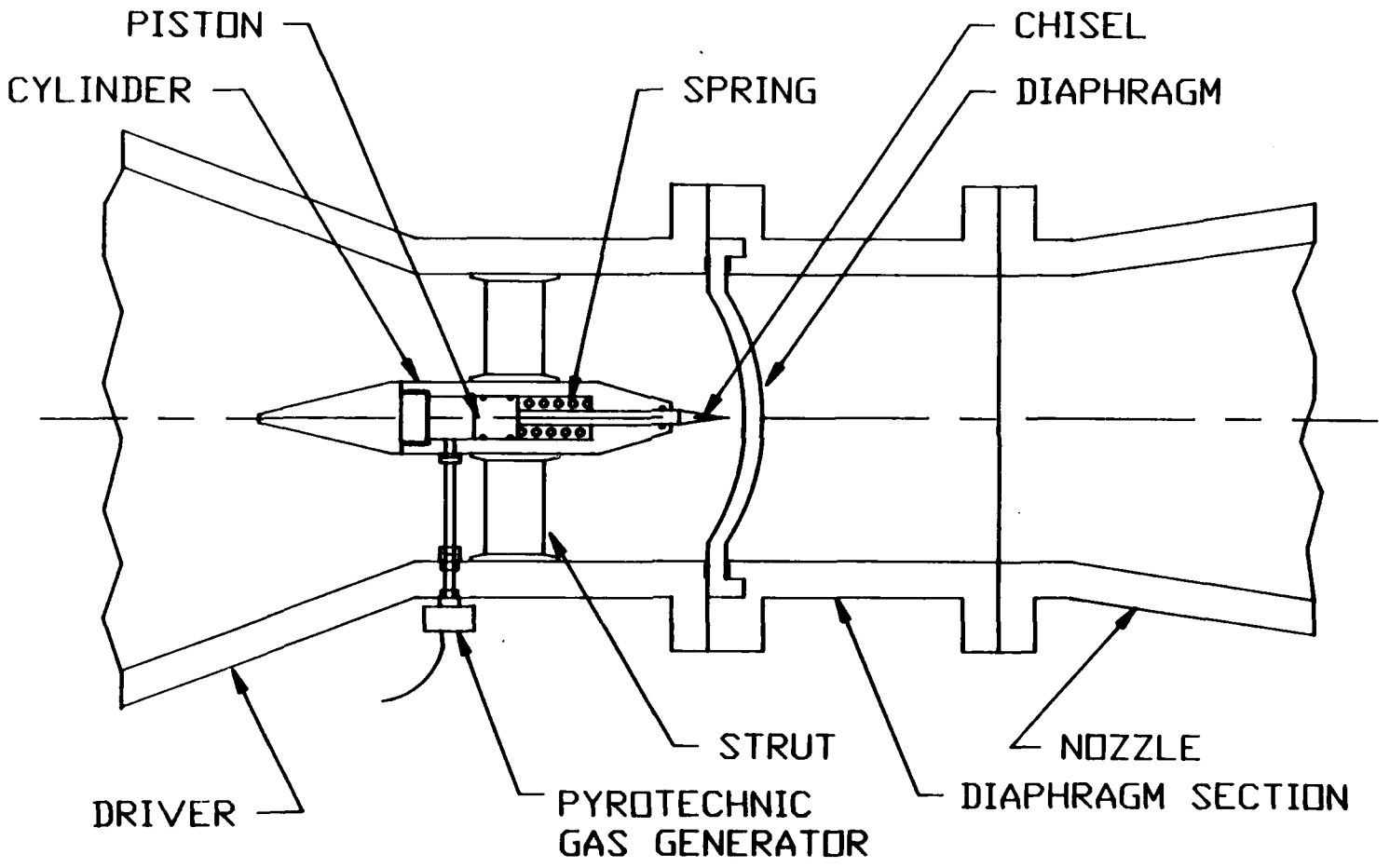

Figure 33. Mechanical diaphragm opener.

increase.

$$v = k\sqrt{2gh} = k\sqrt{2g\frac{p}{\rho}}$$

where

v = velocity of flow through an orifice
k = orifice coefficient ≈ 0.97
g = 32.17 ft/sec^2
p = pressure, PSF
ρ = density, lb/ft^3

For 3,000 psi, the oil could theoretically flow through an orifice as fast as 1800 FPS. Actually, when multiple orifices and pipe losses are accounted for, maximum flow rate will be on the order of 100 FPS and response time can be calculated accordingly.

5.1.4 Petal Formation.

When the diaphragm is sheared into petals (or gores) by the action of explosive or pressure, individual petals are formed as illustrated in Figure 27.

The pressure force acting on the petal surface, normal to the surface, is the static differential pressure, P, acting on a triangular area.

$F = PA$
A = area, inches^2 = $(h-y)\, x_y$
$X_y = (h-y) \tan \theta/2$

Therefore:

$A = (h-y)^2 \tan \theta/2$
$F = P(h-y)^2 \tan \theta/2$ lbs

Force acts through the area centroid $\bar{y}$ where

$$\bar{y} = \frac{(h-y)}{3} + y$$

Therefore, the bending moment, M, that acts to open the petals at any station y is given by the following equation:

$$M = F\bar{y} = P\left[\frac{(h-y)^3}{3} + y(h-y)^2\right] \tan\frac{\theta}{2} \text{ in lb}$$

Section moduls $S = t_y^2 \frac{(h-y)\tan\theta/2}{3}$

Bending stress $S_b = \frac{M}{S} = \frac{P}{t_y^2}\left[(h-y)^2 + 3y(h-y)\right]$

For a typical case of interest

h = 20 inches

S_b max occurs as y = 0

$$S_b \text{ max} = \frac{P(h^2)}{t_y^2}$$

For 1,000 psi differential pressure, the bending stress is greater than the 150,000 psi minimum yield stress of the diaphragm material but as y increases, the bending stress decreases. However, it may be great enough to cause local failure of the petal near the tip, which could bend prematurely like a banana peel and prevent the entire petal from flattening itself at the root. Experiments are necessary to verify the petal formation.

5.2 DIAPHRAGM STRUCTURAL ANALYSIS.

The structural design of the rupture diaphragm is critical to the safe design and operation of the high pressure, high temperature LB/TS driver system. The diaphragm is basically a pressure vessel component and is designed not to fail at its ultimate strength level at the maximum static

working pressure differential and temperature (a suitable design safety factor is included). In the case of a diaphragm designed to rupture, however, additional design criteria must be developed for the precise rupture opening of the diaphragm upon an explosive, mechanical or pressure force initiation. As a result, the diaphragm is designed to operate at very high stress levels. Therefore, manufacturing and inspection processes for the diaphragm must be stringently controlled to minimize material and production flows which could cause accidental catastrophic failure. Additionally, the inherent low design safety factor for the diaphragm creates an unsafe and hazardous condition in the shock tube while the driver is being pressurized and/or heated.

In this section, the design criteria for the rupture diaphragm will be established from the operating characteristics of the LB/Ts driver system, then a materials survey will be used to select several candidate steel alloys which are suitable for the diaphragm design under study and finally a parametric stress analysis will establish the required geometry (i.e., thickness, radius of curvature, etc.) of the diaphragm design.

5.2.1 Design Criteria.

The structural design criteria for the LB/TS diaphragm is derived from its two modes of operation. The first mode is the diaphragm's function as a "safe" pressure vessel component operating at the design pressure and temperature. The second mode is the diaphragm's ability to precisely rupture upon initiation by mechanical means, by explosive cutting charge or gas pressure differential increase. The three operation modes must be considered simultaneously to derive the necessary design criteria for the diaphragm stress analysis.

The LB/TS dual diaphragm system design is shown in Figure 8. As was stated previously, the dual diaphragm system facilitates the use of an explosive cutting charge (limited to 200-300°F temperature operation) on the downstream diaphragm which is thermally isolated from the hot driver gas by the upstream diaphragm. Additionally, the pressure differential across each of the diaphragms is regulated at approximately one half the total driver gage

pressure and thus the two diaphragms are each stressed half as much as a single diaphragm system. The working temperature of the upstream diaphragm is considered to be at the driver gas temperature and the downstream diaphragm at approximately room temperature due to driver gas cooling between the two diaphragms.

The design criteria for mechanical stress is established from a design safety factor imposed on the tensile ultimate strength of the diaphragm material. For the upstream diaphragm, the design safety factor must be less than two to assure that this diaphragm is ruptured by the pressure increase which occurs when the downstream diaphragm is explosively ruptured. Because the initial pressure differential across the upstream diaphragm is only one half the total driver gas pressure, a design safety factor greater than two would not induce sufficient mechanical stress to fracture the upstream diaphragm. To provide adequate assurance that the diaphragm will rupture, a design safety factor of 1.5 is used in the analysis. The downstream diaphragm (in the explosive opening design), however, has a more conservative design safety factor because it is ruptured by explosive cutting charges. In this case, the only limits to the design safety factor are the required safety in the LB/TS test section while the driver gas is being pressurized/heated and the cutting ability of the linear shaped charges which are used to rupture the diaphragm. For the diaphragm in this study, a design safety factor of at least 2 is used to provide sufficient margin of safety to prevent accidental discharge of driver gas. In order for the test section to be man rated while the drivers are pressurized, the ASME pressure vessel code maximum allowable stress specification for the material used must be used for the diaphragm design. A summary of the design criteria for each of the diaphragms is given in Table 7. IT IS OUR RECOMMENDATION THAT NO MEN BE PRESENT DOWNSTREAM OF A PRESSURIZED DIAPHRAGM!

5.2.2 Diaphragm Materials Selection.

The selection of materials for the LB/TS rupture diaphragm is dependent upon its operating environment and opening constraints. The diaphragm is subject to high stress levels at temperatures from 70° to 700°F. The tensile

strength of the diaphragm material is the single most important property to be considered. If the ultimate strength is low (less than 75 ksi) the diaphragm would be excessively thick and heavy. A diaphragm which is very thick (in the order of one inch) would be very difficult to fracture predictably and completely. The required FLSC charge would be heavy enough to cause severe pressure loads on the downstream cartridge walls. A thinner diaphragm would be more likely to fully petal open in a predictable and controllable manner. A heavy diaphragm would make handling and assembly more difficult and would inflict greater damage to the diaphragm housing when it petals and strikes the housing wall. An additional constraint on the diaphragm material is the degradation of strength properties at elevated temperatures. As the material temperature increases, the ultimate strength correspondingly decreases and over time the material tends to creep (elongate) under stress. The hot diaphragm (upstream) should be made from a material which has high strength properties and resists creeping at its operating temperature.

Table 7. Rupture diaphragm design criteria.

Design Criteria	Diaphragm No. 1	Diaphragm No. 2
Location	Upstream	Downstream
Working Pressure (psig)	1150	1150
Rupture Pressure (psig)	2300	1150
Working Temperature (F)	700	<100
Rupture Method	Differential Pressure	Explosive Cutting Charges
Opening Pattern	8 Radial Grooves Min	8 Radial Grooves Min
Safety Factor	1.5	>2.0
Min Thickness Strength Basis	Tensile Ultimate	Tensile Yield
Man Rating	No	No

A second important class of properties to consider for the diaphragm is the fracture strength. The most common type of property affecting fracture strength is elongation. Elongation is the amount of strain a material will exhibit under tensile stress before any fracture is observed. This property is important because when the diaphragm petals open, an excessive amount of

strain will occur at the base of the petal. To prevent the failure of the petal base and thus the possible fracture and release of the petal into the high velocity gas flow, the material must be resistant to fracturing at high strain conditions. The elongation is specified in percent strain which is the percent length per unit length that the material is stretched to failure.

Other fracture strength properties to consider are fracture and notch toughness. The notch toughness of the material is the ability of a metal to absorb energy and deform plastically before fracturing. Fracture toughness, a material property related to notch toughness, describes the resistance of a metal to the propagation of an existing crack. Both of these properties describe the brittleness or low ductility of the material. The diaphragm increase the possibility of an unwanted failure because of stress concentrations produced by the material discontinuity. The fracture roughness of a material is typically specified as the stress intensity factor, K, in units of stress times square root of length (i.e., ksi-$(in)^{1/2}$). The stress intensity factor generally describes and relates the material flaw size, component geometry and fracture toughness. For every structural material which exhibits brittle fractures there is a lower limiting value of K termed the plane-strain fracture toughness, Klc. In a general sense, all high strength alloys (steel, aluminum, etc.) exhibit some degree of brittleness and therefore the fracture roughness must be carefully examined when considering the material for high stress structural use as in the diaphragm operation.

The types of structural materials which were initially considered for the rupture diaphragm are steel, aluminum, and titanium alloys. These alloy groups have available a wide range of strength and toughness properties through the use of different alloying elements and heat treatment practices. For two of these alloy groups, steel and titanium, there are available materials with ultimate strengths in the order of 150 ksi. Aluminum alloys cannot be heat treated or alloyed to the 150 ksi strength level (maximum strength for a 7075-T6 alloy is typically 75 ksi) and thus were eliminated as candidate diaphragm materials. The properties of the alloys are available from several sources. The ASME Boiler and Pressure Vessel Code [Ref. 8] has material specifications for all types of pressure vessel applications (i.e.,

bolting, fittings, plates and sheets, pipes and tubes, forgings, castings, and bars). A second source for property data is the Military Standardization Handbook for Metallic Materials and Elements for Aerospace Vehicle Structures (MIL-HDBK-5C). This handbook tabulates data for a wide variety of metallic materials used in the aerospace industry. A selection was made for materials which have the desired high strength and ductile properties suitable for the rupture diaphragm. The candidate materials were selected based on engineering judgement and reference research. Table 8 gives properties for the various candidate materials.

5.2.3 Diaphragm Stress Analysis.

The diaphragm structural design was performed on the baseline diaphragm configuration shown in Figure 34. The stress analysis was limited to a first order simple stress model to calculate relative thicknesses of the diaphragm shells so that an evaluation of the required fabricating and opening techniques could be made. A higher order design would incorporate a finite element analysis which would provide excellent diaphragm opening/rupturing design data. This analysis, however, was beyond the scope of project and is left for a future study. The diaphragm stress model is composed of three basic structures. The major section of the diaphragm is the spherical dish-like shell. The spherically shaped structure is characterized by its radius of curvature which is assumed to be approximately 40 inches, roughly twice the diaphragm port diameter. The spherical shell transfers it membrane stress to the next structural section, a toroidal shell. The toroidal shell is a smooth transition section from the spherical dish to the mounting ring and is characterized by a major diameter approximately equal to the diaphragm port diameter and a minor diameter chosen based on parametric calculations (range is from 4 to 8 inches diameter). The inner minor diameter of the toroidal shell is assumed to transfer all bending loads caused by the spherical shell deflection to a mating male bearing surface on the flange in which the diaphragm is mounted. This insures that the spherical structure only transfers the membrane stress to the toroidal shell which in turn transfers its membrane stress to the mounting ring where the load is taken out in shear by the diaphragm mounting ring. The mounting ring is the section of the

Table 8. Strength and elongation properties of selected high strength steel alloys.

ALLOY SPEC	HEAT TREAT	ULTIMATE STRENGTH @ RT ksi	STRENGTH @ 700 F ksi	YIELD @ RT ksi	STRENGTH @ 700 F ksi	ELONGATION PERCENT in/in	EXPOSURE LIMIT F
LOW ALLOY STEELS							
AISI 4130	ANNEALED	90	76	70	59	15	-----
	Q & T	125	105	103	87	10	925
	Q & T	150	126	132	111	9	775
	Q & T	180	151	163	137	7	575
AISI 4140	ANNEALED	90	76	70	59	15	-----
	Q & T	125	105	103	87	10	1025
	Q & T	150	126	132	111	9	875
	Q & T	180	151	163	137	7	725
	Q & T	200	168	176	148	6	625
AISI 4340	Q & T	125	105	103	87	10	1100
	Q & T	150	126	132	111	9	950
	Q & T	180	151	163	137	7	800
	Q & T	200	168	176	148	6	700
	Q & T	260	218	215	181	5	350
INTERMEDIATE ALLOY STEELS							
AMS 6523	Q & T	190	160	180	151	10	900
AMS 6526	Q & T	220	185	190	160	10	900
HIGH ALLOY STEELS							
AMS 6520	Q & T	252	212	242	203	5	900
STAINLESS STEELS							
AM-355 SS							
AMS 5749	SCT850	190	160	150	126	10	800
AMS 5749	SCT1000	165	139	140	118	12	800
17-4PH	H900	190	154	170	133	8	<900
	H925	170	138	155	121	8	<925
	H1025	155	126	145	113	8	<1025
	H1075	145	117	125	98	9	<1075
	H1150	135	109	105	82	10	<1150

Q & T--QUENCHED AND TEMPERED TO ULTIMATE STENGTH GIVEN

Reference: MIL-HDBK-5C-Metallic Materials and Elements for Aerospace Vehicle Structures

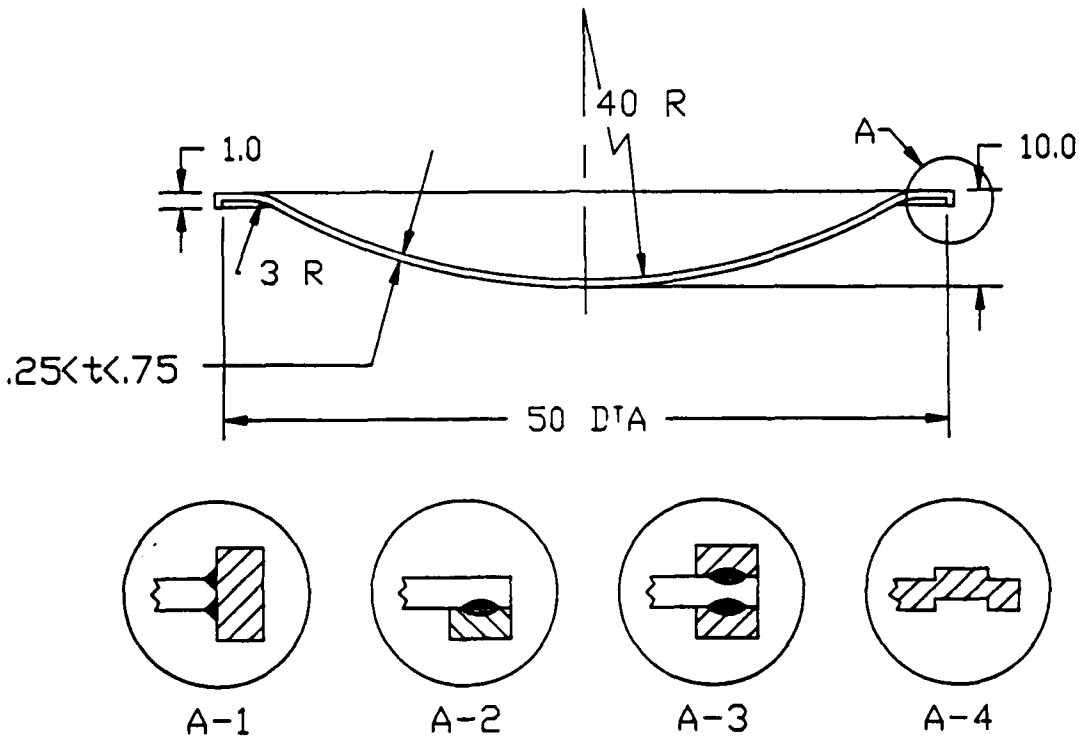

Figure 34. LB/TS diaphragm schematic.

AD-A193 372 AUTOMATED DIAPHRAGM LOADING FOR THE LB/TS (LARGE 2/2
BLAST/THERMAL SIMULATOR).. (U) SCIENCE APPLICATIONS INC
SAN DIEGO CA I B OSOFSKY ET AL. 28 FEB 86 SAIC-86-1529
UNCLASSIFIED DNA-TR-86-66 DNA001-85-C-0315 F/G 14/2 NL

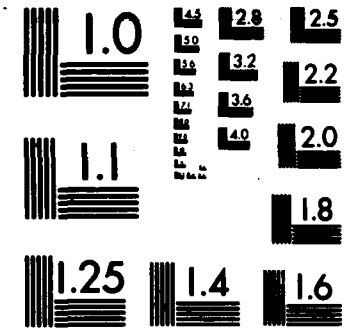

diaphragm that has two functions. First it provides a flat surface to seal against the driver pressure and second it provides structural support for the diaphragm while it is under high stress during operation. The ring is characterized by a lip that is inserted into a slot in the mounting flange to firmly hold the diaphragm in place. This lip is under shear stress and prevents the diaphragm from pulling out of its mounting.

The stress analysis was based on the following assumptions:

1. Driver pressure is exerted only on the spherical shell.
2. Only membrane stresses due to differential pressure are transferred at the interface of the spherical shell and the toroidal shell.
3. The mounting ring lip is in shear stress only.
4. Each section (i.e., spherical, toroidal and ring) is treated independently and the end deflections are matched for each section.

The stress analysis is performed by first choosing a membrane thickness, then calculating the membrane stress and deflection of the spherical shell where it meets the toroidal shell and then calculating the deflection of the toroidal shell due to the spherical shell end conditions. The last step is to calculate the deflection of the ring due to the toroidal end conditions. The results will provide two values, the stress state of the membranes and the shear force of the diaphragm at the ring outer diameter. Two pressures were used in the analysis, first the initial differential pressure of 1150 psi and then the final differential pressure of 2300 psi exerted on the upstream diaphragm when the downstream diaphragm is ruptured. Table 9 shows results of calculations performed for various thicknesses of the diaphragm configuration previously shown at 1150 psi. Table 9 also gives calculation results for the same thicknesses and configuration at 2300 psi. The stress values given are actual tensile and shear stresses and must be modified by a safety factor for a design allowable stress. The stress values are based on a uniform thickness diaphragm, including the ring lip which is in shear stress only. The shear stress levels for the diaphragm are much less than the tensile stress levels as indicated by the table. For a 2300 psi diaphragm operating at the 150 ksi stress level, the shear stress taken out by a single shear area is less than half the tensile stress. This shows that a double shear configuration (see Figure 34, Section A-3) is not necessary for the diaphragm. The

thickness for a 2300 psi diaphragm operating at a design allowable stress of 150 ksi would typically be about 5/8ths of an inch as the table shows. For a 1150 psi diaphragm, the thickness is about 3/16ths of an inch. The material selection would be based on the material working stress (i.e., yield stress times an appropriate safety factor) and the working temperature. The preliminary structural design analysis indicates that the materials previously chosen and given in Table 8 are applicable for this design and represent excellent candidates for the diaphragm configuration under study.

Table 9. Diaphragm structural design results for 1150 and 2300 psi.

Diaphragm Nominal Thickness in	Maximum Bending Tensile Stress @1150 ksi	@2300 ksi	Maximum Single Shear Stress @1150 ksi	@2300 ksi	Maximum Double Shear Stress @1150 ksi	@2300 ksi
0.250	182	363	84	168	42	84
0.375	122	243	56	112	28	56
0.500	91	182	42	84	21	42
0.625	73	146	33	67	17	33
0.750	61	122	28	55	14	28
1.000	46	92	21	41	10	21

5.3 DIAPHRAGM FABRICATION TECHNOLOGY.

5.3.1 Fabrication Methods.

The diaphragms that are required for the LB/TS are best described as circular sheets of steel of uniform thickness which are formed into a partial spherical segment. The steel that is selected for the diaphragm must be cross rolled sheet with uniform properties. The steel must be free from inclusions, pits and flaws. The shape of the diaphragm is shown on Figure 34. The spherical radius of curvature and other radii will be determined after a detailed structural trade study is accomplished. for purposes of this study, a 40 inch spherical radius was selected and the transition radius was three inches. This geometry places the diaphragm in almost pure tension. Shear forces are reacted by the tension component acting on the support frame.

Minimum tensile yield stress is specified as 150,000 psi. A number of manufacturing processes were investigated and some are described in detail below. The processes were designed to provide a uniformly thick diaphragm with vee grooves machined or formed in the convex spherical side.

5.3.1.1 Explosive Forming. Figure 35 schematically illustrates the explosive forming process. A diaphragm blank with a preformed flange or with bolt holes is held to a very heavy alloy steel female die by edge clamps. For illustrative purposes, the clamps are shown bolted by hydraulic or mechanical clamps could be used in practice. The female die may be several feet thick and a steel such as AISI 4340 could be used. A vacuum pump is used to evacuate the void between the diaphragm blank and the die. The entire assembly is submerged in a tank of water. A small explosive charge is suspended at or near the center of curvature of the die and detonated. The intense hydraulic pressure generated by the detonation forms the diaphragm blank to the contour of the die. If grooves are desired in the finished diaphragm, a pattern of wires outlining the grooves may be positioned on the concave face of the die. The impact of the diaphragm blank on the die face is so fast that the blank will locally flow around the wires to form grooves. If round wires are used, round grooves will be formed. Therefore, if vee grooves are desired, wires of the proper cross section must be used on the die.

Unfortunately, the forming process stretches the metal and the most severe stretch will result near the 45 degree radial line of the spherical segment. Therefore, the diaphragm thickness must be sized at this thinnest area or the diaphragm must be machined to a final contour after forming. It is likely that the sealing face of the diaphragm will require machining or polishing.

In any case, the diaphragm is formed from annealed material and is heat treated after forming. Jigs will be required to prevent warping during heat treat and in some cases, straightening dies would be required to eliminate residual warping.

Explosive forming is a rapid, relatively inexpensive process. It is

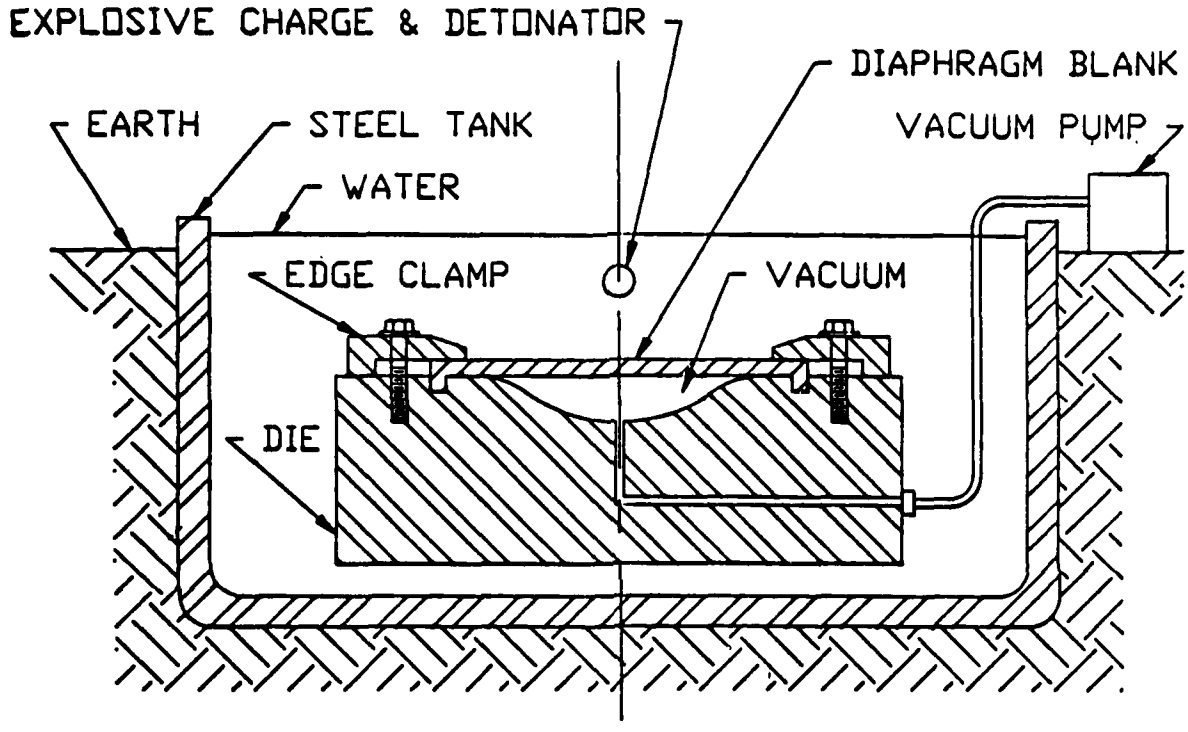

Figure 35. Explosive forming of diaphragms precision die method.

likely that a number of dies would be required to get the required production rate. One advantage is that only one die size is required to handle the range of thickness of diaphragms that will be required for the LB/TS.

This process can be used to form scale diaphragms for BRL scale model shock tubes.

5.3.2 Hydroform.

In the hydroform process, a female die such as that illustrated in Figure 35 is constructed and the diaphragm blank is mounted as before. Instead of submerging the die in water, a heavy pad of rubber is used to cover the diaphragm blank and a huge hydraulic press squeezes the rubber and metal blank into the forms cut into the die.

Because hydroforming cannot be used for heavy steel parts, the process was not thoroughly investigated, however, because many of the diaphragms will be "thin," hydroforming should be investigated for these cases in future studies.

5.3.3 Forging.

Both Ladish and Wyman-Gordon said that the one meter diameter diaphragm was too thin for them to forge in male and female dies. For the flange diameters of interest (about 50 inches O.D.) they would start with a billet of steel and end up with a diaphragm that was approximately two inches thick. This would then require machining to the final thickness which is in the order of 0.5 inches or less. This makes the process uneconomical for the thin diaphragms of interest.

5.3.4 Spinning.

SAIC had detailed engineering discussions with Spincraft in North Billerica, Massachusetts. Spincraft has another plant in New Berlin, Wisconsin. The diaphragm would be formed from AISI 4130 steel or 17-4PH precipita-

tion hardening stainless steel. The forming is carried out by spinning a flat disk shaped diaphragm blank against a male die rotating on the spindle of a power spinning machine. The same die can be used for any thickness of diaphragm. During the spin forming operation, the metal flows and the thickness of the finished part varies along the radius. Figure 36 shows a large conical dish being formed on the spinning machine.

Thickness is reduced as follows for the diaphragms of interest.

Initial Thickness Inches	Minimum Spun Thickness Inches
0.7	0.550
0.5	0.375
0.375	0.290
0.250	0.180

Therefore, we would end up with a diaphragm whose thickness varies along the radius with the minimum thickness located approximately at the 45° point on the spherical segment.

The radial vee groove pattern would have to be machined after forming. Also, Spincraft says that the sealing surfaces must be machined after spinning. The heat treat would take place after machining.

Spincraft has estimated the ROM unit cost of diaphragms based on 1000 units. Their estimate is given below.

Spincraft ROM cost.

17-4 PHG precipitation hardening stainless steel.

Bank Thickness Inches	Unit Price Including Material	Unit Material Cost
0.7	$3,200	$2,069
0.5	2,500	1,380
0.375	1,975	1,035
0.25	1,450	690

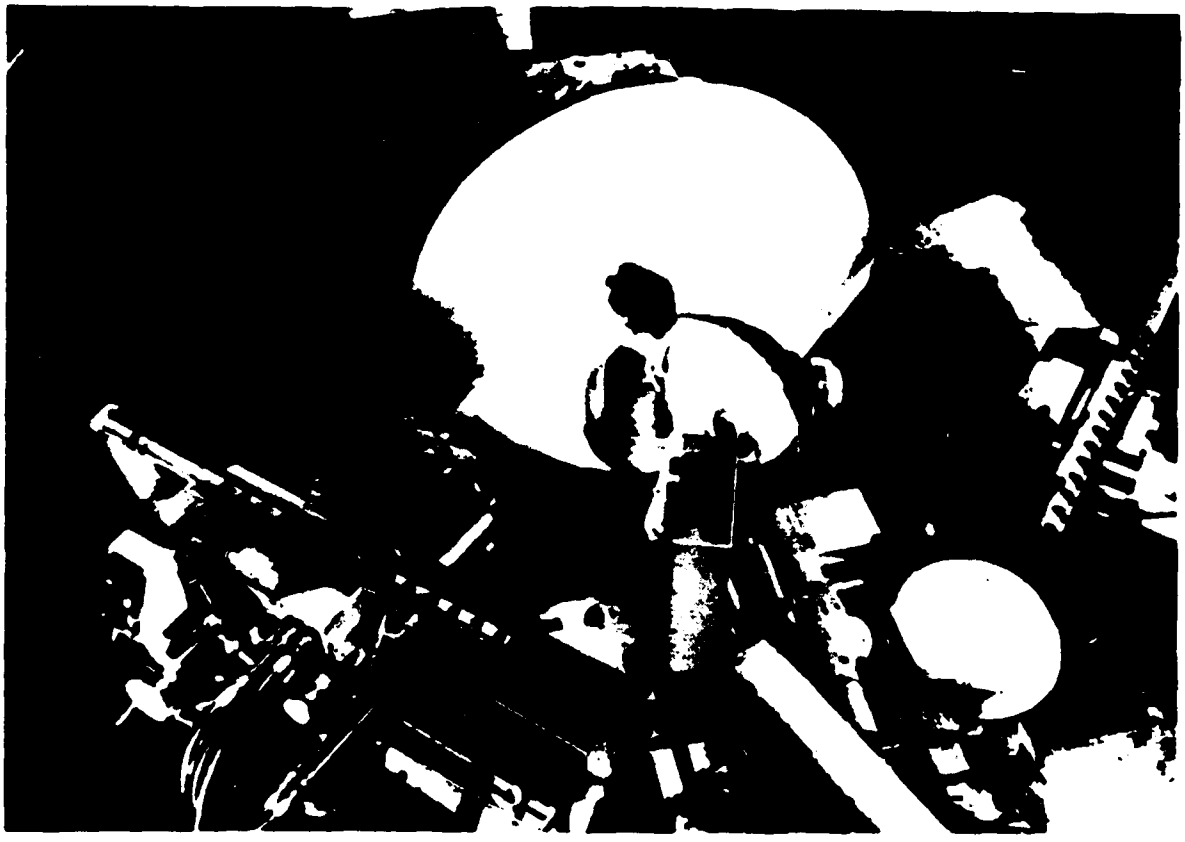

Figure 36. Spincraft power spinning machine.

This shows that metal flow is significant. Flatness of the seal area can be held to within 0.020 inches by machining. As spun, the flatness will vary ± .063 inches.

5.3.5 Hydraulic Forming.

Diaphragms can be free formed by subjecting them to hydraulic pressure in a fixture similar to that shown in Figure 37. The diaphragm is held in place by a bolted clamp and hydraulic pressure is applied to one side by a hydraulic pump. Water is usually used as the pressurizing fluid so that it can be drained without recovery. The deflection of the diaphragm is measured and pumping is stopped when the deflection reaches a predetermined amount. The metal is stretched beyond the yield point but setback will occur when the pressure is released. As in any of the other processes, the diaphragms will be thinner at preferential radial stations and may need to be machined and grooved after deflection.

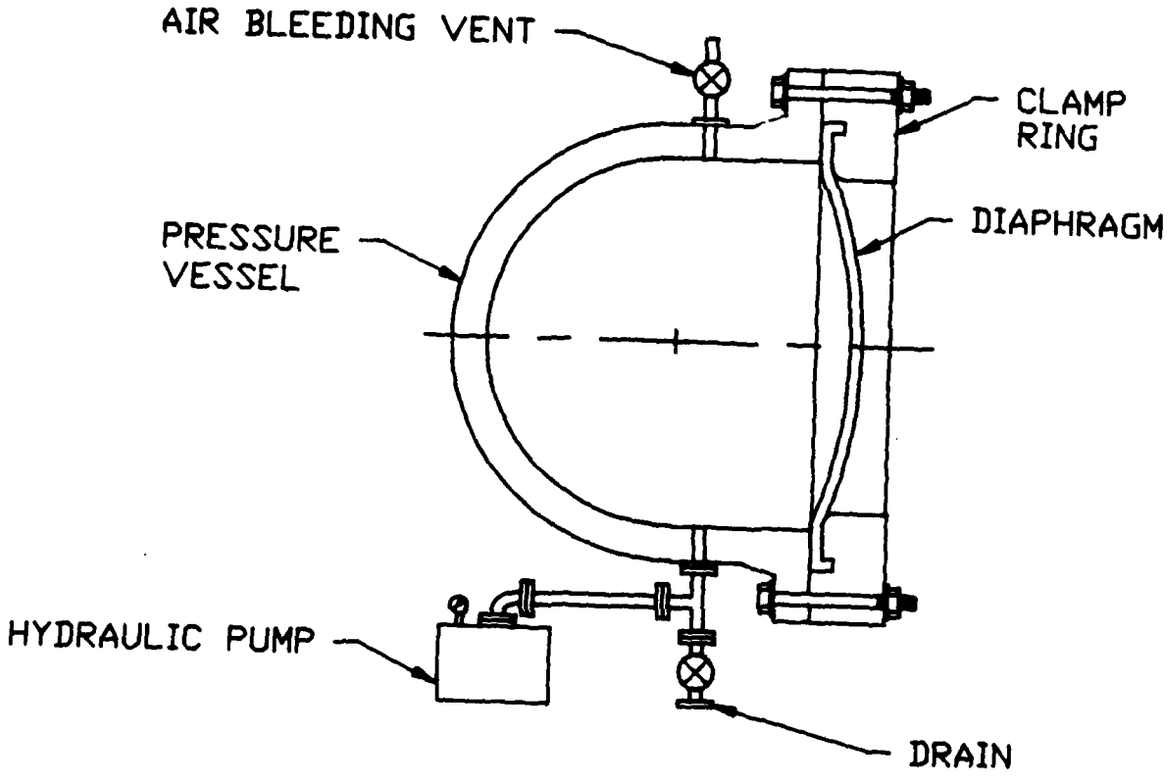

Figure 37. Hydraulic forming of diaphragm.

SECTION 6
OPENING TECHNIQUES DEMONSTRATION TEST PLAN

This section very briefly describes a test plan that would be used to evaluate the opening techniques and obtain test data. It is designed to utilize the linear shaped charges on a dual diaphragm installation.

6.1 FLSC CHARACTERIZATION TESTS.

Test panels of metal shall be fitted with a length of FLSC at the proper standoff distance and the charge shall be fired. The test panel shall be unsupported except at the edges. Depth of cut shall be measured. Metallographic cross sections shall be prepared for each cut. Test panels shall be six inches by twelve inches. Three measurements per cut shall be made at the beginning, center and end of the cut.

FSLC TEST MATRIX

Panel Thickness Inches	Charge Size	Panel Material Type A	B	C
.125	1	AISI 4130	17-4PH	AMS 6523
.125	2	AISI 4130	17-4PH	AMS 6523
.125	3	AISI 4130	17-4PH	AMS 6523
.25	1	AISI 4130	17-4PH	AMS 6523
.25	2	AISI 4130	17-4PH	AMS 6523
.25	3	AISI 4130	17-4PH	AMS 6523
.375	1	AISI 4130	17-4PH	AMS 6523
.375	2	AISI 4130	17-4PH	AMS 6523
.375	3	AISI 4130	17-4PH	AMS 6523
.50	1	AISI 4130	17-4PH	AMS 6523
.50	2	AISI 4130	17-4PH	AMS 6523
.50	3	AISI 4130	17-4PH	AMS 6523

For valid data, three panels/test point should be tested. Tests should take place at room temperature.

6.2 DIAPHRAGM OVERPRESSURE TESTS.

At least three scaled diaphragms of each material and each thickness shall be tested in a pressure vessel in which the diaphragm is pressurized to design pressure on both sides. The convex side should have the pressure slowly released until the diaphragm ruptures. This will characterize the particular design to obtain the initial bursting point.

After the diaphragms have been tested for initial opening, the above tests should be repeated with very rapid venting of the downstream pressure by means of a large ball valve or diaphragm to obtain data on the petal formation and bending as the diaphragm opens. A test rig similar to that illustrated in Figure 8 should be used with the aft diaphragm replaced by a quick opening valve. The test matrix is shown below.

DIAPHRAGM PRESSURE BURST TEST MATRIX

Maximum Test Pressure	Diaphragm Configuration	Diaphragm Material		
P_1	1	A	B	C
P_1	2	A	B	C
P_1	3	A	B	C
P_2	1	A	B	C
P_2	2	A	B	C
P_2	3	A	B	C
P_3	1	A	B	C
P_3	2	A	B	C
P_3	3	A	B	C

Petal formation will be noted as a function of the various variables.

6.3 DIAPHRAGM EXPLOSIVE OPENING TESTS.

At least three scaled diagrams of each material and thickness shall be tested in a test rig similar to that illustrated in Figure 8. The FLSC shall be mounted on the diaphragm and actuated. Petal formation shall be observed.

Local blast pressures shall be measured aft of the diaphragms and strain gages shall measure the response of the chamber walls.

EXPLOSIVE OPENING TEST MATRIX

SINGLE DIAPHRAGM

Diaphragm Configuration	Charge Size	Pressure	Material		
A	1	1 2 3	A	B	C
	2	1 2 3	A	B	C
	3	1 2 3	A	B	C
B	1	1 2 3	A	B	C
	2	1 2 3	A	B	C
	3	1 2 3	A	B	C
C	1	1 2 3	A	B	C
	2	1 2 3	A	B	C
	3	1 2 3	A	B	C

6.4 DUAL DIAPHRAGM EXPLOSIVE OPENING TESTS.

The scale test series described in Section 6.3 shall be repeated with a test rig similar to that illustrated in Figure 8. Dual diaphragms shall be installed. Explosives shall be installed on the aft diaphragm. The system shall be pressurized with P_0 upstream and $P_0/2$ between the two diaphragms. The explosive shall be fired to open the aft diaphragm and measurements made of complete system response time.

These tests will result in designs and performance data for explosively opened or pressure opened single and dual scaled diaphragms. The test matrix is shown below.

EXPLOSIVE OPENING TEST MATRIX
DUAL DIAPHRAGM

Diaphragm Configuration		Charge				
Upstream	Downstream	Size	Pressure	Material		
A	D	1 2 3	1	A	B	C
A	E	1 2 3	2	A	B	C
A	F	1 2 3	3	A	B	C
B	D	1 2 3	1	A	B	C
B	E	1 2 3	2	A	B	C
B	F	1 2 3	3	A	B	C
C	D	1 2 3	1	A	B	C
C	E	1 2 3	2	A	B	C
C	F	1 2 3	3	A	B	C

SECTION 7
CONCLUSIONS

7.1 HEATING.

(a) The design of a diaphragm system for heated driver gas is feasible.

(b) A single diaphragm may be used in combination with a mechanical diaphragm rupturing device.

(c) A dual diaphragm system is required if explosive release of heated driver gas is required.

(d) Cooling is required on the upstream sealing piston if suitable insulation is not available.

(e) Cooling may be required if explosive charges are used to open the diaphragm.

7.2 DIAPHRAGMS.

(a) Thin diaphragms of high tensile-high elongation steel are preferred because:

1. They are easier to form.
2. Less explosive energy is required for rupture.
3. There is less chance of petal separation upon opening.
4. Full opening is more likely.

(b) Diaphragms for the LB/TS will be an expensive expendable item with 15 to 30 units being used per test.

(c) Diaphragm thickness will be matched to the driver pressure.

(d) Explosive charge performance must be obtained experimentally.

(e) Diaphragms must have vee grooves machined on their convex faces to assure uniform tearing patterns during opening.

7.3 DIAPHRAGM CARTRIDGES.

(a) The diaphragm cartridge loading system is a feasible design.

(b) No bolting is required to install or remove a diaphragm cartridge.

(c) Automatic programmed "cherry picker" type manipulators can be used to exchange diaphragms in the drivers if cartridges are used.

(d) Sealing is best accomplished by an upstream annular piston.

(e) Although not illustrated in the design drawings, all gas and coolant connections can be automatically coupled when a cartridge is installed and disconnected when the cartridge is removed. Ports and valving can be provided in the downstream flange which faces the nozzle.

7.4 STRUCTURES.

(a) The ASME boiler code should be used for the design of all man-rated structures such as the diaphragm housing and cartridges.

(b) A safety factor should be used in the diaphragm's bursting strength design.

(c) All assemblies should be proof tested.

SECTION 8
RECOMMENDATIONS

1. A scaled diaphragm test facility should be designed and fabricated. This facility would be used to pressure test, rupture test, opening test and evaluate diaphragms. The facility should have heating capability so that actual exposure to heated environments can be made.

2. A diaphragm opening test should be conducted to characterize the opening of the diaphragms and quantify the design parameters.

3. An explosive opening test should be conducted to determine the proper explosive charge and standoff distance for the diaphragm materials which are heat treated to design conditions.

4. Explosive overpressures as a function of system pressure, geometry and charge weight should be analytically and experimentally determined for structural design of the LB/TS diaphragm/nozzle hardware.

5. Very detailed thermal design analyses should be conducted to verify the heat transfer due to the higher pressures and natural/forced circulation in the diaphragm region of the LB/TS. Experiments should be conducted on heated scaled diaphragm sections to correlate data and theory.

6. A scaled mechanical diaphragm opening system should be designed, fabricated and used to evaluate this technique and obtain full scale design parameters.

7. Diaphragm fabrication technology should be evaluated by making and testing scaled diaphragms that are fabricated by various processes that can be used on full size diaphragms.

SECTION 9
LIST OF REFERENCES

1. Osofsky, I.B., G.P. Mason, D.T. Hove, and D.K. McLaughlin, "Support of the Characterization of the LB/TS Facility Final Report," SAIC Report SAIC-86/1528.

2. McLaughlin, D.K., F.Y. Su, and D.T. Hove, "Gas Dynamics and Heat Transfer Analysis in Support of the Characterization of the LBTS Facility," Dynamics Technology, Inc. Report DT-8425-02, January 1985.

3. Osofsky, I.B., G.P. Mason, and D.T. Hove, "Heated Diaphragm Investigation - Progress Report," SAIC-1-108-860-112 HB, January 1986.

4. Casslaw, H.S. and J.C. Jaeger, Conduction of Heat in Solids, Second Edition, Oxford Press, 1980.

5. "SINDA User's Manual," COSMIC Program #TSC-12671, Revised by Sperry Support Services, 1980.

6. Edwards, D.K., V. E. Denny, and A.F. Mills, Transfer Process, Second Edition, Hemisphere Publishing Corporation, 1979.

7. Roark, R.J. and W.C. Young, Formulas for Stress and Strain, Fifth Edition.

8. ASME Boiler Code, American Society of Mechanical Engineers.

DISTRIBUTION LIST

DEPARTMENT OF DEFENSE

ASSISTANT TO THE SECRETARY OF DEFENSE
ATOMIC ENERGY
ATTN: EXECUTIVE ASSISTANT

DEFENSE INTELLIGENCE AGENCY
ATTN: RTS-2B

DEFENSE NUCLEAR AGENCY
2 CYS ATTN: TDTR
4 CYS ATTN: TITL

DEFENSE NUCLEAR AGENCY
ATTN: NMHE
ATTN: TTST

DEFENSE TECHNICAL INFORMATION CENTER
12CYS ATTN: DD

DEPARTMENT OF THE ARMY

DEP CH OF STAFF FOR RSCH DEV & ACQ
ATTN: DAMA-CSM-N

HARRY DIAMOND LABORATORIES
2 CYS ATTN: SCHLD-NW-P
ATTN: SCLHD-DTSO
ATTN: SLCIS-IM-TL (TECH LIB)

U S ARMY BALLISTIC RESEARCH LAB
ATTN: SLCBR-SS-T (TECH LIB)
2 CYS ATTN: SLCBR-TBD-B R PEARSON
ATTN: SLCBR-TBD, DR MARK

U S ARMY CORPS OF ENGINEERS
ATTN: DAEN-RDL
ATTN: DAEN-RDL
ATTN: DAEN-RDM B BENN
ATTN: DAEN-ZCM

U S ARMY ENGR WATERWAYS EXPER STATION
ATTN: D OUTLAW
ATTN: TECHNICAL LIBRARY
ATTN: WESSE (J K INGRAM)

U S ARMY FOREIGN SCIENCE & TECH CTR
ATTN: DRXST-SD

U S ARMY MATERIEL COMMAND
ATTN: AMCCN
ATTN: AMCLD
ATTN: AMCON
ATTN: OFFICE OF PROJECT MGMT

U S ARMY NUCLEAR & CHEMICAL AGENCY
ATTN: LIBRARY
ATTN: MONA-NU
ATTN: MONA-NU (A RENNER)

U S ARMY TEST AND EVALUATION COMD
ATTN: AMSTE-TE-F R GALASSO

U S ARMY WHITE SANDS MISSILE RANGE
ATTN: STEWS-FE-R
ATTN: STEWS-TE-AN J OKUMA
2 CYS ATTN: STEWS-TE-N

DEPARTMENT OF THE NAVY

MARINE CORPS DEV & EDUCATION COMMAND
ATTN: D091 CPT POTOCKI

NAVAL RESEARCH LABORATORY
ATTN: CODE 2627 (TECH LIB)
ATTN: CODE 4700 W ALI
ATTN: CODE 4720 J DAVIS
ATTN: CODE 5584 E FRIEBELE
ATTN: CODE 7780

NAVAL SURFACE WEAPONS CENTER
ATTN: CODE H14
ATTN: CODE X211 (TECH LIB)

THEATER NUCLEAR WARFARE PROGRAM OFC
ATTN: PMS-42331C (R. JONES)

DEPARTMENT OF THE AIR FORCE

AIR FORCE INSTITUTE OF TECHNOLOGY/EN
ATTN: LIBRARY/AFIT/LDEE

AIR FORCE WEAPONS LABORATORY
ATTN: NTE
ATTN: NTED J RENICK
ATTN: NTES
ATTN: SUL

DEPUTY CHIEF OF STAFF/AF-RDQM
ATTN: AF/RDQI

DEPARTMENT OF ENERGY

LAWRENCE LIVERMORE NATIONAL LAB
ATTN: L-53 TECH INFO DEPT LIB

LOS ALAMOS NATIONAL LABORATORY
ATTN: REPORT LIBRARY

SANDIA NATIONAL LABORATORIES
ATTN: EDUCATION & TECH LIB DIV

SANDIA NATIONAL LABORATORIES
ATTN: TECH LIB 3141 (RPTS RCVG CLRK)

OTHER GOVERNMENT

FEDERAL EMERGENCY MANAGEMENT AGENCY
ATTN: OFC OF RSCH/NP H TOVEY
ATTN: P BETTGE/NP-CP

DEPARTMENT OF DEFENSE CONTRACTORS

APPLIED RESEARCH ASSOCIATES, INC
ATTN: R GUICE

BDM CORPORATION
ATTN: LIBRARY

BLACK & VEATCH
ATTN: H LAVERENTZ

DYNAMICS TECHNOLOGY, INC
ATTN: D HOVE

INSTITUTE FOR DEFENSE ANALYSES
ATTN: CLASSIFIED LIBRARY

KAMAN SCIENCES CORP
ATTN: D COYNE
ATTN: L MENTE
ATTN: LIBRARY

KAMAN SCIENCES CORP
ATTN: LIBRARY/B. KINSLOW

KAMAN SCIENCES CORPORATION
ATTN: F BALICKI

KAMAN SCIENCES CORPORATION
ATTN: DASIAC

KAMAN TEMPO
ATTN: DASIAC

PACIFIC-SIERRA RESEARCH CORP
ATTN: H BRODE, CHAIRMAN SAGE

S-CUBED
ATTN: R DUFF

SCIENCE & ENGRG ASSOCIATES, INC
ATTN: J STOCKTON

SCIENCE APPLICATIONS INTL CORP
ATTN: J DISHON
ATTN: TECHNICAL LIBRARY

SCIENCE APPLICATIONS INTL CORP
2 CYS ATTN: D HOVE
2 CYS ATTN: G MASON
2 CYS ATTN: I OSOFSKY

SCIENCE APPLICATIONS INTL CORP
ATTN: TECHNICAL LIBRARY

SCIENCE APPLICATIONS INTL CORP
ATTN: J COCKAYNE
ATTN: W CHADSEY
ATTN: W LAYSON

SPARTA INC
ATTN: I OSOFSKY

THERMAL SCIENCES, INC
ATTN: R FELDMAN

END

DATE

FILMED

6-1988

DTIC